AFRL-RX-TY-TP-2012-0040

IMPROVING PROTECTION AGAINST VIRAL AEROSOLS THROUGH DEVELOPMENT OF NOVEL DECONTAMINATION METHODS AND CHARACTERIZATION OF VIRAL AEROSOL

Myung–Huei Woo

Department of Environmental Engineering Sciences
University of Florida
Gainesville, FL 32611

Contract No. FA8650-06-C-5913

April 2012

AIR FORCE RESEARCH LABORATORY
MATERIALS AND MANUFACTURING DIRECTORATE

■ **Air Force Materiel Command** ■ **United States Air Force** ■ **Tyndall Air Force Base, FL 32403-5323**

NOTICE AND SIGNATURE PAGE

Using Government drawings, specifications, or other data included in this document for any purpose other than Government procurement does not in any way obligate the U.S. Government. The fact that the Government formulated or supplied the drawings, specifications, or other data does not license the holder or any other person or corporation; or convey any rights or permission to manufacture, use, or sell any patented invention that may relate to them.

This report was cleared for public release by the 88th Air Base Wing Public Affairs Office at Wright Patterson Air Force Base, Ohio available to the general public, including foreign nationals. Copies may be obtained from the Defense Technical Information Center (DTIC) (http://www.dtic.mil).

AFRL-RX-TY-TR-2012-0040 HAS BEEN REVIEWED AND IS APPROVED FOR PUBLICATION IN ACCORDANCE WITH ASSIGNED DISTRIBUTION STATEMENT.

WANDER.JOSEPH.D.1230231660 Digitally signed by WANDER.JOSEPH.D.1230231660 DN: c=US, o=U.S. Government, ou=DoD, ou=PKI, ou=USAF, cn=WANDER.JOSEPH.D.1230231660 Date: 2012.05.08 14:50:07 -05'00'

JOSEPH D. WANDER, PhD
Work Unit Manager

HENLEY.MICHAEL.V.1231823332 Digitally signed by HENLEY.MICHAEL.V.1231823332 DN: c=US, o=U.S. Government, ou=DoD, ou=PKI, ou=USAF, cn=HENLEY.MICHAEL.V.1231823332 Date: 2012.06.22 14:46:48 -05'00'

MICHAEL V. HENLEY, DR-IV
Chief, Airbase Sciences Branch

RHODES.ALBERT.N.III.1175488622 Digitally signed by RHODES.ALBERT.N.III.1175488622 DN: c=US, o=U.S. Government, ou=DoD, ou=PKI, ou=USAF, cn=RHODES.ALBERT.N.III.1175488622 Date: 2012.07.17 12:42:32 -05'00'

ALBERT N. RHODES, PhD
Chief, Airbase Technologies Division

This report is published in the interest of scientific and technical information exchange, and its publication does not constitute the Government's approval or disapproval of its ideas or findings.

REPORT DOCUMENTATION PAGE

Form Approved
OMB No. 0704-0188

PLEASE DO NOT RETURN YOUR FORM TO THE ABOVE ADDRESS.

1. REPORT DATE *(DD-MM-YYYY)*	2. REPORT TYPE	3. DATES COVERED *(From - To)*
16-APR-2012	Technical Paper (Thesis)	15-SEP-2007 -- 30-APR-2012

4. TITLE AND SUBTITLE

Improving Protection against Viral Aerosols Through Development of Novel Decontamination Methods and Characterization of Viral Aerosol

5a. CONTRACT NUMBER

FA8650-06-C-5913

5b. GRANT NUMBER

5c. PROGRAM ELEMENT NUMBER

0609120

6. AUTHOR(S)

Woo, Myung-Huei

5d. PROJECT NUMBER

5e. TASK NUMBER

5f. WORK UNIT NUMBER

QL102008

7. PERFORMING ORGANIZATION NAME(S) AND ADDRESS(ES)

Department of Environmental Engineering Sciences
University of Florida
Gainesville, FL 32611

8. PERFORMING ORGANIZATION REPORT NUMBER

9. SPONSORING/MONITORING AGENCY NAME(S) AND ADDRESS(ES)

Air Force Research Laboratory
Materials and Manufacturing Directorate
Airbase Technologies Division
139 Barnes Drive, Suite 2
Tyndall Air Force Base, FL 32403-5323

10. SPONSOR/MONITOR'S ACRONYM(S)

AFRL/RXQL

11. SPONSOR/MONITOR'S REPORT NUMBER(S)

AFRL-RX-TY-TP-2012-0040

12. DISTRIBUTION/AVAILABILITY STATEMENT

Distribution A: Approved for public release; distribution unlimited.

13. SUPPLEMENTARY NOTES

Ref Public Affairs Case # 88ABW-2012-4138, 24 July 2012. Document contains color images. Document is reproduced as received.

14. ABSTRACT

Although respirators and filers are designed to prevent the spread of pathogenic aerosols, a stockpile shortage is anticipated during the next flu pandemic. Contact transfer and reaerosolization are also concerns. An option to address these potential problems is to decontaminate used respirators/filters for reuse. In this research a droplet/aerosol loading chamber was built and used in decontamination testing to proved a fair comparison of the performance of different decontamination techniques, including antimicrobial chemical agents, microwave irradiation and ultraviolet (UV) irradiation, which were incorporated into filtration systems and tested.

The inactivation efficacy of dialdehyde cellulose and starch filters s biocidal filters was investigated. In sufficiently humid conditions both media showed higher removal efficiency and better disinfection capability at lower pressure drop than conventional media. In microwave-assisted filtration systems temperature (T) was found to be a key factor. Relative humidity (RH) was another pivotal parameter at warm-to-hot-water temperatures but became insignificant above 90 C. An examination of the effect of T and RH on UV inactivation revealed that absorption of UV by water and shielding of viruses inside aggregates suppressed inactivation. Varying the spray medium showed that artificial saliva (AS) and beef serum extract (BE) produce a protective effect against UV compared to deionized (DI) water, that RH was not a factor in stability of MS2 coli phage sprayed in AS or BE, and that infectious MS2 particles in DI water displayed a volume-based size distribution but in AS and in BE the size dependence was of a lower order. Whereas AS and BE enhanced stability, adding salts had the opposite effect.

15. SUBJECT TERMS

bioaerosols, disinfection, infectivity, influenza, respiratory protection, viruses

16. SECURITY CLASSIFICATION OF:			17. LIMITATION OF ABSTRACT	18. NUMBER OF PAGES	19a. NAME OF RESPONSIBLE PERSON
a. REPORT	b. ABSTRACT	c. THIS PAGE			Joseph D. Wander
U	U	U	UU	163	19b. TELEPHONE NUMBER *(Include area code)*

Reset

IMPROVING PROTECTION AGAINST VIRAL AEROSOLS THROUGH DEVELOPMENT OF NOVEL DECONTAMINATION METHODS AND CHARACTERIZATION OF VIRAL AEROSOL

By

MYUNG-HEUI WOO

A DISSERTATION PRESENTED TO THE GRADUATE SCHOOL
OF THE UNIVERSITY OF FLORIDA IN PARTIAL FULFILLMENT
OF THE REQUIREMENTS FOR THE DEGREE OF
DOCTOR OF PHILOSOPHY

UNIVERSITY OF FLORIDA

2012

To my family in Korea for their constant love and support

ACKNOWLEDGMENTS

I could not have accomplished this study without the valuable assistance of many individuals. Here, I would like to express my deep appreciation to those people. I gratefully acknowledge my advisor, Dr. Chang-Yu Wu for the introduction of aerosol field and giving me an opportunity to join his group for bioaerosol study. His guidance, knowledge, encouragement, critical thinking, and even writing skill have inspired me for research work. I especially appreciate Dr. Joseph Wander who provides valuable comments based on the wide and in-depth knowledge of bioaerosol to improve this study. I wish to express my gratitude to Drs. Ronald Baney and Wolfgang Sigmund for providing the filter materials and valuable comments on filter characteristics. I am also grateful to my committee member, Dr. Ben Koopmen for reading this dissertation and providing the priceless comments.

Great appreciation should go to Dr. Myoseon Jang for guidance and advice for the present and future research fields. I also thank Brian Heimbuch and Dr. William Wallace in Air Force Research Laboratory in Tyndall AFB for their guidance and advices. I also wish to acknowledge the staffs in MAIC, PERC and ICBR who instruct me the use of instruments and helped me with operation.

I would like to thank all aerogators, Dr. Jin-Hwa Lee, Dr. Yu-Mei Hsu, Lindsey Riemenschenider, Alex D. Theodore, Qi Zhang, Danielle Hall, Brian Damit, Seungo Kim, Dr. Sewon Oh, Jun Wang, Lin Shou, Nima A.-Mohajer, Dr. Hsing-Wang Li, and Matt Tribby for their discussions and friendship. Many thanks go out to my undergraduate students, Kyle Brown, Kyle Ulmer, Diandra Anwar, Arian Tuchman, Sang-Gyou Rho, Christiana Lee, Tammy Smith, and Adam Grippin for their helps for my research. My special thanks go to my friends, Drs. Youngmin Cho, Sejin Youn, and Hwan Chul Cho.

TABLE OF CONTENTS

page

LIST OF TABLES

LIST OF FIGURES

LIST OF ACRONYMS

ABI	Applied Biosystem
ANOVA	Analysis of Variance
APS	Aerodynamic Particle Sizer
AS	Artificial Saliva
ATCC	American Type Culture Collection
BE	Beef Extract
BSL	Biosafety Level
CCF	Coarse pore Cellulose Filter
CDC	Center for Disease Control and Prevention
CF	Cellulose Filter
CFU	Colony-Forming Unit
CMD	Count Median Diameter
CPC	Condensation Particle Counter
CV	Coefficient of Variation
DAC	Dialdehyde Cellulose
DAS	Dialdehyde Starch
DI	Deionized
DLS	Dynamic Light Scattering
DMA	Differential Mobility Analyzer
DNA	Deoxyribonucleic Acid
E. coli	Escherichia coli
ELISA	Enzyme-Linked Immunosorbent Assay

ESP	Electrostatic Precipitator
FCF	Fine pore Cellulose Filter
FDA	Food and Drug Administration
FFR	Filtering Facepiece Respirators
FT-IR	Fourier Transform Infrared
HEPA	High-Efficiency Particulate Air
HRH	High Relative Humidity
HVAC	Heating, Ventilating, and Air-Conditioning
IE	Inactivation Efficiency
LD	Lethal Dose
LRH	Low Relative Humidity
MMD	Mass Median Diameters
MPPS	Most Penetrating Particle Size
MRH	Medium Relative Humidity
MS2	MS2 bacteriophage
NIOSH	National Institute for Occupational Safety and Health
PBS	Phosphate Buffered Saline
PCR	Polymerase Chain Reaction
PF	Polypropylene Filter
PFU	Plaque-Forming Unit
PSD	Particle Size Distribution
qPCR	Quantitative Polymerase Chain Reaction
QF	Quality Factor

Q-T-Q	Quarter-to-Quarter
RH	Relative Humidity
RNA	Ribonucleic Acid
RS	Relative Survival fraction
RT	Room Temperature
SARS	Severe Acute Respiratory Syndrome
SEM	Scanning Electron Microscopy
SF	Survival Fraction
SMPS	Scanning Mobility Particle Sizer
STDA	Simultaneous Differential Thermal Analysis
S-T-S	Sample-to-Sample
TSB	Tryptone Soy Broth
TGA	ThermoGravimetric Analysis
UVGI	Ultraviolet Germicidal Irradiation
VRE	Viable Removal Efficiency
WHO	World Health Organization

Abstract of Dissertation Presented to the Graduate School
of the University of Florida in Partial Fulfillment of the
Requirements for the Degree of Doctor of Philosophy

IMPROVING PROTECTION AGAINST VIRAL AEROSOLS THROUGH DEVELOPMENT OF NOVEL DECONTAMINATION METHODS AND CHARACTERIZATION OF VIRAL AEROSOL

By

Myung-Heui Woo

May 2012

Chair: Chang-Yu Wu
Major: Environmental Engineering Sciences

Although respirators and filters are designed to prevent the spread of pathogenic aerosols, a stockpile shortage is anticipated during the next flu pandemic. Contact transfer and reaerosolization of collected microbes from used respirators are also a concern. An option to address these potential problems is to decontaminate used respirators/filters for reuse. In this research, a droplet/aerosol loading chamber was built and applied for decontamination testing for fair comparison of the performance of different decontamination techniques. Different decontamination techniques including antimicrobial chemical agents, microwave irradiation, ultraviolet irradiation, were incorporated into the filtration system and evaluated.

As biocidal filter, dialdehyde cellulose/starch filters were investigated for their inactivation efficacy. Both filters with sufficient moisture content had a higher removal efficiency, lower pressure drop, and better disinfection capability, which are all important attributes for practical biocidal applications. For microwave-assisted filtration system, temperature was identified to be a key factor. Relative humidity was another pivotal parameter for viability of viruses at warm-to-hot-water temperatures, but it became insignificant at temperatures above 90 ℃. As environmental conditions greatly affect the viability of microorganism, the effect of relative

humidity and spray medium on UV inactivation was examined. Absorption of UV by high water content and shielding of viruses near the center of the aggregate are considered responsible for lower inactivation. Across different spray media, inactivation efficiencies in artificial saliva (AS) and in beef extract (BE) were much lower than in deionized water for both aerosol and droplet transmission, indicating that solids present in AS and BE exhibited a protective effect. For particles sprayed in a protective medium, relative humidity was not a significant parameter.

The distribution of infectious MS2 aerosols followed volume-based size distribution for pure viral aerosol whereas these of infectious MS2 generated with solid contents followed lower dimensions. Aggregation by MS2 itself and encasement by inert salts yielded higher stability factor because of shielding effect and reduction of the air/water interface whereas the soluble salts resulted in adverse effect. The knowledge and technologies developed in this study can better protect the general public as well as healthcare facilities against viral aerosols.

CHAPTER 1
INTRODUCTION

Biological Threat

The public's concern of bioterrorism and airborne pathogens has significantly increased in recent years. During the 20th century, three major influenza pandemics occurred from a major genetic change in the influenza strain: the Spanish flu in 1918 (20-100 million deaths), the Asian flu in 1956 (2 million deaths), and the Hong Kong flu in 1968 (1 million deaths). The 2002 and 2003 Severe Acute Respiratory Syndrome (SARS), caused over 8000 cases and 700 deaths. The recent swine flu outbreak, due to a new strain of H1N1 influenza A, has caused illness in over 70 countries and resulted in at least 14,000 deaths worldwide as of January 2010 (ECDC, 2010). On June 11st, 2009, World Health Organization (WHO) raised the pandemic alert level to Phase 6 indicating the onset of a global pandemic (CDC, 2009). These incidents increased the public's awareness and concern of viruses of low infectious dose viruses and spread of airborne pathogens.

Viral Aerosol

Bioaerosols are airborne particles with biological origins such as non-viable pollen, and viable fungi, bacteria, and viruses (Burge, 1990). The adverse health effect of bioaerosols depends on several factors, such as microorganism type and dose. Among them, virus is the smallest one in size (Prescott et al., 2006). Although the size of a single virion is small (20 nm - 300 nm), viruses in nature exist in a wide range of sizes because of aggregation of several viruses, attachment of viruses onto other material, or encasement of viruses by droplets of respiratory secretions. One important concern of the aggregates is the adverse health effect imposed by the deposition in the respiratory system. Inhaled particles can deposit in various respiratory regions. After they are deposited, the aggregates may disperse into numerous individual virions. More

than 400 different viruses with different lethal doses (LDs) result in human diseases such as rubella, influenza, measles, mumps, smallpox, and pneumonia, which involve the respiratory system either directly or indirectly (Prescott et al., 2003). The aggregation, attachment, and encasement of viruses also facilitate resistance to environmental stresses, such as heat, dryness, toxic gases, and ultraviolet (UV) light because of shielding effect (Kowalski & Bahnfleth, 2007). Although the aggregation state of virus with other materials, infectivity of viruses in aggregates under different environmental stress are key parameters to assess the health risk, very limited research has been carried out with respect to this aspect.

Transmission Mode

The understanding of the transmission modes of viral aerosol is critical to the protection of the public against major airborne pathogen pandemics. Effective prevention and treatment of infectious viral aerosols (i.e. vaccination and respiratory protection) also require specific information on the transmission mode. For the spread of infectious viruses, there are three critical transmission modes (CDRF, 2006): (1) Droplet transmission mode: Droplet transmission results from infected individuals generating droplets containing microorganisms by coughing, sneezing, singing, and talking, (2) Contact transmission mode: Contact transmission includes a direct body-to-body contact and an indirect contact through a contaminated object (e.g., needle and towel). This mode frequently occurs in a healthcare facility, and (3) Aerosol transmission mode: Aerosol transmission includes the dispersion of droplet nuclei, which remains in air after evaporation of droplet, and dust particles containing the microorganism.

Filtration

Filtration is one of the most commonly used methods for collecting bioaerosols because of low cost and simple structure (Hinds, 1999). Aerosol filtration has been widely applied in various applications such as respiratory protection, air purification, and clean rooms (Lin et al., 2003). High efficiency particulate air (HEPA) filter is defined as one having at least 99.97% filtration efficiency for 0.3 μm diameter particles, which is the most penetrating particle size MPPS (Hinds, 1999). Filtration efficiency is determined by several mechanisms such as interception, impaction, diffusion, gravity, and electrostatic force, depending on fiber density, diameter, filter thickness, and other factors (Hinds, 1999).

The filtration efficiency at the MPPS is mainly determined by three mechanisms (Hinds, 1999): (1) interception, where particles following an airstream flow line come within one radius of a fiber and adhere to it; (2) impaction, where larger particles are unable to follow the curving contours of airstreams around the fiber and are forced to strike on the fiber; and (3) diffusion, which is a result of the collision of small particles with gas molecules, which are thereby impeded in their path through the filter. Heating, ventilating, and air-conditioning (HVAC) systems with HEPA filters can effectively control and reduce airborne contaminants including bioaerosols based on the above mechanisms; however, reaerosolizations of virus collected inside an HVAC system in hospitals and residential buildings can be problems with this control strategy.

Surgical masks approved by the Food and Drug Administration (FDA) and filtering facepiece respirators (FFRs) certified by the National Institute for Occupational Safety and Health (NIOSH) are intended to be worn by healthcare persons and the general public during a pandemic event. Virus might be filtered by the fibers of a regular surgical mask through diffusion. Also, aggregated viruses might be captured by impaction and interception. However,

using surgical masks and N95 FFRs as countermeasures for bioaerosols has not been demonstrated to provide a complete response: (1) Although using surgical masks and N95 FFRs for tuberculosis has been shown to meet CDC guidelines, the same is not true for viral agents such as the swine flu virus. (2) There is no experimental basis upon which the FFR's life span in an H1N1 scenario can be estimated. (3) The stockpile of FFRs will be exhausted in the event of a severe pandemic. CDC estimates that more than 90 million FFRs will be required for healthcare workers in the US if a pandemic influenza event persists for 42 days (CDRF, 2006).

Decontamination Methods

One possible approach to resolve insufficient supplies of FFRs is to decontaminate the FFRs by using disinfection agents/processes such as microwave irradiation, UV irradiation, bleach solution, and peroxide and then reuse the decontaminated respirator. For this, no change of FFRs characteristics and no adverse health effect from the chemicals should occur. However, currently there exists no protocol for decontamination test for this purpose because of various limitations. First of all, there is no standard test method for simulating bioaerosol contamination of the FFRs. Secondly, the unique properties of bioaerosols generated by respiratory secretions may affect the effectiveness of the decontamination process, and the proper operating conditions to obtain controlled and consistent properties are not known. Thus, methods that can produce representative human respiratory secretions and device for a consistent and controlled delivery of aerosolized droplets containing viral agents need to be developed in order to properly evaluate techniques for decontamination.

Once a standard protocol for decontamination test is established, different methods can be fairly evaluated. There have been several inactivation methods that can be applied to decontaminate filters loaded with viral aerosol. (Fisher et al. 2009; Brion et al. 1999; Lee et al.

2009; Zhang et al. 2009), including microwave irradiation, UV irradiation, and antimicrobial chemicals.

Microwaves are electromagnetic waves with wavelengths between 1 m and 1 mm, or frequencies between 300 MHz and 300 GHz (Jones et al., 2002). Microwaves used in microwave ovens generally operate at a frequency of 2.45 GHz corresponding to a wavelength of 12 cm and energy of 1.02×10^{-5} eV. Microwave radiation is non-ionizing but is sufficient to cause polar molecules such as water to vibrate, thereby resulting in friction, which produces heat. The use of microwave irradiation for killing microorganisms through thermal and non-thermal effects has been demonstrated in various studies in liquid media (Pellerin, 1994; Kiel et al., 2002; Awuah et al., 2005; Campanha et al., 2007). However, no study for decontamination of virus in air has been done. Consequently, it is necessary to evaluate the performance of microwave irradiation against viral agent for air filtration system.

UV light has sufficient energy to be a practical anti-microbial method. UV irradiation is now a recognized method for inactivating a wide variety of biological agents and in particular airborne microorganisms (Prescott, 2006). Recent increases in the incidence of airborne diseases such as tuberculosis have focused attention upon the use of UV. With a wavelength of 254 nm, UV light strikes the biological cells and the energy is specifically absorbed by adjacent thymine nucleotide bases in deoxyribonucleic acid (DNA), causing them to form covalent bonds with each other rather than forming hydrogen bonds with adenine based in the complementary DNA strain (Perier et al., 1992). Phyrimidine dimers in thymine base distort the shape of DNA and change the double helix structure. Phyrimidine dimers make it impossible for the cell to accurately transcribe or replicate its genetic material which ultimately leads to the death of the cell (Kowaiski et al., 2007; Prescott, 2006). UV intensity, exposure time, lamp placement, air

movement patterns and the relative humidity of the air determine the effectiveness of UV. Most studies have focused on the UV intensity and exposure time to increase the decontamination efficacy (Chang et al., 1985; Rastogi et al., 2006; Duleba-Majek, 2009). None of them has considered the important parameters (e.g., relative humidity, nebulized media, and transmission mode) related to susceptibility of viral agent. Therefore, the investigation of the effects of these parameters on decontamination efficiency is important in determining the optimal conditions.

Incorporating antimicrobial agents such as aldehyde, phenolics, alcohols, halogens, heavy metals, and quaternary ammonium compounds into air filters are common methods to inactivate viruses. Among them, aldehydes such as formaldehyde and glutaraldehyde are highly reactive molecules which combine with protein and nucleic acids by cross-linking and alkylation. Recently, dialdehyde starch by glycol cleavage oxidation of starch through periodate reaction was shown to have antimicrobial effect with advantages such as low toxicity and low cost compared to glutaraldehyde (Hou et al. 2008; Para et al. 2004). Song (2008) demonstrated that dialdehyde polysaccharides including dialdehyde starch and dialdehyde cellulose synthesized by periodate oxidation act as biocides in aqueous suspension and by surface contact. However, its incorporation into air filtration media has not been explored. As a consequence, evaluation of the decontamination performance of dialdehyde cellulose filter against airborne viral agent to determine the feasibility of its use in a wide range of application is necessary.

Research Objectives

The ultimate goal of this doctoral research was to improve protection against viral aerosol through development assessment and comparison of novel decontamination technologies. The first objective was to develop a method for consistent and controlled delivery of droplets containing viral agents onto surface that would allow fair comparison of different contamination

technologies. The second and third objectives were to evaluate the performance of dialdehyde cellulose filter and dialdehyde starch filter against viral aerosol, respectively. The fourth objective was to evaluate microwave irradiation assisted filtration for capture and inactivation of viral aerosols for collective protection. The fifth objective was to investigate the effects of relative humidities and nebulized media on UV decontamination of viral aerosols and viral droplets loaded filter for individual protection. The sixth objective was to investigate the stability of MS2 virus by comparing infectious virus to total virus under different environmental conditions.

The comprehensive study about development and evaluation of inactivation technologies based on the characteristics of viral aerosol will lead to mitigation of the shortage problem of respirator stockpile and to provide novel means for inactivating airborne biological agents, subsequently to alleviate the threat of disease transmission by viral aerosol. If successfully accomplished, the knowledge learned and technologies developed can better protect the general public as well as healthcare facilities against viral agents.

CHAPTER 2
METHOD FOR CONTAMINATION OF FILTERING FACEPIECE RESPIRATORS BY DEPOSITION OF MS2 VIRAL AEROSOLS[*]

Background

The public's concern about bioterrorism (e.g., the 2001 anthrax attack) and spread of airborne pathogens (e.g., Severe Acute Respiratory Syndrome (SARS) and avian flu (H5N1)) through the aerosol route has increased greatly in recent years (Tellier, 2006). For example, in 2002 and 2003 SARS caused over 8000 illnesses and 700 deaths and there is still no adequate treatment (Yang et al., 2007). The recent swine flu outbreak due to a new strain of H1N1 influenza A has caused illness in over 70 countries and resulted in at least 6000 deaths worldwide as of October 2009 (ECDC, 2009). On June 11, 2009, the World Health Organization (WHO) raised the pandemic alert level to Phase 6, indicating the onset of a global pandemic (CDC, 2009).

One effective method for protection against airborne pathogens during pandemic spread through droplet and aerosol transmission is to wear a filtering facepiece respirator (FFR) certified by National Institute for Occupational Safety and Health (NIOSH). This approach considerably decreases the incidence and severity of infection. The Center for Disease Control and Prevention (CDC) has issued guidelines about the use of face masks and respirators to protect against H1N1 transmission in healthcare facilities (CDC, 2009). However, using medical masks and N95 FFRs as countermeasures for bioaerosols has not been demonstrated to provide a complete response: (1) Although using surgical masks and N95 FFRs for tuberculosis has been shown to meet CDC guidelines, the same is not true for viral agents such as the swine flu virus. (2) There is no experimental basis upon which the FFR's life span in an H1N1 scenario can be

[*] Reprinted with permission from Woo, M.-H., Hsu, Y.M, Wu, C.-Y, Heimbuch, B., Wander, J. (2010). Method for contamination of filtering facepiece respirators by deposition of MS2 viral aerosol. *Journal of Aerosol Science* 41, 9 44–952.

estimated. (3) The stockpile of FFRs will be exhausted in the event of a severe pandemic. CDC estimates that more than 90 million FFRs will be required for healthcare workers in the US if a pandemic influenza event persists for 42 days (CDRF, 2006).

One possible approach to resolve insufficient supplies of FFRs is to decontaminate the FFRs by applying disinfection agents/processes such as microwave irradiation, ultraviolet germicidal irradiation (UVGI), bleach solution, peroxides, etc, and then reusing the decontaminated respirator. To qualify a method to decontaminate an FFR for reuse, one must provide a statistically robust demonstration that the technologies applied do not alter the mechanical properties of the FFR, do not leave any toxic byproduct on the FFR, and achieve at least four-log virucidal efficacy on the materials of construction of the FFR. However, no protocol has been reported for such decontamination testing, a consequence of two main limitations. First, no standard test method has been reported for simulating bioaerosol contamination of the FFRs. Second, the unique properties of bioaerosols generated by respiratory secretions can be expected to affect the efficacy of the decontamination process, and the window of operating conditions affording controlled and consistent properties is not known. Therefore, development and validation of methods that are representative of human respiratory secretions is a necessary condition before one can realistically evaluate techniques for decontamination.

Influenza is commonly thought to be transmitted by three mechanisms (droplet, contact, and aerosol (droplet nuclei)) (CDRF, 2006). Some diseases (e.g., tuberculosis) are known to be mainly transmitted by the droplet nuclei route whereas droplet transmission is considered by many to be the dominant route for some other diseases (e.g., mumps), although the actual routes are still being debated (Fiegel et al., 2006; Yang et al., 2007; Tellier, 2006). Salgado et al. (2002) suggested different roles in influenza between droplet and aerosol transmission. Influenza is

mainly spread through droplet transmission by coughing and sneezing from infectious people while aerosol transmission is important for long-distance and sporadic infection. An infected human can be a source of large droplets generated by coughing and sneezing. During airborne transmission, these droplets will shrink in size with the consequence that both droplets and droplet nuclei contact surfaces. Although many researchers have examined the droplet size generated from humans, the actual size is not clear. Yang et al. (2007) reported that most droplets from coughing, sneezing, and talking have diameter between 1 and 20 μm and these droplets may contract depending on the humidity and medium generated. Viruses in these droplets can aggregate with each other or be encased by the saliva component, both enhancing persistence of viability. Meanwhile, viability of viruses in saliva can be attenuated by enzyme action (Dia & Marek, 2002). Therefore, it is important that the transmission medium be factored into the design of the test method.

The focus of this study was to develop a method for reproducibly applying fixed amounts of representative viral particles generated from droplets/aerosols onto FFRs for decontamination testing. This study had specific objectives: (1) to build a droplet/aerosol chamber system that generates droplets/aerosols containing viruses to emulate those from coughing and sneezing, (2) to deliver the droplets and resulting aerosol onto specimens of six commercially available FFRs, and (3) to demonstrate uniformity of deposition within a sample and across independent samples by achieving quarter-to-quarter (Q-T-Q) and sample-to-sample (S-T-S) coefficients of variations (CVs) of less than 20% and 40%, respectively. While the focus of this study was FFRs and a biosafety level (BSL)-I virus, the system was designed to be used with BSL-II microorganisms which require advanced containment. This fact limited the overall size of the unit due to the

requirement for secondary containment of the test system. The system also has utility outside of FFRs and could be used to load any surface (e.g., surgical scalpel or glove).

Materials and Methods

Virus and Nebulization Fluid Preparation

MS2 bacteriophage (MS2; ATCC®, 15597-B1™) was applied as the first challenging bioaerosol because it requires only a BSL-I facility. MS2 has a nonenveloped, icosahedral capsid with a nominal diameter of 27.5 nm (Prescott, Harley, & Klein, 2006; Valegard, Lijas, Fridborh, &Unge, 1990). MS2 infects only male *Escherichia coli* (*E. coli*) and is commonly used as a non-pathogenic surrogate for human pathogenic viruses (e.g., poliovirus, influenza A, and rhinovirus) because of its similarity in resistance to antimicrobial agents and ease of preparation and assay (Brion & Silverstein, 1999; Aranha–Creado & Brandwein, 1999; Fisher et al., 2009). Freeze-dried MS2 was suspended in deionized (DI) water to a titer of approximately $10^{10} – 10^{11}$ plaque-forming units (PFUs) per mL and stored at 4 °C.

Artificial saliva was used as the nebulization fluid to emulate droplets generated by coughing and sneezing. Saliva is a very dilute fluid composed of more than 97% water, plus electrolytes, proteins, and enzymes (Diaz & Marek, 2002). Varieties of inorganic ions maintain osmotic balance and offer buffering (Humphrey & Williamson, 2001; Diaz–Arnold & Mark, 2002; Dodds et al., 2005). The compounds and their corresponding amounts of artificial saliva are listed in Table 2-1 (Veerman et al., 1996; Wong & Sissions, 2001; Aps & Martens, 2005; Edward et al., 2004). Mucin from porcine stomach (Sigma–Aldrich, M1778) was chosen as the representative mucus stimulant (Vingerhoeds et al., 2005).

Test Material

Six different models of FFRs approved by NIOSH were employed in this study. Three of those models were also approved by the Food and Drug Administration (FDA) as surgical

devices. Each type of FFR has different characteristics, such as number of layers, hydrophilicity, and physical shape. Prior to FFR testing, 110-mm diameter discs of flat glass-fiber filter (Gelman Science, 61630) were used to determine workable operating conditions of virus concentration, flowrate, and loading time.

Droplet/Aerosol Loading System

A droplet/aerosol loading system was custom built for this study with the following requirements: (1) the width and height are less than 120 cm so that it can be placed in a biosafety cabinet; (2) parts can be easily disassembled for sterilization; (3) droplets/aerosols can be distributed uniformly onto substrates; (4) the droplet size distribution is consistent; (5) environmental conditions that can affect the droplet size, such as relative humidity (RH) and temperature, can be controlled. The schematic design of the loading system is shown in Figure 2-1. The system consists of a chamber body, an ultrasonic generator (241T, Sonaer® , Farmingdale, NY) for producing the droplets, a bubbler for generating moisture, compressed cylinder air for controlling RH and diluting virus concentrations, an RH meter for measuring humidity, a six-port manifold for distributing the aerosols, a thermometer for measuring temperature, and six supports to hold the flexible-form FFRs during loading (Baron et al., 2008; Feather & Chen, 2003; Fisher et al., 2009). This system can also include a charge neutralizer (Model 3012, TSI Inc., Shoreview, MN). The chamber body was fabricated from stainless steel sheet with welded seams to withstand the high temperature for sterilization. The turntable and six perforated sample plates were employed to increase uniformity of deposition. The particle size distributions (PSDs) were measured by an aerodynamic particle sizer (APS; Model 3321, TSI Inc., Shoreview, MN) through a port on the side of the chamber. Before building the droplet loading chamber, an experiment was conducted to verify the uniform deposition of aerosols using a small chamber, presented in Appendix A.

Chamber Operation and Determination of Operating Conditions

Before and after experiments, the chamber was decontaminated by wiping the interior of the chamber with isopropyl alcohol then allowing the chamber to set for 30 minutes. Six samples were placed onto the supports on the turntable using sterile forceps. Theoretically, a titer of around 10^7 PFU/mL in the ultrasonic nebulizer with 5-min loading time should provide sufficient loading density (>10^3 PFU/cm^2). The titer was prepared by adding 0.3 mL virus stock suspension into 30 mL artificial saliva. The droplets from the ultrasonic nebulizer after passing the distributor entered the chamber through six inlets. The size of droplets generated and loaded can be affected by the frequency of the ultrasonic generator and by environmental conditions such as RH and temperature. For this study, the frequency of the generator was 2.4 MHz and the environmental conditions were 20±2 ℃ and 35±5%. Low RH was chosen because the survivability of MS2 is high under this condition. After loading, the residual droplets were allowed to clear for 5 mins, and the FFR samples were taken out for extraction and assay.

Various operating parameters were evaluated to determine the conditions that would provide desired droplet characteristics, including loading time (1–30 mins), virus titer (10^7–10^8 PFU/mL), turntable speed (0–3 rpm), airflow rate (1–5 Lpm), and mucin concentration (0.3–0.9%). The loading density was controlled by adjusting the loading time and the titer of the virus suspension. To evaluate how viability of the virus is influenced by the ultrasonic process, bioaerosols produced at different times were collected by a Biosampler and their viability was compared. The turntable speed was varied to determine its relationship with uniformity. Flow rate and mucin loading were also varied to investigate their effects on the consistency of delivered droplets. Three runs were carried out for each set of conditions.

After loading with virus, each filter sample was cut into four equal quarters. Each quarter was immersed in 25 mL of extraction medium in a 50-mL conical tube. A 0.25 M glycine solution was applied to extract the MS2 from the quarter sample with agitation by a wrist-action shaker (Model 75, Burrell Scientific, Pittsburgh, Pa.) at a 10° angle for 15 mins to analyze the loading density (these conditions showed the best extraction efficiency in preliminary testing). The extracted solution was assayed by using the single-layer method (EPA, 1984) to determine the loading density according to Equation 2-1 with the assumption of 100% extraction efficiency:

$$LD = \frac{PFU}{10^{-n}} \times \frac{V_1}{V_2} \times \frac{4}{\pi d^2} \quad (2\text{-}1)$$

where LD is the loading density, V_1 is the volume of extraction solution, V_2 is the volume of sample, d is the diameter of the filter, and n is the number of dilutions (Lee et al., 2009).

A single layer bioassay was used to enumerate the infectious viruses with a host of *Escherichia coli* (*E. coli*; ATCC, 15597). The freeze-dried *E. coli* was suspended in 1X PBS, and isolated into a solidified hard agar plate (1.5% agar) with a sterilized loop, and then incubated at 37 ^{o}C overnight. The single colony from the plate was transferred to the tryptone soy broth (TSB) 271 for *E. coli* growth at 37 ^{o}C overnight. The MS2 media 271 (100 mL) was inoculated with 0.3 mL of the *E. coli* culture from TSB 271 and then incubated at 37 ^{o}C for 3 hrs. The TSB 271 and culture medium 271 were prepared following the American Type Culture Collection (ATCC) procedure for MS2 assay. One millimeter of MS2 sample and 3 hrs- incubated *E. coli* host were added to the sterile conical blue tube containing 9 mL of soft agar (0.5% agar) in a water bath between 40 ^{o}C and 50 ^{o}C. To get the countable range of 30-300 PFU/mL, the serially diluted MS2 samples were used. The mixture was shaken thoroughly and then poured into a petri dish. After the agar hardened, the plate was inverted and placed in an incubator at 37 ^{o}C

overnight. The plagues on the plate were enumerated and the titer of the sample was determined after multiplying the dilution factor to the plaque count. To visualize the particle loading, scanning electron microscopy (SEM, JEOL JSM-6330F, JEOL Inc.) of the filter before and after loading particles.

Statistical Analysis

The Q-T-Q and S-T-S CVs of loading density were obtained to evaluate the uniformity. R2 8.1 software (CRAN) and Microsoft Excel® were used to calculate one-way analysis of variance (ANOVA) and CV, respectively.

Results and Discussion

Determination of Operating Conditions

The impact of ultrasonic nebulization on viability of virus in the nebulizer reservoir was investigated by measuring the viable counts over time. The results present no significant difference in virus viability between 0 and 30 mins (p=0.10) (data not shown). Apparently, the heat shock from ultrasonic vibration did not cause damage to the MS2 in the reservoir during droplet generation. To determine the effect on virus of ultrasonication during droplet generation, viability of the viruses collected in the BioSampler after 5 and 10 mins of generation was examined. The theoretical concentration in the BioSampler after 5 mins of nebulization is 3×10^5 PFU/mL when the virus titer in the reservoir is 1.0×10^7 PFU/mL. The 5-min time-weighted (0–5 and 5–10 mins) average concentration of collected viruses in the BioSampler was around 3.2×10^5 PFU/mL, which is similar to the theoretical value. As demonstrated, the ultrasonic nebulizer can be used to produce droplets containing MS2 virus without adverse effects on viability.

Figure 2-2A displays the virus loading density as a function of loading time and Figure 2-2B shows the loading density as a function of the viral titer. As shown, the loading density had a linear relationship with time and with virus titer in the nebulization medium, as expected based on the initial viability tests. The results show that these two parameters can be adjusted to acquire a desired loading density. It should be noted that in determining the loading density the extracted fraction was assumed to be 1; however, different types of FFRs will have different values that depend on the material property and structure.

The uniformity tests were conducted with the turntable at various speeds because Marple & Rubow (1983) observed increased uniformity of CV from 4.3% to 1.5% when they rotated their aerosol chamber at 0.56 rpm. Figure 2-3 shows the CVs from three runs as a function of turntable speed. The variation of the CVs was somewhat larger than Marple & Rubow (1983) reported due to variability working with a viable system (MS2) vs. a non-viable system (PSL and dust).

The flow rate (2 Lpm) of this work is much lower than the rate (100 Lpm) used by Marple & Rubow (1983), and delivers a distribution of droplets that is sufficiently uniform (CV < 20%) even without the turntable, which appears to provide a moderate decrease in CV with increasing rotation rate. The difference among the six positions was not statistically significant ($p = 0.73$) for flat-sheet glass fiber filters. The reason for this uniformity is likely because settling is the dominant mechanism for large droplets in our system and a six-port distributor delivered the bioaerosols. A straight fog stream was observed through the front window during the loading. Therefore, the turntable speed was not an important parameter to meet the uniformity criteria when the flatsheet filter was employed. The deposition of the particles on FFRs after loading for

1 min was also confirmed by SEM. As shown in Figure 2-4, particles were randomly distributed on fiber surface without any specific pattern.

The criterion for minimum loading density—10^3 PFU/cm^2—was achieved for all conditions tested and could be easily increased if needed. Based on these results, the operating conditions to be discussed later were chosen to be 5-min loading time at a titer of 10^7 PFU/mL and 2 rpm turntable speed.

Droplet Size Distribution

Figure 2-5 shows the size distribution of droplets generated by the ultrasonic nebulizer at different flow rates. The size distributions of droplets generated at 1–3 Lpm were similar, with count median diameters (CMDs) and mass median diameters (MMDs) of 3.5 μm and 10 μm, respectively. The droplet size distributions at 4 and 5 Lpm were slightly shifted to a smaller diameter. Bimodal distribution was observed in the mass-based size distribution, with modes at 4–6 μm and over 20 μm. The theoretical CMD from the ultrasonic nebulizer can be determined from Equation 2-2 (Lang, 1962):

$$d_p \text{ (CMD)} = 0.73 \times \sqrt[3]{\frac{\sigma}{\rho f^2}} \tag{2-2}$$

where d_p is the nebulized droplet size, σ is the surface tension of the liquid, ρ is the density of the liquid, and f is the frequency of the nebulizer. As shown, the droplet size is independent of the flow rate. The gentle airflow within 1–3 Lpm just carries the aerosol away from the liquid surface. However, at a higher flow rate, the larger volume of dry dilution air promotes evaporation and therefore results in a smaller droplet size. To generate droplets of other sizes, the frequency can be adjusted. For example, droplets are expected to be 12.1 and 6.6 times larger, respectively, when lower frequencies of 60 kHz or 150 kHz are used instead of 2.4 MHz (Lang, 1962).

The mucin concentration also plays an important role in determining the initial droplet size because it affects surface tension and density of the artificial saliva used. Mucin at 0.3% was chosen for the artificial saliva in this study to match the protein content in human saliva. Increasing the mucin concentration threefold would reduce the median size to 40% of its original size because of the decrease in surface tension. In summary, the droplet size can be controlled by adjusting the composition of the spray medium, the frequency of the ultrasonic generator and the flow rate.

The droplet size decreases from the point of generation at the ultrasonic nebulizer all the way to the filter surface due to evaporation, and the size deposited depends on the environmental conditions (i.e., temperature and RH). The flowrates of the ultrasonic generator, dilution air, and temperature of the bubbler can be used to control RH, and heating tape (part (b) in Figure 2-1) can be used to adjust the temperature. Figure 2-6 displays the droplet size distribution generated and loaded at 2 Lpm through the aerosol generator plus 3 Lpm dry air to provide 35% RH. For this condition, the cylinder air without a bubbler was applied to achieve the low-RH condition. The MMDs for droplets generated and loaded were 9.2 and 3.2 μm, respectively, with corresponding CMDs of 3.4 and 1.8 μm , which are similar to the droplet size reported in the literature (Yang et al., 2007; Morawska et al., 2009) to have been generated by humans. The droplet's residence time is 0.13 s when settling is considered the main mechanism acting in this chamber. The droplet's theoretical life time at 35% RH is around 0.15 s, which means that droplets just reaching the FFR are almost completely evaporated. The size of a completely evaporated droplet can be calculated according to Equation 2-3:

$$d_p = d_d \times \sqrt[3]{F_v} \tag{2-3}$$

where d_p is the diameter of the aerosol particle and *Fv* is the volume fraction of solid material in the suspension in the nebulizer. For 0.3% mucin, the volume fraction is 6.00×10^{-2}, so d_p is calculated to be 1.9 μm when d_d is 9.2 μm. The reason the measured value is higher than the theoretical value is incomplete evaporation. After running the experiment, we noted that the filter surface was slightly damp, which is consistent with the above interpretation.

Loading onto NIOSH-certified FFRs

The CVs for uniform deposition of droplets/aerosols onto substrates for six different FFRs were calculated by analyzing the infectivity of viruses extracted from the loaded filter (Table 2-2). The flexible nature of the FFRs makes it difficult to achieve deposition on the same spot with the same shape each time. Therefore, a holding medium is necessary to achieve low CV values. Even for fixed-form FFRs, some inherently cannot produce equal quarters because the shape is not symmetric. Operational variation while cutting the sample (e.g., uneven quarters) can also contribute to larger CV values. Consequently, the CV for Q-T-Q was higher than that for S-T-S over all FFRs. It is possible to use circular areas punched from a FFR so that the difference in shape will not influence the results. However, this was outside the scope of the study, which aimed to evaluate decontamination effectiveness using the entire FFR. Nevertheless, the average CVs for both Q-T-Q and S-T-S for all FFRs were lower than the criteria—20% and 40%, respectively—demonstrating the system's ability to consistently load the test agents. Table 2-2 also displays the results of the loading densities. As shown, all sets had sufficient quantity to meet the threshold criteria.

Due to differences in surface properties, the loading density of different respirator models can be different even when the same operating conditions are applied. Figure 2- 7 shows the extraction efficiency of three different FFRs at various extraction times. Different layer structures and properties of the FFRs are responsible for the differences as discussed. The shape

of the FFR is another reason for differences in loading density. The loading density reported in Table 2-2 was calculated based on the FFR's projected area. The FFR having a duck-bill shape showed a lower loading density owing to its different curvature. As shown, both factors can affect loading density. Nevertheless, the loading density can be easily met in a controlled fashion using the specified conditions and can be conveniently increased by adjusting the loading time, virus titer, or both.

Summary

A simple system for producing, delivering, and loading of consistent challenges of droplets/aerosols containing virus onto FFRs has been developed and assessed. The respective CVs for S-T-S and Q-T-Q for the six NIOSH-certified FFRs tested were lower than 20% and 40%. The droplet size can be altered by tuning the frequency of the ultrasonic nebulizer, by changing the composition of the dispersion aerosolized, and by adjusting the temperature and RH inside the chamber. Droplets emulating bioaerosols released during coughing and sneezing can be produced using specific conditions and the loading density can be achieved by controlling the loading time and the virus titer in the nebulization medium. This system allows for development and validation of a standard method for loading bioaerosol challenges when different decontamination techniques are to be compared. It also has utility for loading surfaces to study fomite transmission and reaerosolization of particles from surfaces. It can be further applied to generate and load droplets and aerosols of different sizes and to load onto materials other than FFRs.

Table 2-1. Composition of artificial saliva (Based on 979 mL of DI water)

Chemical Species	Amount	Chemical Species	Amount
$MgCl_2 \cdot 7\ H_2O$	0.04 g	KSCN	0.19 g
$CaCl_2 \cdot H_2O$	0.13 g	$(NH_2)_2CO$	0.12 g
$NaHCO_3$	0.42 g	NaCl	0.88 g
0.2 M KH_2PO_4	7.70 mL	KCl	1.04 g
0.2 M K_2HPO_4	12.30 mL	Mucin	3.00 g
NH_4Cl	0.11 g	DMEM*	1mL

DMEM*: Dulbecco's modified Eagle's medium

Table 2-2. Loading density and CVs of Q-T-Q and S-T-S for 6 different FFRs (N = 3, Criteria of CV for Q-T-Q and S-T-S: 20% and 40% respectively)

Shape	Type	No	Loading density (PFU/cm^2)	CV for Q-T-Q (%)	CV for S-T-S (%)
Fixed	P††	1	$2.3\times10^3\pm0.3\times10^3$	12.07±2.74	9.05±2.22
	P	2	$2.9\times10^3\pm0.2\times10^3$	10.92±2.09	5.89±0.68
	S‡‡	3	$1.0\times10^3\pm0.1\times10^3$	15.41±6.89*	10.12±3.75*
	P	4	$2.6\times10^3\pm0.2\times10^3$	18.04±2.97	6.94±3.26
Flexible (duckbill)	S	5	$1.2\times10^3\pm0.1\times10^3$	13.70±1.59	9.17±3.86
	S	6	$1.8\times10^3\pm0.2\times10^3$	13.19±7.19	10.27±1.71

*N = 2, P††:Particulate respirator, S‡‡:Surgical respirator

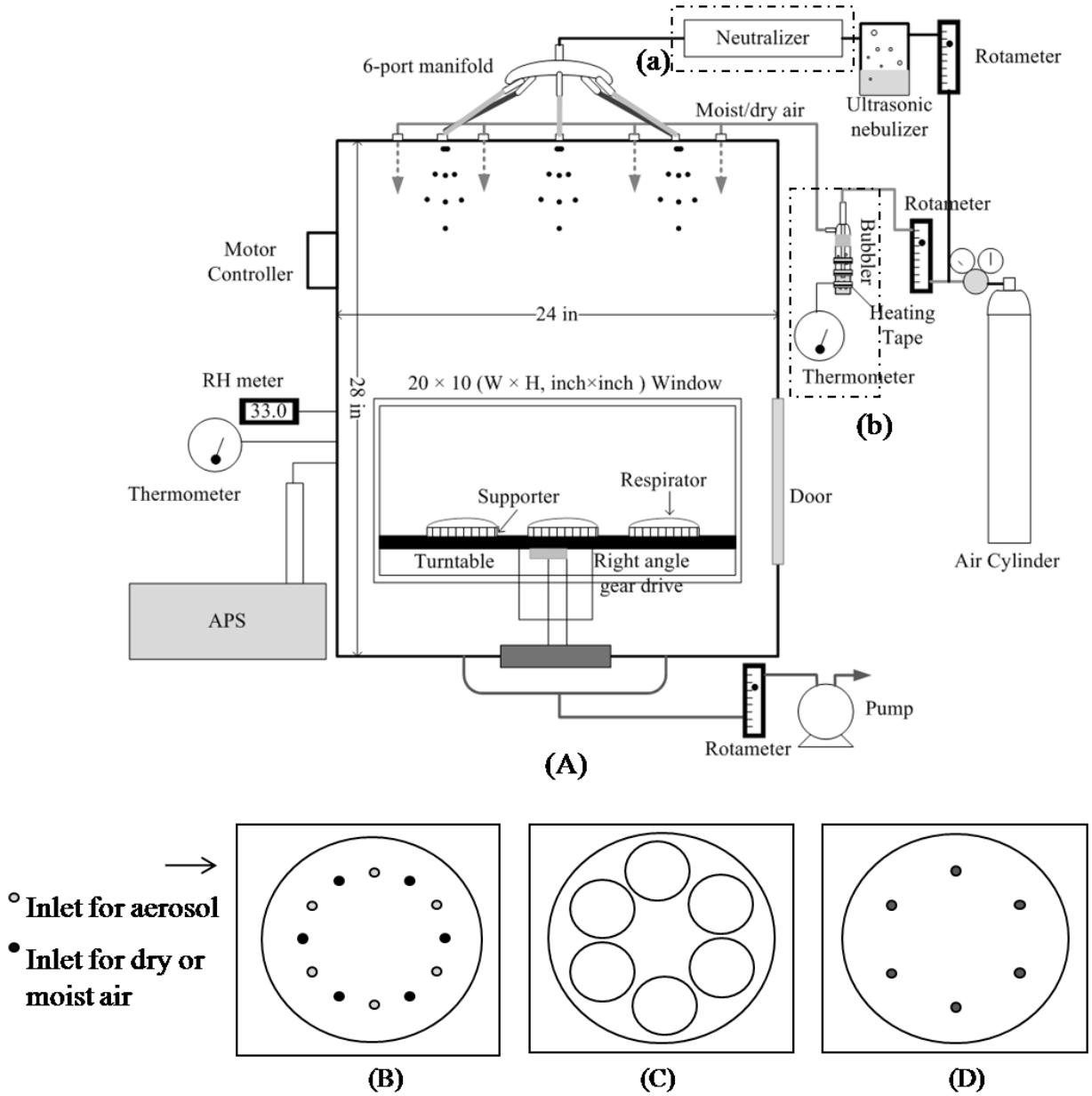

Figure 2-1. Schematic diagram of droplet loading system: A) entire system B) distributor on top C) turntable D) air outlet at bottom (a) and b) are needed only in certain conditions)

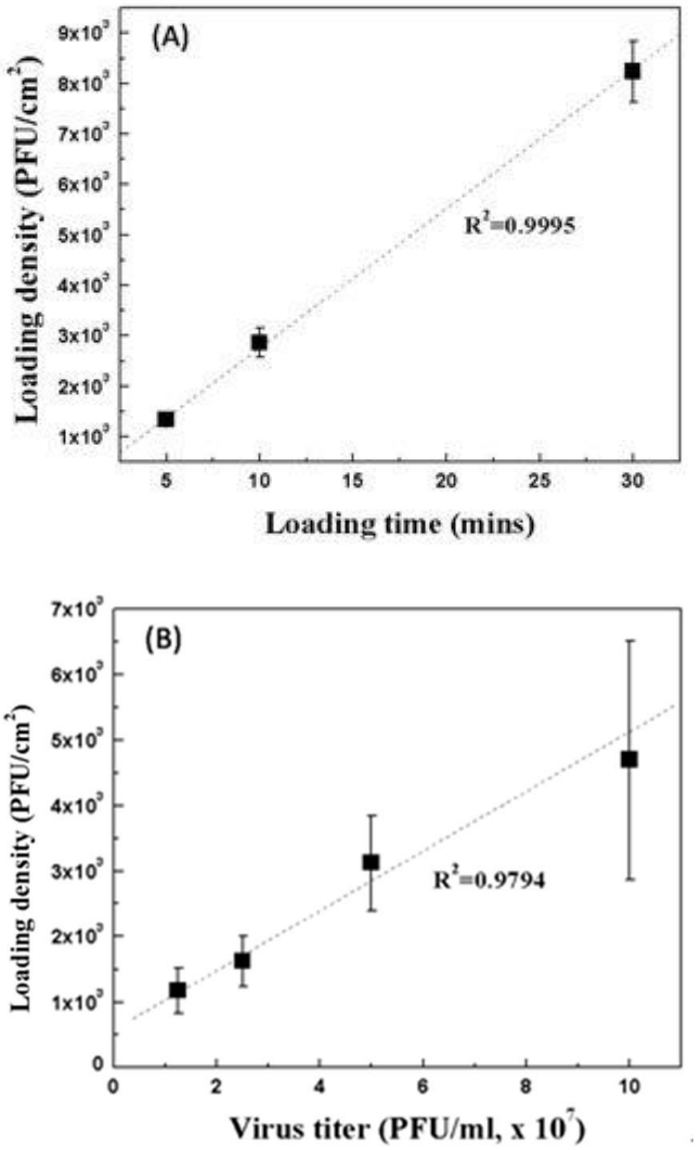

Figure 2-2. Loading density as a function: A) loading time and B) virus titer in the nebulizer

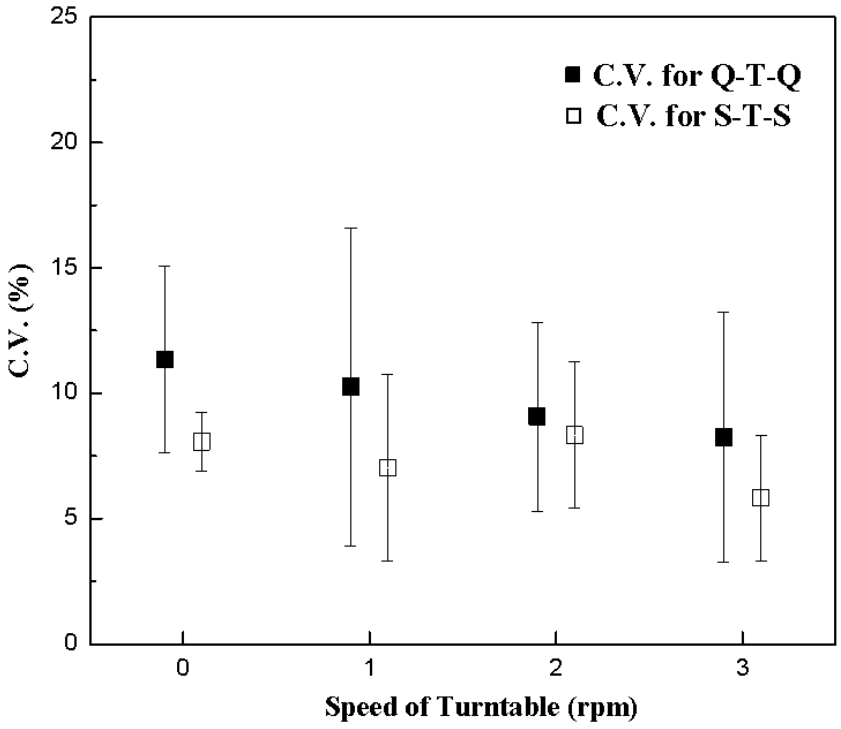

Figure 2-3. CVs for Q-T-Q and S-T-S as a function of turntable speed

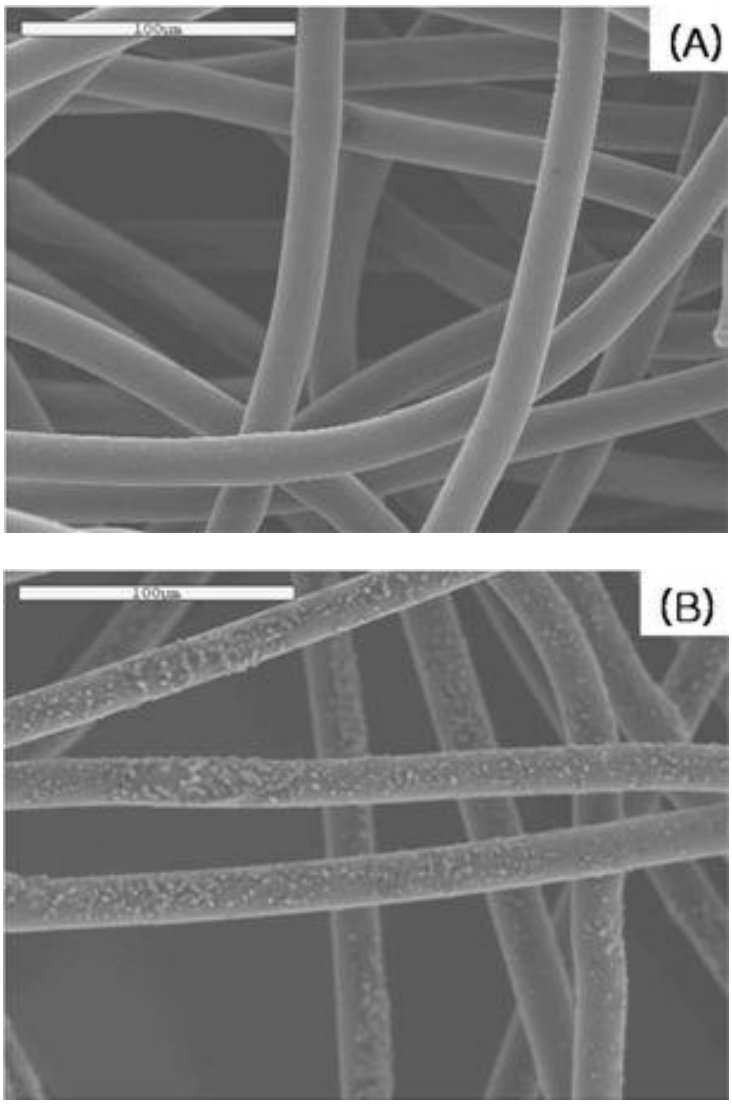

Figure 2-4. Scanning electron microscopy images: A) untreated FFR and B) treated FFR at 250x

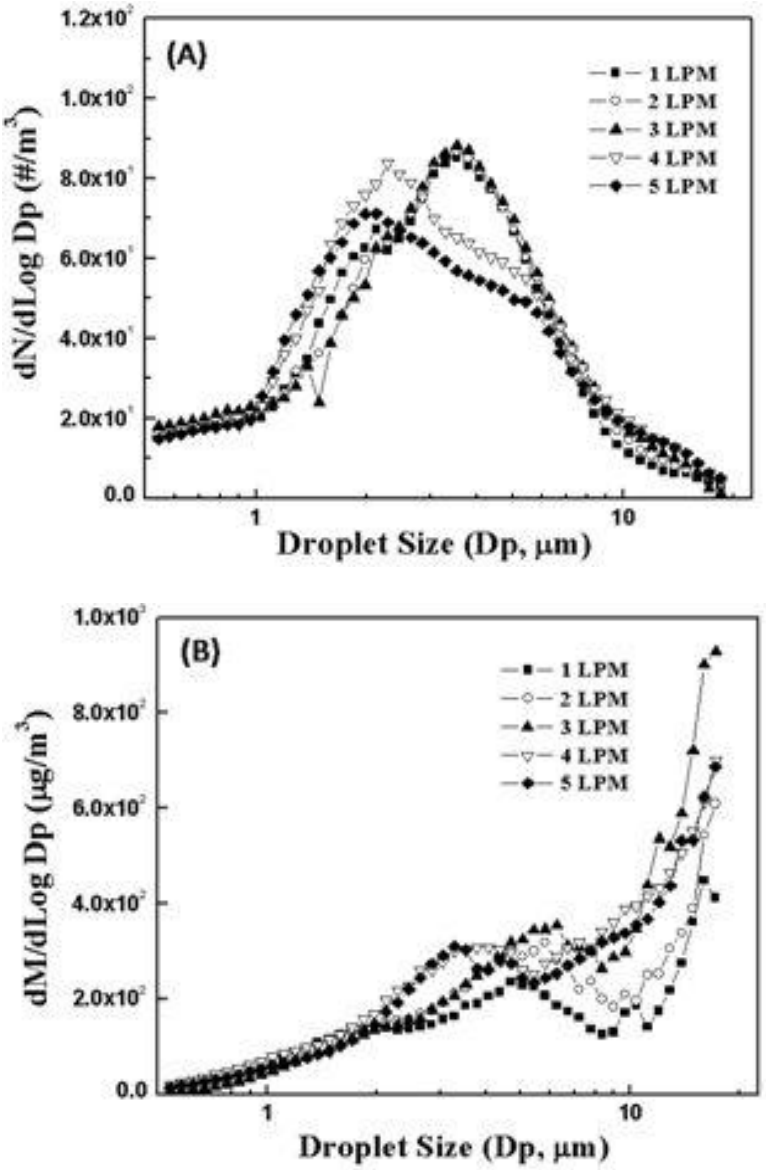

Figure 2-5. Size distribution of droplets generated by ultrasonic nebulizer at five flow rates: A) N umber- and B) mass-based

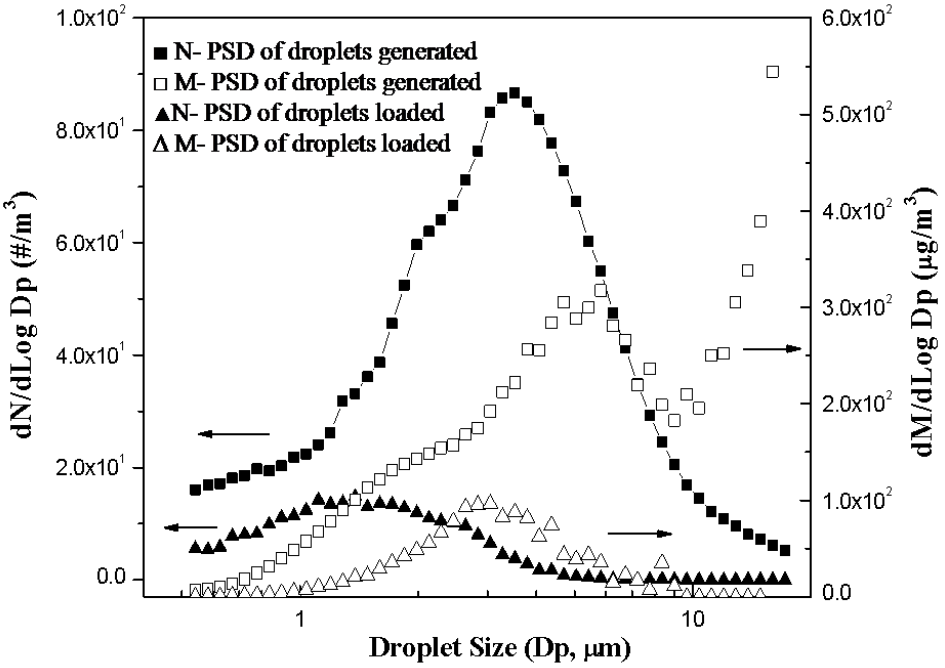

Figure 2-6. The number- and mass-based particle size distributions of generated droplets and loaded droplets at 2 Lpm through the aerosol generator plus 3 Lpm dry air and 2-rpm turntable speed

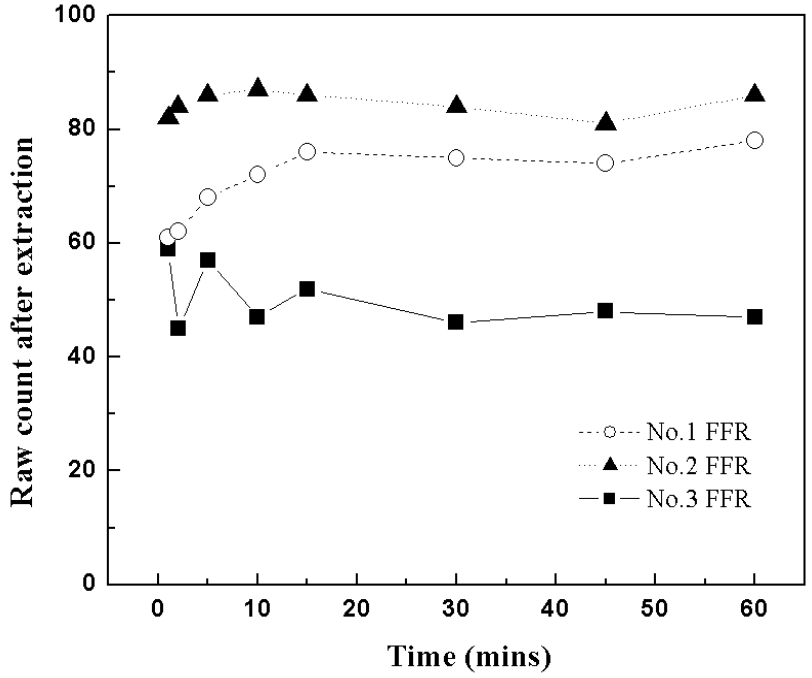

Figure 2-7. Recovery of viable MS2 as a function of extraction time for three FFRs

CHAPTER 3
EVALUATION OF THE PERFORMANCE OF DIALDEHYDE CELLULOSE FILTERS AGAINST AIRBORNE AND WATERBORNE BACTERIA AND VIRUSES[†]

Background

The increasing concern of bioterrorism (*e.g.* anthrax attack), the spread of waterborne pathogens (*e.g.* typhoid fever) and airborne pathogens (*e.g.* avian flu, Severe Acute Respiratory Syndromes, and swine flu) have raised the public's concern about the health effects of microorganisms and protection methods against them (Prescott, 2006; CDC, 2008). Filtration is one of the most commonly applied methods to remove airborne and waterborne microorganisms because of its low cost, simple structure, and high efficiency (Hinds, 1999). Air filtration has been widely applied as respiratory protection and air purification (Lin & Li, 2003), while water filtration has been applied for drinking water purification and waste water treatment (Metcalf, 2004). Although filtration is an efficient method to capture viable microorganisms as well as nonviable particles, it does not inhibit the survival of viable microorganisms collected on the filter, thus allowing the filter to be a fomite. The viable particles may grow on the filter and even reaserosolize from the filter through high air stream, causing adverse health effects. Therefore, inactivation treatment is necessary to decontaminate the loaded filters.

Several disinfection technologies, including irradiation, dry heat, and chemical treatment have been studied to decontaminate loaded filters. Ultraviolet (UV) irradiation is used for air and water sterilization because UV-C with wavelength of 254 nm breaks the molecular structure within deoxyribonucleic acid (DNA) or ribonucleic acid (RNA) and makes thymine dimmers; however, it has a limitation of low penetration due to short wavelength (Kujunnzic et al., 2006). Microwave irradiation is also applied for wet/dry disinfection with the thermal effect by water

[†] Reprinted with permission from Woo, M.-H., Lee, J. H., Rho, S. G., Ulmer, K., Welch, J., Wu, C.-Y., Song, L. & Baney, R. (2011) Evaluation of the performance of dialdehyde cellulose filter against airborne and waterborne bacteria and virus. *Industry & Engineering Chemistry Research.* 50, 11636-11643

vibration and non-thermal effects such as cell damage, membrane distortion, and change of enzyme activities (Wu & Mao, 2010). Recently, flash infrared radiation disinfection has been introduced as fomite disinfection (Damit et al., 2010). However, all irradiation based methods require an additional energy source and a facility for the treatment. Besides radiation based methods, dry heat and chemical treatment have also been used (Viscusi et al., 2009). High temperature can cause protein denature and chemical reaction can distort biomolecular functions. Viscusi et al. (2009) showed the decontamination effect of autoclave and 160 ^{o}C dry heat, 70% isopropyl alcohol, and soap water against MS2, but also reported the significant degradation of filtration efficiency after one-time decontamination treatment. Therefore, a decontamination technology without additional energy source and without causing filter degradation is necessary.

Without the above limitations, biocidal filters have been approached to take advantage of combined disinfection and mechanical filtration. Halogen compounds are effective antimicrobial agents that can be incorporated to filters because of their ability to damage the capsid protein (Ratnesar-Shumate et al., 2008). Ratnesar-Shumate et al. (2008) reported that iodine-quaternary ammonium-treated filter has biocidal effects against *Micrococcus luteus* and *E. coli*, and Lee at al. (2009) demonstrated that the iodine dislodged from the filter can inactivate MS2 for air filtration. Verdenelli et al. (2003) also demonstrated that chloride-treated filters (cis-1-(3-chloroallyl)-3,5,7-triaza-1-azoniaadamantane chloride and octadecylmethyltrimethoxysilylpropyl ammonium chloride) have higher filtration efficiency, lower microbial colonization, and longer lifetime against 10 different bacteria and 6 different fungi for air filtration. Miller (2009) reported that perlite covalently bonded by quaternary amine organosilane (3-trihydroxysilylpropyl-dimethyloctadecyl ammonium chloride) destroys pathogens (*E. coli*) by piercing the outer

membrane during water filtration. However, with these types of biocial filters there is a possibility of toxic chemical release chemicals to humans.

First reported in 1964, aldehydes such as glutaldehyde have also been used as antimicrobial agents against bacteria, spores, fungi, and viruses (Mcdonnell & Russell, 1999). Several studies demonstrated that aldehydes work through the following mechanisms: (1) strong interaction with outer cell layers in bacterial spores, (2) cross-linking in protein, transport inhibition, and strong association with outer layers in both gram negative and positive bacteria, (3) interaction with cell wall in fungi, and (4) inhibition of DNA and RNA synthesis in viruses (Power & Russell, 1990; Bruck, 1991; Favero, 1991). However, the small molecular aldehyde is also toxic. In contrast, larger aldehyde compounds are less toxic. Recently, dialdehyde starch by glycol cleavage oxidation of starch through periodate reaction has been shown to have antimicrobial effect, low toxicity and low cost compared to glutarldehyde (Hou et al., 2008; Para et al., 2004). Song (2008) demonstrated that dialdehyde polysaccharides including dialdehyde starch and dialdehyde cellulose synthesized by periodate oxidation act as biocides in aqueous suspension and by solid contact. However, its incorporation into air and water filtration media has not been explored.

The objective of this study was to investigate the filtration efficiency of the dialdehyde cellulose filter synthesized by one step periodate oxidation. The inactivation performance of this filter against airborne and waterborne bacteria and viruses under different environmental conditions was evaluated. For water filtration, the viable removal efficiency and the relative survival fraction of untreated and treated filters of different treatment times were investigated by testing with both *E. coli* and MS2 bacteriophage. For air filtration, the physical removal

efficiency, viable removal efficiency, and relative survival fraction of filters under different relative humidities (RHs) were investigated.

Materials and Methods

Test Filters

The dialdehyde cellulose (DAC) filters were prepared by periodate oxidation of cellulose filters (No. 50, Whatman, Φ=55 mm) with different treatment times (*i.e.*, 4, 8, and 12 hrs) (Song, Cruz, Farrah, & Baney, 2009). The cellulose filters were immersed into 100 mL of deionized (DI) water containing 0.2 M sodium periodate ($NaIO_4$, Fisher Chemical) with pH of 3-4. The reaction was performed in a shaker at 200 rpm of speed in the dark at 37 ℃ for the varying treatment times. Subsequently, the filter was rinsed five times with DI water. The filter was then immersed in the same volume of DI water in a shaker at room temperature (RT) overnight. This filter was again washed several times to remove excess periodate. After rinsing out the residual periodate, the DAC filter was dried in a hood at RT for 24 hrs. As a control, an untreated cellulose filter was used. To ensure no residual periodate, the treated filter was tested with 2 mL of 0.5% (w/v) sodium metabisulfite aqueous solution and 1 mL of 0.1 N silver nitrate to observe if there was any color change resulting from the residue. To determine the change of chemical structure after treatment, Fourier Transform-InfraRed (FT-IR; Nicolet Magma 560) spectroscopy in the wave number range of 4000-500 cm^{-1} was used.

Test Bacteria and Bacteriophages

E. coli (ATCC® 15597) and MS2 (ATCC® 15597-B1™) were used as the challenging agents for water and air filtration. *E. coli*, a gram-negative rod-shaped bacterium with an aerodynamic diameter 0.7-0.9 μm, is commonly used as a representative of vegetative cell. Freeze-dried *E. coli* was suspended with 1% tryptone soy broth (TSB, BD 211705) to a titer of 10^{11}-10^{12} colony forming units (CFUs)/mL. *E. coli* stock was prepared by inoculating the *E .coli*

onto a nutrient agar (Becton, Dickinson and Company) plate and then transferring the inoculate to a slant. This slant was incubated for 24 hrs, and *E. coli* suspension extracted from the slant through vortexing with 1X phosphate buffer saline (PBS) was used as the bacteria stock.[10] The final titer of *E. coli* was around 10^8-10^9 CFU/mL after serial dilution.

MS2 is a single-strand RNA, unenveloped, and icosahedra-shaped virus with a single size diameter of 27.5 nm. Because of similar physical characteristics, MS2 has been used as a surrogate for human pathogenic RNA viruses such as poliovirus and rotavirus (Prescott et al., 2006; Woo et al. 2010). Freeze-dried MS2 was suspended with 1% TSB to a titer of 10^{11}–10^{12} plaque forming units (PFUs)/mL as the virus stock suspension and stored at 4 °C. The stock was serially diluted to 10^8-10^9 PFU/mL by sterile DI water before being used for the experiment.

Water Filtration

The water filtration system was comprised of a vacuum-based filter (Model XX1104700, Sterifil® Aseptic System, Millipore Co.) loaded with either an untreated cellulose or a treated DAC filter, as shown in Figure 3-1. Ten mL of bacterial or virus suspension with a titer of 10^8-10^9 CFU (or PFU)/mL were dripped through the filter at 0.5 Lpm under vacuum for 1 min (Herrera et al., 2004). To demonstrate the applicability for real-life scenario, Suwannee river water sample prefiltered through a 0.45 μm filter was also used. The filtered suspensions were assayed to investigate their viable titers using suitable dilution to an adequate count (*i.e.*, 30–300 CFU or PFU) by the single-layer method (EPA, 1984). For enumeration of bacteria and virus, 9 mL of agar medium 271 was prepared in a 15 mL conical tube (Falcon, Becton, Dickinson and Company) and placed in a water bath at 50 ^{o}C (Fisher et al., 2009). For *E. coli*, 1 mL of diluted *E. coli* suspension was added to the tube. For MS2, 1 mL of diluted MS2 suspension and 1 mL of log phase *E. coli* prepared in medium 271 were added to the tube (Fisher et al., 2009). The agar

containing *E. coli* or MS2 was mixed by swirling and then the mixture was poured into the Petri dish. The agar solidified at room temperature and then the dish was put into the incubator at 37 ^{o}C for 24 hrs before counting. Scanning electron microscopy (SEM, JEOL JSM-6330F, JEOL Inc.) and dynamic light scattering (DLS, Nanotrac NPA252, Microtrac Inc.) combined with Zetasizer (Malvern Instruments) were used to confirm the aggregation of the viruses.

Air Filtration

The experimental set-up for air filtration is displayed in Figure 3-2 with two compartments for viable removal efficiency and physical removal efficiency measurements. Compressed air was passed through two rotameters. One allowed 7 Lpm of dry air to pass though a six-jet Collison nebulizer (Model CN25, BGI Inc.) to aerosolize a bacterial suspension with a titer of 10^{7}–10^{8} CFU/mL, and the other allowed the air to go through a humidifier. The two flows joined and passed through a 2.3-L glass mixing chamber, and then proceeded towards the filtration unit at 3 Lpm, corresponding to a face velocity of 5.3 cm/s, which is a standard value used in military filtration testing (US Army, 1999). Based on this velocity, the residence time through the mixing chamber was 0.21 s, which was sufficient for microbes to come into equilibrium with the relative humidity. One of the two units was operated without a filter as a control and the other was equipped with the experimental variable, a circular filter with a diameter of 35 mm. The pressure drop across the filter, ΔP, was measured using a Magnehelic gauge connected between upstream and downstream of the test filter. The bacterial aerosols that penetrated the filter were collected in BioSamplers (SKC Corp.) containing 15 mL of 1X PBS at 5.5 Lpm for 5 mins and then 1mL of sample was assayed after serial dilution to get the countable range between 30-300 CFU/mL as mentioned before. Experiments were conducted at RT (23±2 °C) and two relative humidities (RHs): low RH (30±5%, LRH) and high RH (90±5%, HRH). For the virus, the same conditions

were employed, except for changes to DI water in lieu of 1X PBS as the collection medium and PFU instead of CFU. Physical removal efficiency was obtained by using the Aerodynamic Particle Sizer (APS; Model 3321, TSI Inc.) and Scanning Mobility Particle Sizer (SMPS; Model 3936, TSI Inc.) for *E. coli* and MS2 aerosol, respectively (in Figures 3-2B and 3-2C).

Removal Efficiency, Relative Survival Fraction and Statistical Analysis

Removal efficiency of the test filters for water filtration can be expressed as viable removal efficiency. For air filtration, both physical removal efficiency and viable removal efficiency were considered. Removal efficiency was calculated according to Equation 3-1:

$$\text{Removal efficiency (\%)} = \left(1 - \frac{N_E}{N_C}\right) \times 100 \tag{3-1}$$

where N_C is the concentration for the control part and N_E is the concentration for the experiment part. The viable removal efficiency was obtained by comparing the microbial concentrations of original suspension (*Nc*) and filtered one (N_E) for water filtration and the concentrations of control (*Nc*) and experimental BioSampler (N_E) for air filtration. For physical removal efficiency, *Nc* was the number of particles entering the test filter and N_E was the number of particles exiting the test filter obtained by APS or SMPS. The filter quality factor, a useful criterion for comparing filters, based on the physical removal efficiency of the test filters at 5.3 cm/s face velocity was calculated according to Equation 3-2

$$\textit{Quality factor} = \frac{-\ln p}{\Delta P} \tag{3-2}$$

where p is the particle penetration.

After the removal efficiency experiments, the test filters were taken off from the filter holder in the experimental system and subjected to a wrist action shaker (Model 75, Burrell Scientific) to investigate the viability of microbes collected on the filter. The filter was placed in

25 mL of autoclaved DI water in a 50 mL conical tube and shaken for 15 mins. The survival fraction (SF), defined as the ratio of the microbe in the extraction solution to the total microbe count collected on the filter, was used to compare the results of the treated DAC filter with the untreated filter. Herein, the total microbes collected on the filter for air filtration tests were determined by the BioSampler count of the control subtracted by the BioSample count of the experimental flow. Because the collection efficiency of Biosampler is dependent on air flow rate and particle size, relative survival fraction (RS) was introduced by comparing survival fractions of both filters to remove the effects of air flow rate and particle size:

$$\text{Relative survival fraction (RS)} = \frac{SF_{treated\ filter}}{SF_{untreated\ filter}} \tag{3-3}$$

Statistical analysis was carried out using analysis of variance (ANOVA) and student's t-test on a completely randomized design with three or more replications with Design-Expert® 8.0 software.

Results

Water Filtration

The experimental results, including viable removal efficiency and relative survival fraction, are summarized as averages of 5 trials and 3 trials, respectively, for each test filter in Table 3-1. For pure cultures (e.g., DI water and 1X PBS), there was no significant difference in viable removal efficiency among the four tests for *E. coli* although higher removal efficiency was expected because of increase of hydrophobicity after periodate reaction (Varavinit et al., 2001). However, the increased treatment time resulted in significantly lower relative survival fraction (p=0.03) for *E. coli*. For MS2, viable removal efficiency increased and relative survival fraction decreased significantly (p=0.005 and p=0.01) as treatment time increased. Compared with *E. coli*, the slightly lower viable removal efficiency and higher relative survival fraction indicate the

higher resistance of MS2 compared to *E. coli*. For real water samples (i.e., the Suwannee river), the tendency was similar to those for pure cultures, indicating the material's practicality under real conditions such as emergency response or drinking water purification. In general, infectious bacteria and virus concentrations on the filter decreased as treatment time for the DAC filter increased, indicating the inactivation effect of the DAC filter through direct contact.

Air Filtration

The particle size distribution of *E. coli* and MS2 aerosols upstream of the test filters had a mode at approximately 0.8 μm and 28 nm respectively at LRH/RT, as shown in Figure 3-3. The pressure drops across the untreated filter and three DAC filters (4-, 8-, and 12-hr treated filters) are listed in Table 3-2. Since the pressure drop of the test filter at 3 Lpm was out of the measurable range of the Magnehelic gauge, the expected pressure drop of the filter was calculated by using the pressure drag (S_{drag}, filter's aerodynamic resistance to air flow) as shown in Equation 3-4 after measuring the pressure drop of the filter at 1 Lpm.

$$S_{drag} = \frac{\Delta P}{V_f} \tag{3-4}$$

where ΔV_f is the face velocity. As shown in Table 3-2, the pressure drop of the treated filter was lower than that of the untreated filter. The effect of RH on the pressure drop was negligible (data not shown). During the filtration experiment, variation in the pressure drop of the test filters was negligible. Regarding the physical removal efficiency, the 12-hr treated DAC filter presented the lowest value among the test filters as a function of particle size, and the most penetrating particle size shifted to smaller size (~110 nm for untreated filter vs. 30 nm for 12-hr treated filter) as shown in Figure 3-4. The quality factor is also presented in Table 3-2. As shown, increasing the treatment time for the DAC filter increased the quality factor for the virus, but led to a decreased quality factor for the bacteria.

The removal efficiencies, relative survival fractions, and quality factors based on viable removal efficiencies of the untreated filter and the 12-hr treated DAC filter under various environmental conditions are displayed in Table 3-3. For *E. coli*, RH was not an important parameter for the untreated filter in that the differences of the viable removal efficiency (p=0.17), relative survival fraction (p=0.14), and quality factor (p=0.18) results under two different RH conditions were within experimental error. On the other hand, at HRH, the 12-hr treated DAC filter presented increased viable removal efficiencies (p=0.002) compared to the results at LRH (p=0.08). The possible reason is that moisture in HRH might react with conjugated aldehyde in treated DAC filter to make carboxylic acid which can react with amine structure of RNA (Song, 2008). The relative survival fraction of the 12-hr treated filter (p<0.001) was significantly lower than that of the untreated filter at HRH whereas the difference was negligible at LRH (p=0.12), indicating the antimicrobial effect of the DAC filter under moist conditions on the *E. coli* collected on the treated filter. Inhibiting survival and growth of microorganisms collected on the filter is critical in preventing reaerosolization of collected microbes from the filter. For MS2, increasing RH resulted in an increased viable removal efficiency for both the untreated and the 12-hr treated DAC filter (p=0.004 and p<0.001).

Discussion

Water Filtration

Difference in the viable removal efficiencies of *E. coli* and MS2 was expected because their singlet sizes are very different. Contrary to that expectation, the difference was not significant even though *E. coli* has a much larger singlet diameter than MS2. One possible reason for this phenomenon is the increased size by aggregation and/or encasement of the virus in the feed solution. The aggregation made the virus behave more like a larger particle, which in turn narrowed the difference between the bacteria and virus test results. The aggregation was

confirmed by SEM and DLS, as shown in Figure 3-5. In studies related to aggregation of viruses in water, Floyd & Sharp (1977) found that poliovirus, having a similar physical property to MS2, existed in the aggregation state in DI water. Riemenschneider et al. (2010) also showed MS2 aggregation in DI water at high concentrations.

As displayed previously, the pressure drop of the filter decreased as treatment time increased, which indicates increases in porosity and also possible changes in mechanical filtration efficiencies. Extraction efficiency was originally expected to be small due to the high retention capability of the resin filter reported in Lee et al. (2009) In contrast, the SEM images (Figure 3-6) of *E. coli* loaded on the 12-hr treated DAC filter before and after agitation treatment show that most microbes collected on the filter were extracted successfully after wrist action shaking. The possible reason for the difference is dissimilar filter materials (cellulose filter vs. quaternary ammonium-resin).

Air Filtration

The shift of the most penetrating particle size along with lower pressure drop of the treated filter than that of an untreated filter suggests possible morphology change of the filter media by treatment. This suggestion is supported by the FT-IR spectra of 12-hr treated DAC filter using untreated cellulosed filter as background as shown in Figure 3-7. Three characteristic bands of DAC appeared around 1730, 960, and 880 cm^{-1}. The sharp peak at 1730 cm^{-1} is a characteristic band of carbonyl groups and the broad bands at 960 and 880 cm^{-1} are assigned to the hemiacetal and hydrated form of the DAC filter, indicating increasing oxidation levels. In addition, a weak absorbance at around 1690 cm^{-1} corresponds to the conjugate aldehyde stretching, representing degradation of cellulose (Kim, & Kuga, 2004). In general, these increased bands represented increased oxidation level. The oxidation degree by comparison of the absorbance of two bands, C=O stretching and CH_2 stretching, was 50% for the 12-hr treated filter (Bruck, 1991). Figure 3-

8 displays the SEM images of the filters before and after treatment. As seen, increased pore size was apparently confirmed.

Although the removal efficiency of the treated filter was lower due to increased pore size distribution, the pressure drop was also lower. For fair comparison, the viable removal efficiency was calculated for a thicker 12-hr treated filter with the same pressure drop as the untreated filter using the quality factor relationship (Equation 3-2). The corresponding viable removal efficiencies of 12-hr treated filter at LRH for *E. coli* and MS2 are 97.56 % and 94.77 %, respectively. As shown, they outperform the untreated filter even at LRH (Table 3-3).

The difference between physical removal efficiency and viable removal efficiency of the untreated filters might be attributed to the different principles of measurements and intrinsic properties of the microorganisms. APS and SMPS were applied to count particles physically for physical removal efficiency, whereas the single-layer method was used to determine the concentration of only viable bacteria and viruses in the entire range for viable removal efficiency. Aggregated viruses counted as a single particle by the SMPS can be assayed as several single viruses after dispersion in the collection medium, and empty droplet counted by SMPS does not register any count by the bioassay. Since environmental conditions (*e.g.* RH) affect the virus viability, the concentration of viable agents for viable removal efficiency also changes as RH varies. All these contribute to a difference between viable removal efficiency and physical removal efficiency.

As mentioned, the relative survival fraction is an important parameter in evaluating the reliability of the filter as an antimicrobial filter for air filtration and determining the mechanism. The relative survival fraction was used to fairly compare the effect of RHs on inactivation. Accordingly, 1.03 and 0.43 for *E. coli* and 0.96 and 0.38 for MS2 were obtained at LRH and

HRH, respectively. The fact that these ratios decrease as relative humidity increased for both microorganisms (p <0.001 for *E. coli* and p=0.001 for MS2) suggests sufficient water contents are important to the biocidal effect of DAC.

The relative survival fractions of other biocidal filters are listed in Table 3-4. Rengasamy et al. (2010) reported that four different biocidal filters (i.e., silver copper, envizO$_3$, iodine, and TiO_2 treated filters) showed 0.25-0.79 and 0.001-0.08 of relative survival fractions at LRH and HRH, respectively. However, it should be cautioned to make any direct comparison with the DAC filter because of different incubation times and conditions. Lee et al. (2009) used similar test conditions to the current study for an iodine treated filter and reported a relative survival fraction of 0.63. The iodine treated filter exhibited insignificant difference among different RH conditions unlike the DAC treated filter. Another category of inactivation technology is the energetic method. Heimbuch et al. (2010) reported the relative survival fractions by energetic methods of microwave generated steam, UV, and moist heat to be less than 10^{-5} for H1N1 virus. Although the inactivation performance of the DAC treated filter was lower than those energetic methods, it requires no additional energy source as mentioned earlier.

Summary

The retail cost of 50 cellulose filters is around $60. The only chemical required for the filter treatment is sodium periodate, which costs less than $2 for treating 50 filters through the soaking method. This 3% additional treatment cost to the original media yields a product with a higher removal efficiency, lower pressure drop, and better disinfection capability. These are all important attributes of an effective biological filtration medium for practical applications such as respiratory protection, ventilation, and water purification system.

Table 3-1. Viable removal efficiency and relative survival fraction of untreated filter and three DAC filters treated under different treatment times in water filtration.

Test medium	Test filter	Test microbe	Viable removal efficiency (%)*	Relative survival fraction †
1X PBS	Untreated	*E. coli*	89.92±6.14	1.00±0.24
	4-hr treated		88.24±5.72	0.44±0.05
	8-hr treated		90.51±6.68	0.29±0.02
	12-hr treated		92.34±5.04	0.15±0.01
Suwannee River	Untreated	*E. coli*	91.55±1.04	1.00±0.24
	12-hr treated		92.87±1.27	0.15±0.10
DI water	Untreated	MS2	81.27±2.03	1.00±0.07
	4-hr treated		83.64±3.36	0.63±0.19
	8-hr treated		86.90±2.00	0.32±0.07
	12-hr treated		88.63±1.12	0.28±0.02
Suwannee River	Untreated	MS2	84.46±1.23	1.00±0.07
	12-hr treated		88.95±1.27	0.28±0.18

Average for *5 trials and † 3 trials

Table 3-2. Pressure drop and quality factor based on physical removal efficiency for four filters at HRH

Test filter	Pressure drop at 5.3 cm/s (Pa)	Quality factor (kPa^{-1})	
		MS2	*E. coli*
Untreated	3936	0.54	3.5
4-hr treated	3116	0.68	NM*
8-hr treated	2952	0.72	NM
12-hr treated	1619	0.98	1.56

*Not Measured

Table 3-3. Removal efficiency, relative survival fraction, and quality factor based on viable removal efficiency of untreated filter and 12-hr treated DAC filter at two relative humidities in air filtration system

Test microbe	Relative humidity	Test filter	Physical removal efficiency (%)	Viable removal efficiency* (%)	Relative survival fraction†	Quality factor*, # (kPa^{-1})
E. coli	LRH	Untreated	99.9999±0.0001	82.1±2.6	1.00±0.33	0.44±0.04
		12-hr treated	92.0663±2.4392	78.3±4.9	1.03±0.34	0.94±0.16
	HRH	Untreated	99.9999±0.0000	79.8±1.7	1.00±0.42	0.41±0.02
		12-hr treated	99.7137±0.1172	89.2±3.7	0.43±0.05	1.37±0.26
MS2	LRH	Untreated	92.3401	72.1±5.3	1.00±0.06	0.32±0.05
		12-hr treated	78.5355	70.3±2.4	0.96±0.10	0.78±0.02
	HRH	Untreated	83.1872	88.1±3.3	1.00±0.02	0.54±0.08
		12-hr treated	80.8232	93.3±6.7	0.38±0.12	1.59±0.40

Table 3-4. Comparison of other disinfection technology

Target microbe	Disinfection technology	Condition	Relative survival fraction
MS2[*]	Biocidal filter	Silver-copper	30 min loading/ 22 ^{o}C/ 30% RH/ 2 hrs	0.63
		EnvizO_3-sheied		0.79
		Iodinated resin		0.63
		TiO_2		0.25
		Silver-copper	30 min loading/ 37 ^{o}C/ 80% RH/ 4 hrs	0.04
		EnvizO_3-sheied		0.08
		Iodinated resin		0.001
MS2[†]	Biocidal filter	Iodinated resin	30 mins/ In-flight test/HRH	0.63
H1N1[#]	Energetic method	Microwave-generated steam	1250 W/ 2 mins	1.3×10^{-5}
		Ultra violet germicidal	1.6-2.0 mW/cm^2/ 15 mins	5.0×10^{-6}
		Warm moist heat	65 ^{o}C/ 85% RH	1.0×10^{-5}

[*]Rengasamy et al. 2010 [†]Lee et al. 2009 [#]Heimbuch et al. 2010

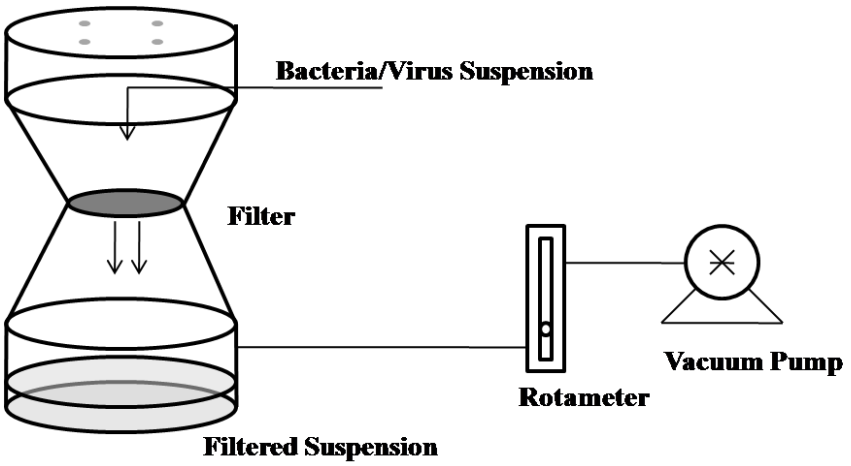

Figure 3-1. Experimental set-up for the removal efficiency of the test filter in water filtration

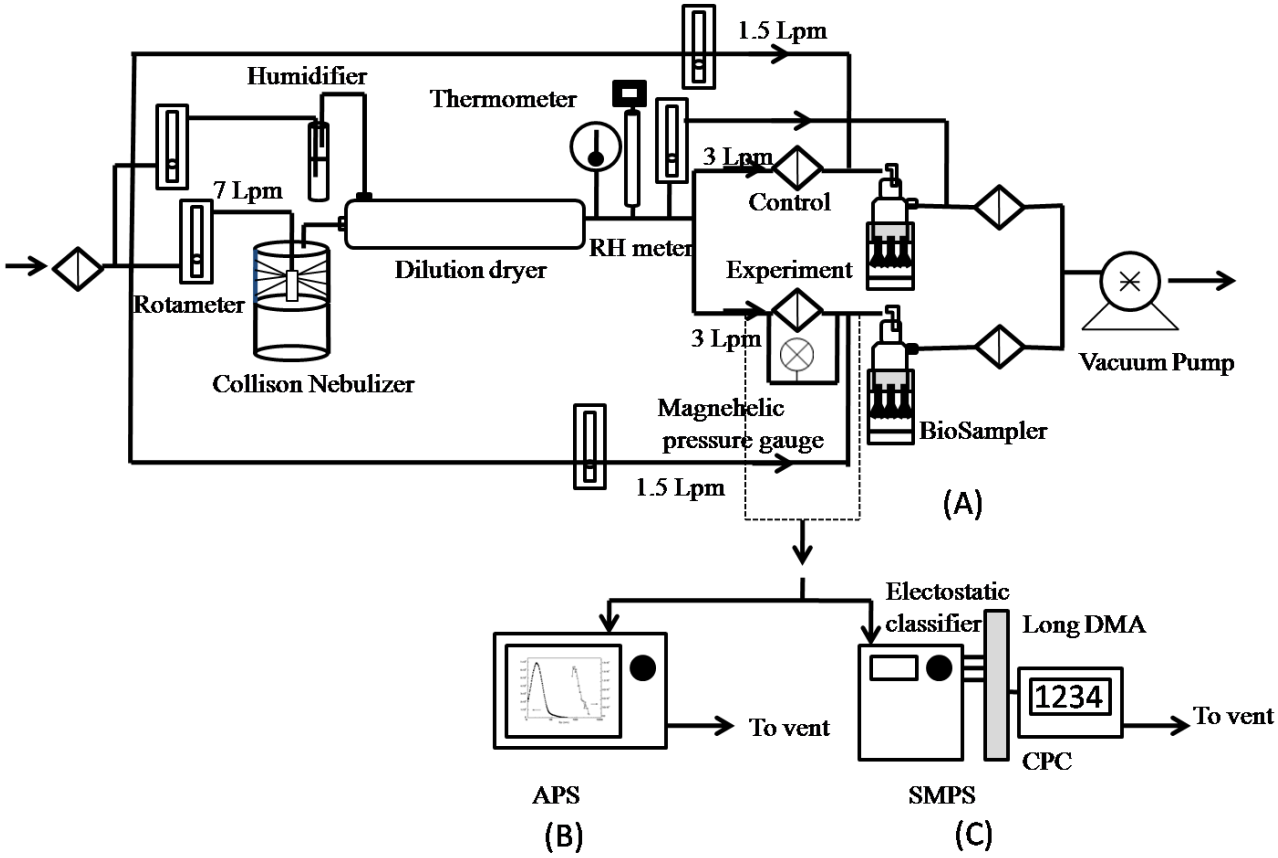

Figure 3-2. Experimental set-up: A) viable removal efficiency and physical removal efficiency against B) *E. coli* and C) MS2 of the test filter in air filtration

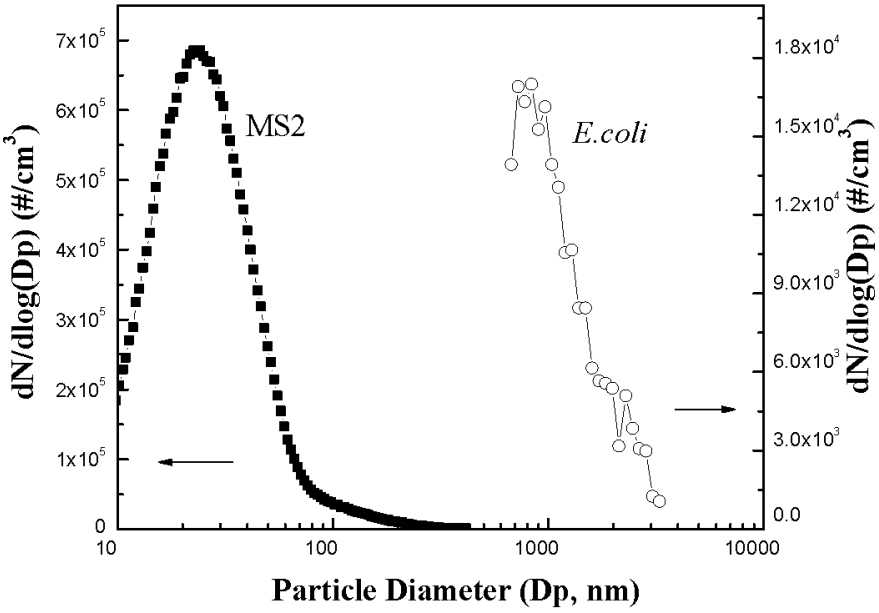

Figure 3-3. The number based particle size distribution of aerosols entering the filter at room temperature and low relative humidity

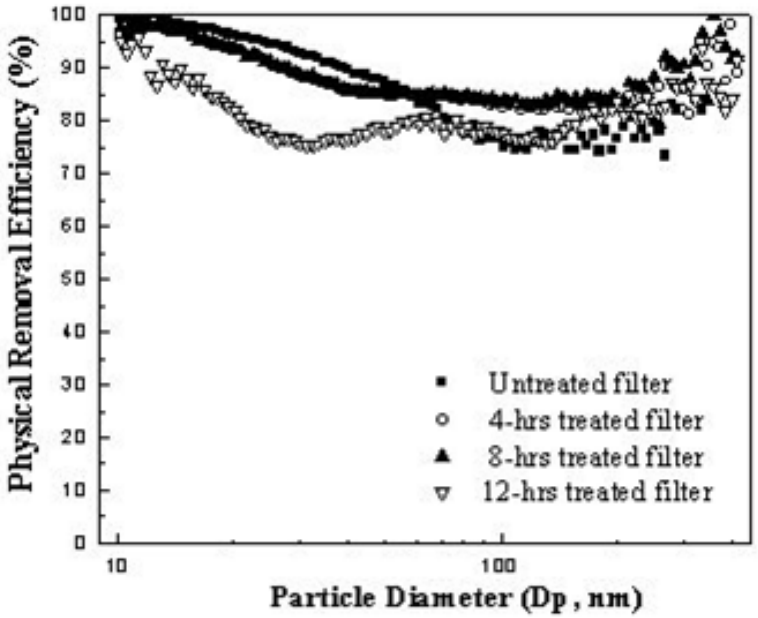

Figure 3-4. Physical removal efficiency of four different filters as a function of particle size at room temperature and low relative humidity

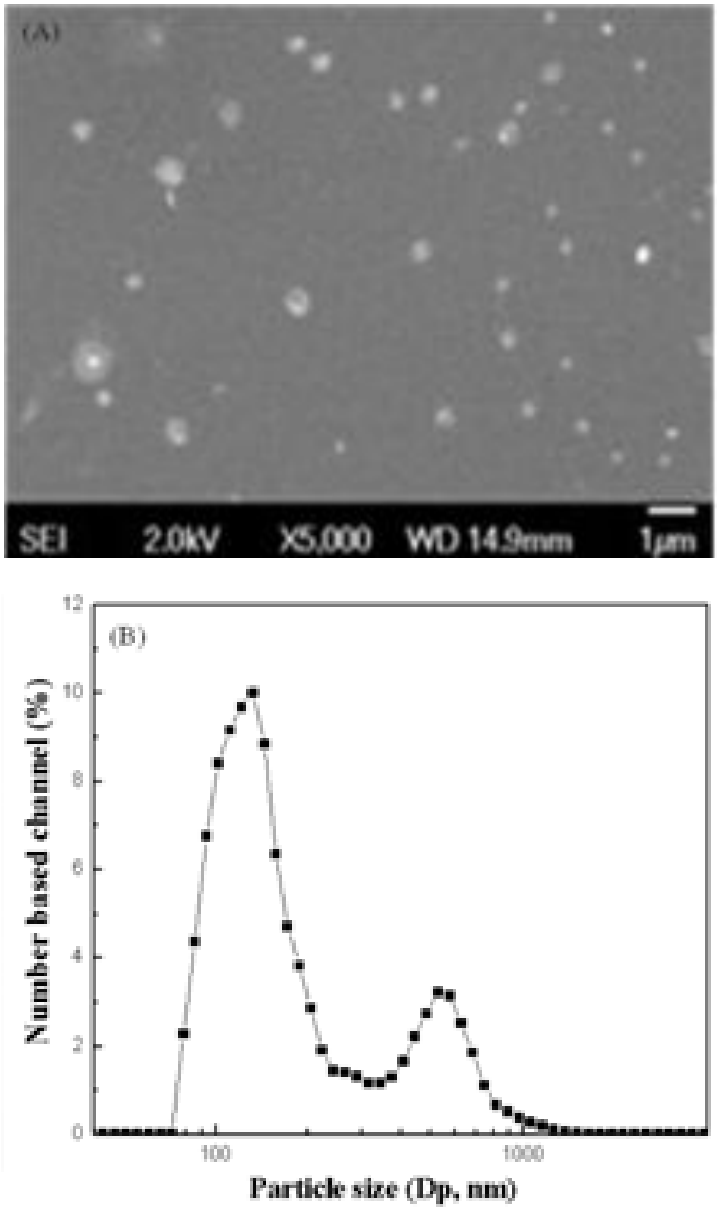

Figure 3-5. Particle size distribution of the MS2 virus titer of 10^9 PFU/mL by A) SEM image and B) particle size distribution by DLS

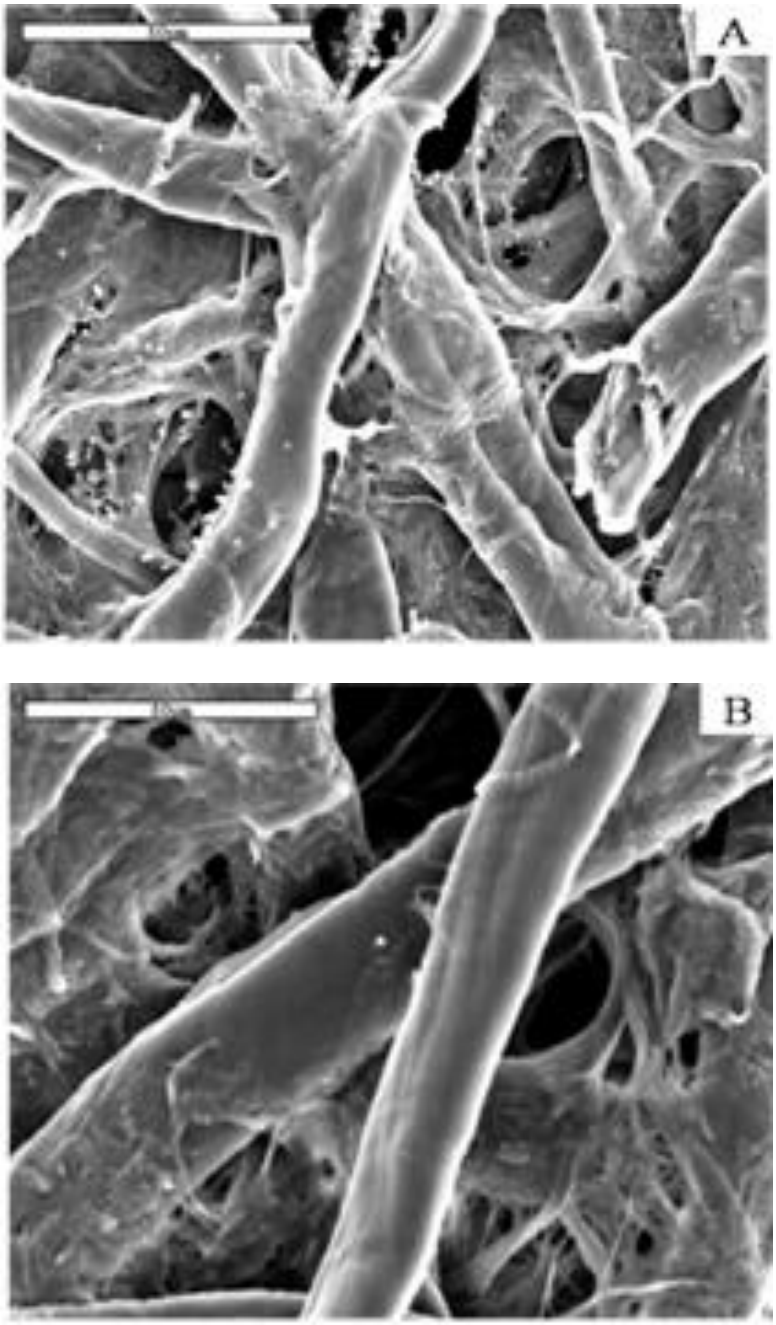

Figure 3-6. SEM images of the 12-hr treated DAC filter with collected *E. coli* before and after extraction

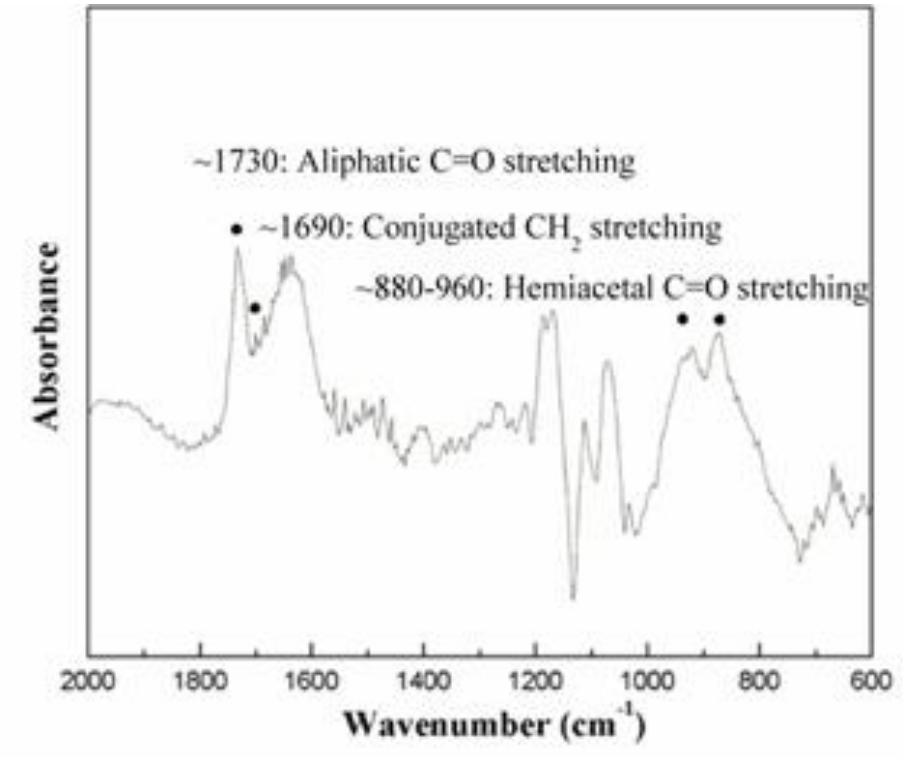

Figure 3-7. FT-IR spectra of 12-hr treated DAC filter when untreated filter was used as background

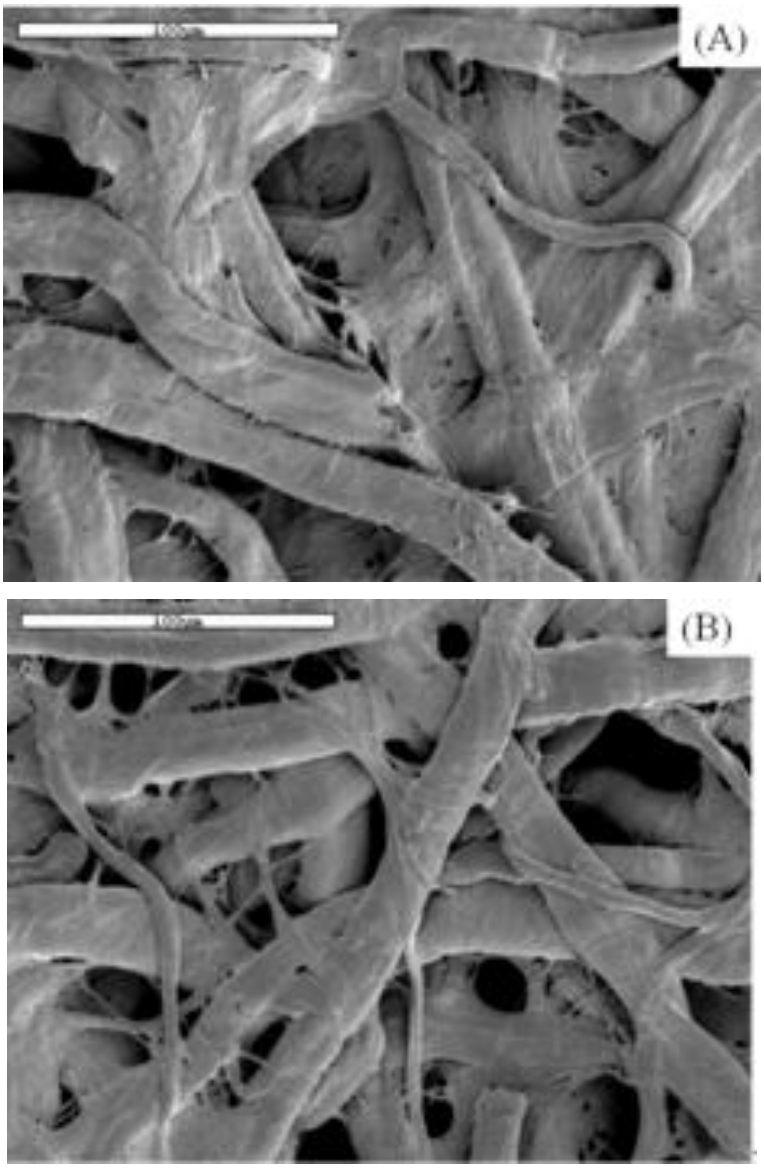

Figure 3-8. SEM images: A) untreated DAC filter and B) 12-hrs treated DAC filter

CHAPTER 4
USE OF DIALDEHYDE STARCH TREATED FILTERS FOR PROTECTION AGAISNT AIRBORNE VIRUSES[‡]

Background

The increasing threat of pathogenic virus outbreaks such as Severe Acute Respiratory Syndrome (SARS), avian flu, and the more recent swine flu have spurred the public's concerns in regards to the health related issues and protection methods against viral aerosols (CDRF, 2006). Filters are one of the most commonly used devices to remove viral aerosols because of their affordability, ease of application, and effectiveness (Fisher et al., 2009). Filtration efficiency is determined by several mechanisms such as interception, impaction, diffusion, gravity, and electrostatic attraction, depending on fiber density, diameter, filter thickness, and other factors (Hinds, 1999). However, these mechanisms are only related to the physical capture of viruses onto the substrate. Conventional filters still allow these collected viruses to infect others if reaerosolized through the respiratory processes of exhalation, sneezing, or coughing, or as a fomite (CDRF, 2006).

Filters can be modified by incorporating chemicals as antimicrobial agents to inactivate viruses (Gabbay et al., 2006; Silver et al., 2006; Lee et al., 2009). Aldehydes such as formaldehyde and glutaraldehyde are also well known antimicrobial agents, as they are highly reactive molecules which are able to combine with proteins and nucleic acids of microbes by cross-linking and alkylation. Nevertheless, their use as incorporated agents has been limited in the air filtration field because of the toxic effects if small aldehyde compounds were to be released and inhaled (Mcdonnell & Russell, 1999). For this reason, polymeric dialdehydes, such as dialdehyde starch (DAS), are promising alternatives. They not only react with hydroxyl,

[‡] Reprinted with permission from Woo, M.-H., Grippin, A., Wu, C. Y.& Baney, R. (2011) Use of dialdehyde starch treated filters for protection against airborne viruses. *Journal of Aerosol Scence* 46, 77-82

amino, imino, and sulfurhydryl functional groups, resulting in the inactivation of viruses, but they also show very low toxicity (Mcdonnell & Russell, 1999; Radley, 1976). Our preliminary study demonstrated that a DAS aqueous suspension acted as an effective biocide against MS2 bacteriophage, PRD1 bacteriophage, and poliovirus. Thus, it is of great interest to employ DAS to modify filters for effective and affordable protection against viral aerosols.

The objective of this study was to explore the inactivation efficiency and filtration performance of commercial filters modified by different DAS suspension concentrations. Three different types of filters, namely, two cellulose filters (CFs) that are commonly used for air cleaning and a polypropylene filtering facepiece respirator (PF), were modified with DAS aqueous suspension. Porosity of CFs was factored into the filter selection due to their influence on collection efficiency of viral aerosols.

Materials and Methods

Test Filters

DAS aqueous suspension was prepared by mixing DAS (Granular form, Sigma–Aldrich, P9265) with deionized (DI) water and then cooked at 95 ^{o}C for 2 hrs, as described in Song et al. (2009). After heat treatment to allow the granules to release the DAS polymeric molecules (Veelaert et al., 1997), gel formation was observed.

Coarse pore cellulose filters (CCFs, Whatman No. 54 with a thickness of 185 μm and a pore size of 22 μm), fine pore cellulose filters (FCFs, Whatman No. 50 with a thickness of 115 μm and a pore size of 2.7 μm), and facepiece respirators made of polypropylene (PFs, Dupont 01-361-N) were employed in this study. Test filters were prepared by immersing filters into 100 mL of the suspension with different concentrations (*i.e.,* 1%, 2%, 3%, and 4%) for 5 mins. These filters were immersed in the same volume of DI water overnight and then washed several times

with DI water to rinse out excess DAS. After removing the residuals, the filters were dried at room temperature overnight. In this study, 4% was selected as the maximum concentration because in preliminary test, DAS treated filters with higher concentrations were fragile, indicating unsuitability for air filtration.

Test Agent

MS2 bacteriophage (MS2; ATCC15992-B1^{TM}), which is a commonly used surrogate for human pathogen enterovirus (e.g., rotavirus) due to their similarities in resistance to antimicrobial agents, was used as the test agent. MS2 is easy to prepare and assay, and it only requires a bio-safety level 1 facility. Freeze-dried MS2 was suspended in sterile DI water and diluted to a titer of 10^8–10^9 plaque forming unit (PFU)/mL. Artificial saliva was used as the nebulized medium to emulate aerosols produced from sneezing or coughing. Details of the recipe for artificial saliva are reported in Woo et al. (2010).

Experimental Method

A schematic diagram of the experimental set-up for aerosol filtration is displayed in Figure 4-1. MS2 aerosol was generated by a six-jet Collison nebulizer (Model CN25, BGI Inc.) that had a virus titer of 10^8–10^9 PFU/mL at a flow rate of 7 Lpm with a pressure of 6 psi. The flow rate through the system was controlled by a rotameter, which was calibrated with a primary flow meter (DryCal® DC-Lite, Bio International Co.). The flow containing MS2 aerosol joined the other flow rate of 7 Lpm, passed through a humidifier for HRH condition, and then proceeded towards a 2.3-L glass mixing chamber. Thereafter, the flow was split and each flow then reached the corresponding filtration unit at a flow rate of 3 Lpm. This flow rate corresponds to the face velocity of 14.2 cm/s, which is a standard value for respirator filtration testing (NIOSH, 1995). The excess air passed through a separate line and bypassed the test filter. The viral aerosols that penetrated the test filter (Φ = 22 mm) were collected by BioSamplers (SKC Corp.) containing 15

mL of sterile DI water at a total flow rate of 5.5 Lpm for 30 mins for the experimental line. The reason for using a lower flow rate than the standard 12.5 Lpm is to avoid significant reaserosolization of MS2 at high flow rate (Riemenschneider et al. 2009). An empty filter holder without a filter was used for the control line. The collected sample was assayed with *E.coli* as a host by the single layer method (EPA, 1984). The viable removal efficiency (VRE) was determined by comparing the PFUs from the experimental and control BioSamplers:

$$\text{VRE} = \left(\frac{N_c - N_E}{N_C} \right) \tag{4-1}$$

where N_C and N_E are the viral concentrations collected by the control and the experimental BioSamplers, respectively. To quantify the amount of MS2 virus collected in a given filter, the test filter taken off from the system was immersed into 25 mL of sterile DI water as an eluent and shaken by a wrist action shaker (Model 75, Burrell Scientific) for 15 mins. To evaluate the biocidal efficacy of treated filters compared to untreated filters, relative survivability (RS) of viruses on filters was calculated by comparing survival factors, SFs, of both filters as:

$$RS = \frac{SF_{treated\ filter}}{SF_{untreated\ filter}} \tag{4-2}$$

Herein, SF is defined as:

$$SF = \frac{(\frac{N_S}{\phi_{EE}})}{(\frac{N_C - N_E}{\phi_{CE}})} \times \frac{V_E}{V_B} \tag{4-3}$$

where N_S is the viral concentration obtained from the eluent, Φ_{EE} is the extraction efficiency of microbes from filter , Φ_{CE} is the collection efficiency of the Biosampler, and V_E and V_B are the liquid volumes of the eluent and the Biosampler, respectively. Consideration of the extraction efficiency and the collection efficiency of the BioSampler was not necessary for this relative

value, RS. The pressure drop across the filter was measured by a Magnehelic gauge to evaluate filter performance using quality factor (QF), a useful criterion for comparing filter performance of different filter types and thicknesses. This value is defined as (Hinds, 1999):

$$QF = \frac{-\ln(1-VRE)}{\Delta P} \tag{4-4}$$

where ΔP is the pressure drop. It should be noted that throughout the duration of experiment (30 mins), the variation of the pressure drop was negligible. Experiments were carried out in triplicate and samples were assayed in duplicate. Statistical analysis was conducted using 2-way analysis of variance (2-way ANOVA) with Design-Expert® 8.0 software. Additionally, a scanning electron microscope (SEM, JEOL JSM-6330F, JEOL Inc.) was used to observe morphological changes of the filters.

Results and Discussion

CCFs and FCFs slightly shrank after the DAS treatment, whereas no visible change was observed for PFs. Also, when CFs were subjected to the wrist action shaker, untreated filters were broken after 15 mins whereas treated filters remained intact. This is presumably because of crosslinking or entanglement of DAS with the cellulose. DAS can react with cellulose of CCF and FCF by forming covalent hemiacetal and acetal bond (BeMiller and Whistler, 2009). SEM images of untreated and treated filters with different DAS suspensions, as shown in Figure 4-2, confirm this hypothesis. CFs are composed of main fibers and fibrillates of small diameter. CCF contains small amounts of fibrillates, whereas FCF has numerous fibrillates. DAS was crosslinked with fibrillates of CFs, resulting in the increase of fibrillate diameter (Figures. 4-2D – 4-2I). Granular DAS was also observed on the surface of the main fibers at high DAS concentration (Figures. 4-2D and 4-2H – 4-2I). In contrast, DAS could not react with fibers of PF due to the lack of reaction between hydrophobic propylene filters and hydrophilic DAS (Song,

2008; Yu et al., 2010). Instead, the DAS with gel-formation might coat the fiber surface of PF, resulting in slight increase in fiber diameter. Also, the hydrophilic property by DAS coating might be the possible reason of the folded structure as shown in Figure 4-3C (Yu et al., 2010). The difference in materials yields differences in the impact of the DAS treatment, as will be demonstrated in the following section.

The pressure drop results are listed in Table 1. Both filter type ($p < 0.0001$) and DAS concentration ($p < 0.0001$) are significant as well as the interaction between filter type and DAS concentration. Since the pressure drop of FCFs at 3 Lpm was out of the measurable range, the pressure drop at 0.5 Lpm was measured and then converted for 3 Lpm by Equation 4-5

$$\Delta P_2 = \left(\frac{\Delta P_1}{V_2} \right) \times V_1 \tag{4-5}$$

where V is face velocity. The pressure drops of untreated and DAS treated PFs were less than 1 inch H_2O at a face velocity of 14.2 cm/s. These values were much lower than the inhalation resistance of 2.52 inch H_2O permitted by NIOSH for certified respirators (NIOSH, 1995) and the military standard of 4.21 inch H_2O for HEPA filter media (U.S. Army, 1998). Furthermore, there was no significant change in pressure drop as a function of DAS treatment. The pressure drop of untreated CCF was 3.45 inch H_2O, which is not suitable for the application of a respirator. However, those of treated CCFs ($p < 0.0001$) significantly decreased with increases of DAS concentration. Finally, those treated with the 4% DAS suspension reached the NIOSH limit for respirators. Meanwhile, the pressure drop of untreated FCF was too high to use as a ventilation filter and respirator, but those of the treated FCFs ($p < 0.0001$) significantly decreased although the pressure drops were still over the criterion for respirators.

Figures 4-3A and 4-3B show that the VRE and QF of the test filters as a function of concentration of DAS suspension. For the PF, the DAS treatment did not change the fiber

diameter of the filters, resulting in insignificant change in VRE. Hence, there was no significant change in QF. For the CF, the treatment did not cause discernible impact on the VRE although the treatment reduced air resistance as exhibited as decreased pressure drop. Accordingly, an increase in the QF was observed. The QFs of untreated and 4% DAS treated CCFs were 0.77 and 1.46 kpa^{-1} and those of FCFs were 0.25 and 1.85 kpa^{-1}, respectively. The impact on FCF (e.g., increase of 7.4 times) was larger than on CCF (e.g., increase of 1.9 times). The amount of crosslinking of the fibrillates is likely responsible for the difference.

To evaluate the inactivation capability of DAS treated filter mats, the RS of treated filters as a function of concentrations of DAS suspension is displayed in Figure 4-4. All filters show similar tendencies, with RS decreasing with increasing concentration of DAS suspension, indicating the inactivation effect of the DAS treated filters against the MS2 collected on the treated filter. Aldehyde functionality of polymeric molecules dispersed from gel formation through heating in preparation is the source attributed to the biocidal capacity on treated surfaces. (Song, Cruz, Farrah, & Baney, 2009)

Summary

This study demonstrates that treating filters with inexpensive DAS (less than $1/ 10 filters) is a practicable method for creating biocidal filters. DAS treatments have different impacts on filtration efficiency depending on filter materials. The treatment reduces air resistance in cellulose filters, resulting in lower pressure drop while having no significant impact on removal efficiency. These factors combine to yield an improved quality factor for cellulose filter. Meanwhile, there is no difference in quality factor for treated propylene filters. Nevertheless, the biocidal effect is clearly exhibited for all treated filters. Compared to other decontamination methods, the DAS treatment does not require additional energy sources and facilities (e.g., microwave, IR, and UV irradiation) and it does not release toxic chemicals (e.g., iodine treated

filter). Therefore, the treated filters can be adopted for wide applications such as in health care facilities and at pandemic events.

Table 4-1. Pressure drop (face velocity of 14.2 cm/s) of three types of filters treated with different concentrations of DAS suspension.

Concentration of DAS suspension	Pressure Drop (inch H_2O)		
	PF	CCF	FCF*
0%	0.69 ± 0.01	3.45 ± 0.00	32.40 ± 0.76
1%	0.69 ± 0.01	3.25 ± 0.07	27.00 ± 1.27
2%	0.64 ± 0.01	3.15 ± 0.00	25.92 ± 0.01
3%	0.65 ± 0.00	2.95 ± 0.07	8.10 ± 0.21
4%	0.63 ± 0.04	2.53 ± 0.04	3.24 ± 0.00

*Converted from 0.5 Lpm

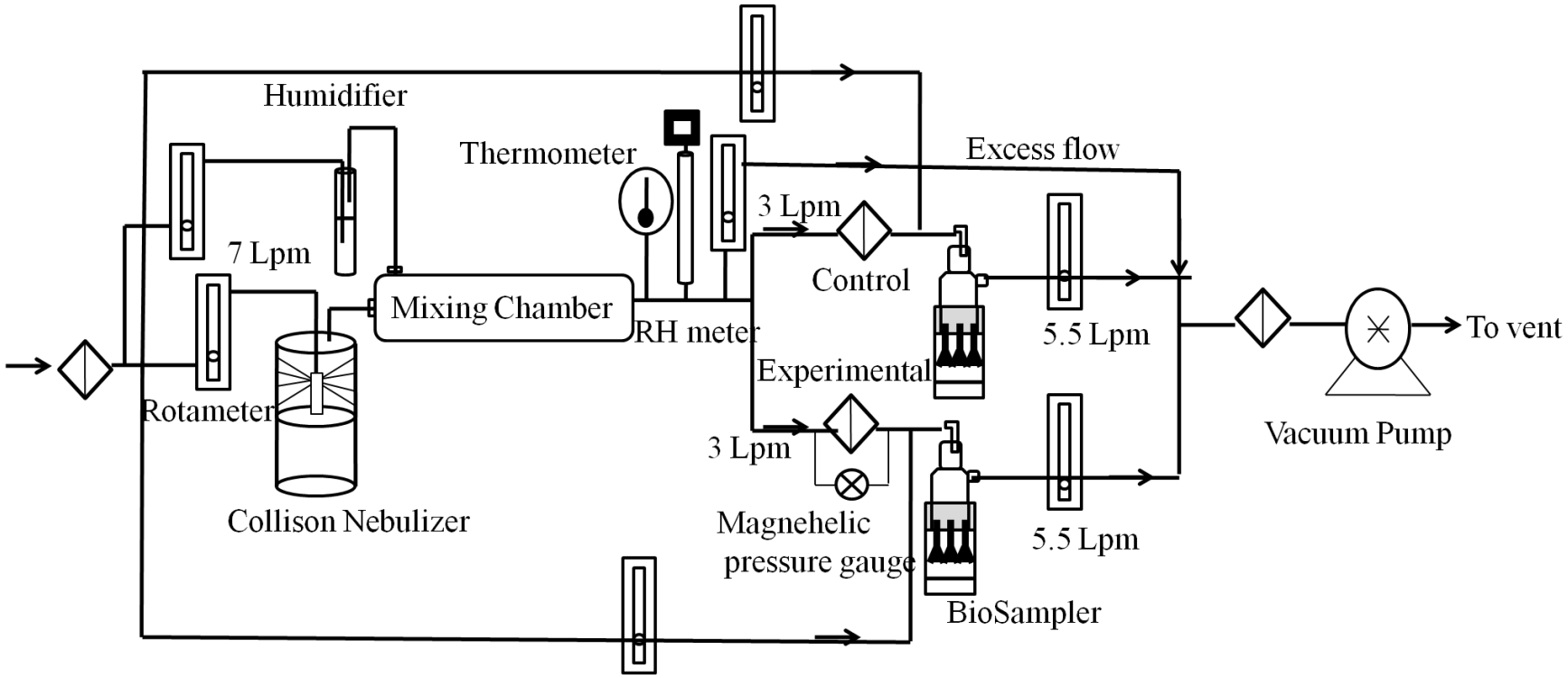

Figure 4-1. Schematic diagram of the experimental set-up: A) SEM image and B) particle size distribution by DLS of the MS2 virus titer of 10^9 PFU/mL

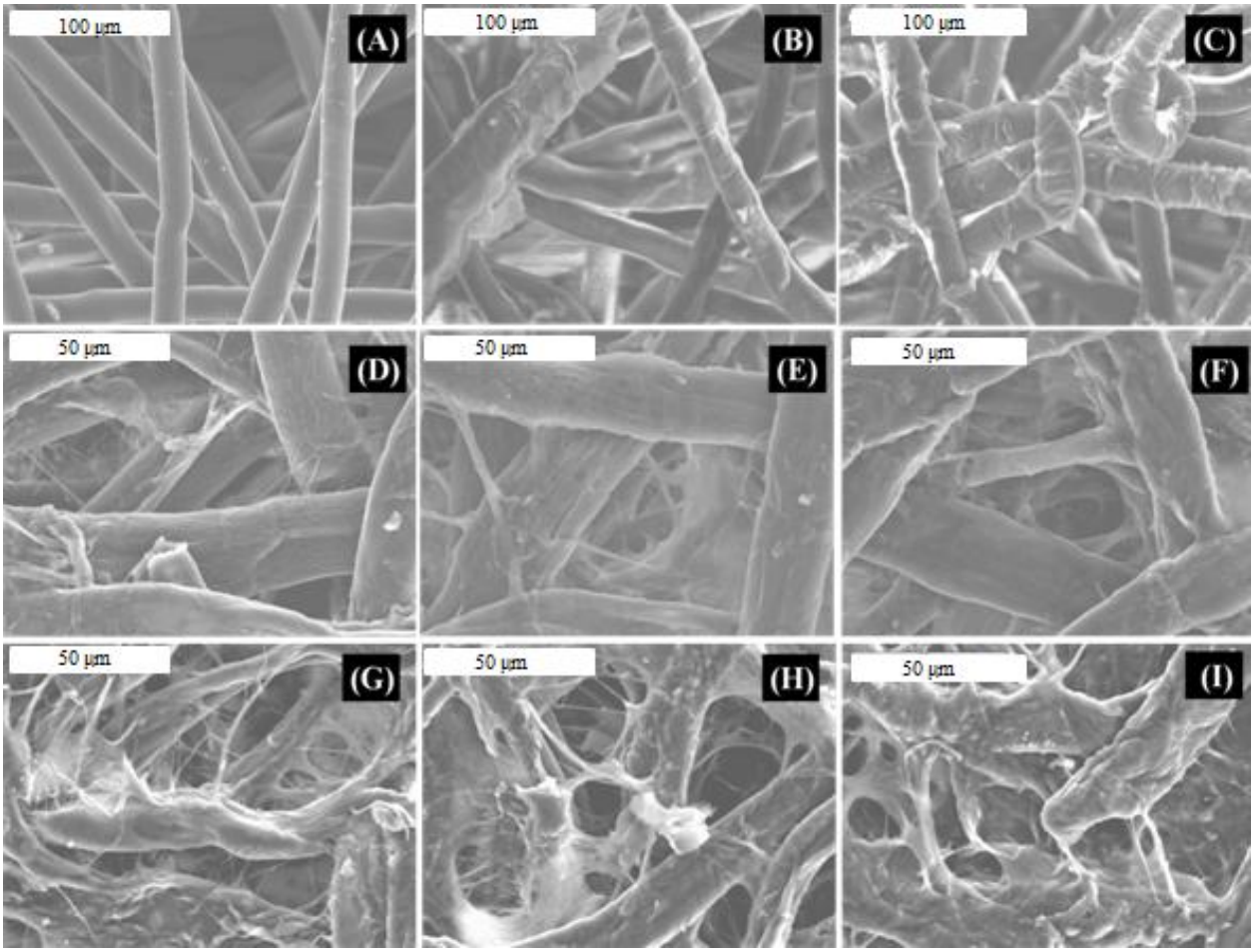

Figure 4-2. SEM images: untreated A) PF, D) CCF, and G) FCF, treated B) PF, E) CCF, and H) FCF with 2% DAS suspension, and treated C) PF, F) CCF, and I) FCF with 4% DAS suspension. Magnifications of A)-C) 500× and D)-I) 1000×, respectively

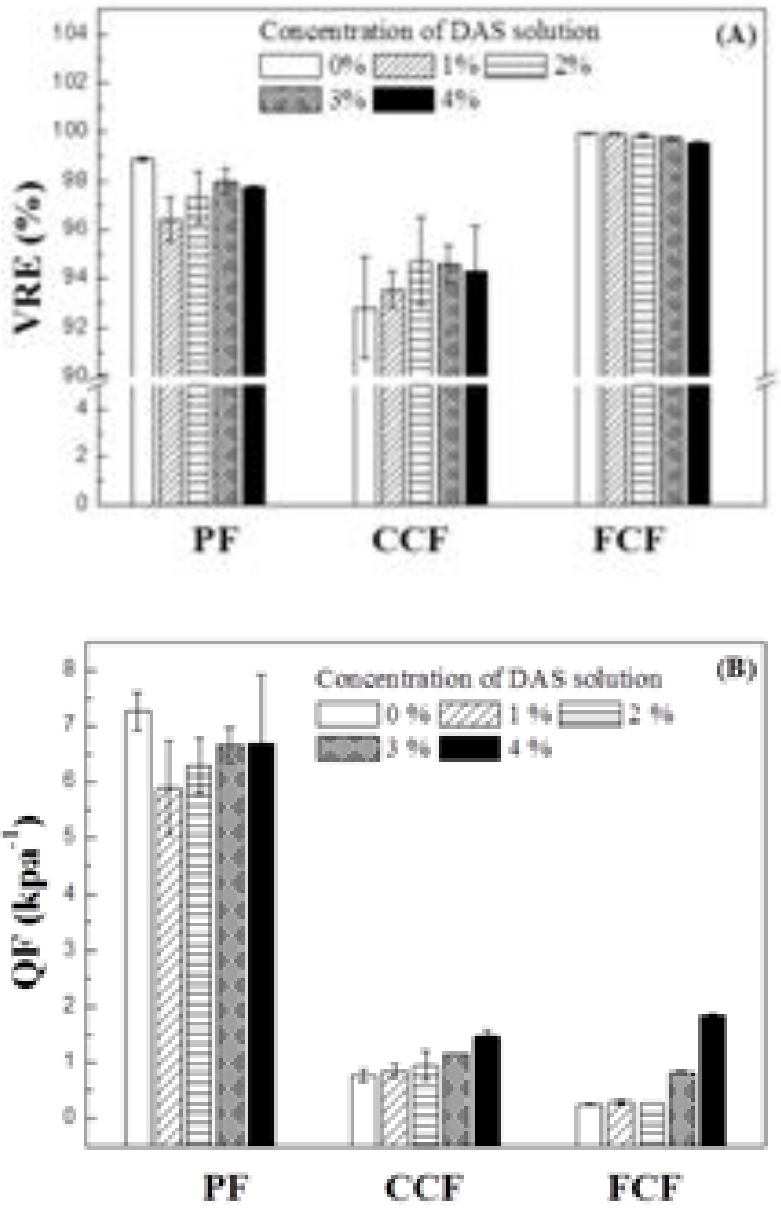

Figure 4-3. Performance of filters treated with different concentrations of DAS suspension: A) viable removal efficiency and B) quality factor

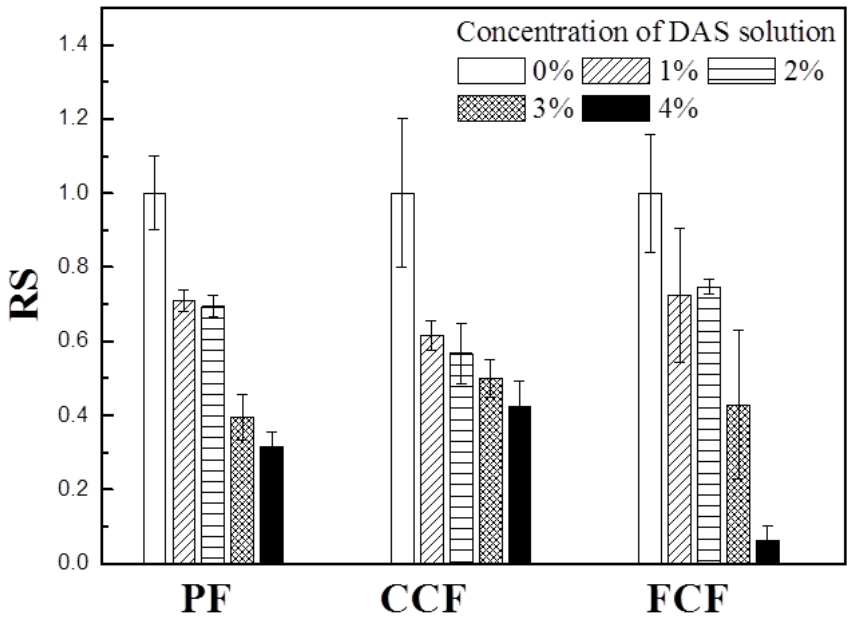

Figure 4-4. Relative survivability of MS2 viruses on filters treated with different concentrations of DAS suspension

CHAPTER 5
MICROWAVE IRRADIATION ASSISTED HVAC FILTRATION FOR INACTIVATION OF VIRAL AEROSOLS[§]

Background

Microwaves—electromagnetic waves with frequencies between 300 MHz and 300 GHz—are widely applied in food processing, wood drying, plastic and rubber treating, curing and preheating ceramics as well as in cleanup processes (Park et al., 2006). Microwaves are non-ionizing but sufficient to cause the molecules in matter to vibrate, thereby causing friction, which is subsequently transformed into heat for various applications. Among the diverse applications, the use of microwaves for decontamination was studied soon after microwaves became available. Goldblith and Wang (1967) and Fujikawa et al. (1992) compared the effect of microwave irradiation on *Escherichia coli* (*E. coli*) and *Bacillus subtilis* (*B. subtilis*). They concluded that the heat produced was a key factor for inactivating the bacteria in solid and aqueous phases. Meanwhile, there has been research demonstrating additional effects, beyond the purely thermal mode of inactivation. For example, distortion of membrane structure and function (Phelan et al., 1994), altered enzyme activity (Dreyfuss and Chipley, 1980), disruption of weak bonds (Betti et al. 2004), increased release of various substances (Campanha et al., 2007; Celandroni et al., 2004; Woo et al., 2000), and increased ionic strength due to an increased current within cells (Watanabe et al., 2000) have all been reported. However, all of the aforementioned research was conducted in the liquid, solid, or aqueous phase.

In recent years, microwave inactivation of airborne microorganisms has gained more interest because of increasing concerns about health-related issues regarding outbreaks of pathogenic airborne viruses (e.g., SARS, H1N1 and swine flu). For examples, Hamid et al.

[§] Reprinted with permission from Woo, M.-H., Grippin, A., Wu, C.-Y., & Wander, J. Microwave irradiation assisted HVAC filtration for inactivation of viral aerosols. Accepted to *Aerosol & Air Quality Research*

(2001) measured 90% inactivation efficiency (IE) by applying microwave irradiation to heterogeneous airborne bacteria and fungi at 600 W for four periods of 2.5 min, each separated by 5 min from the next. Elhafi et al. (2004) demonstrated that infectious bronchitis virus, avian pneumovirus, Newcastle disease virus, and avian influenza virus were inactivated on dried swabs in less than 20 s at 1250 W. Another study, Wu and Yao (2010a) reported IEs of 65% and 6% against airborne *B. subtilis* var niger spore and *Pseudomonas fluorescens*, respectively, in an air stream after exposure to microwaves at 700 W for 2 min and Wu and Yao (2010b) showed gene mutation through polymerase chain reaction-denaturing gradient gel electrophoresis after microwave application.

Other recent studies (Heimbuch et al., 2010; Zhang et al., 2010) have focused on microwave inactivation of contaminated filters. Although filters are effective devices for capturing bioaerosols, and they are utilized in virtually all modern heating, ventilation and air conditioning (HVAC) systems to reduce the spread of infectious viruses and also as filtering facepiece respirators (FFRs) at healthcare facilities, they are limited as a preventive method because they inactivate neither viruses that pass through the filter nor those that are captured.

As some pathogens have a low infectious or lethal dose, viruses that penetrate or reaerosolize have the opportunity to infect people the filter was intended to protect (McCrumb, 1961). Heimbuch et al. (2010) reported that microwave-generated steam at 1250 W for 2 min induced a 5-log IE for H1N1 virus collected on FFRs. Zhang et al. (2010) demonstrated that microwave irradiation could provide an adequate method for inactivating *E. coli* and *B. subtilis* endospores via a microwave-assisted nanofibrous air filtration system.

The air quality of indoor has been determined by HVAC system because the pollutants including infectious viruses exhaled by human and transmitted by objects can be mitigated

through the filtration and recirculation by HVAC system. If the viruses captured on the filter and transmitted during recirculation in HVAC system can be inactivated, the risk of spread of virus can be reduced. However, no research has been conducted to evaluate the applicability of this technology to commercial HVAC filters even though these filters are commonly used in hospitals and residential buildings for collective protection. Therefore, the objective of this study was to evaluate the inactivation performance of microwave-irradiation assistance to HVAC filtration systems during in-flight filtration against MS2 bacteriophage (MS2). Key parameters examined were microwave power levels, microwave application times, and relative humidity. The thermal stability of the filter media was also investigated.

Materials and Methods

Test Filters and Agent[**]

Two commercial HVAC filters made of polyethylene and polypropylene (Filter 1; 3M) and synthetic polymer (Filter 2; True Blue) were selected as test filters, and glass microfiber LydAir MG (Filter 3; Lydall) was used for comparison. MS2 (ATCC® 15597-B1™) was applied as a test agent. It is a surrogate for enteroviruses such as rotavirus because of their similar structural properties and resistance to heat and chemicals (Brion et al., 1999; Prescott et al., 2006). Freeze-dried MS2 was suspended in DI water with a titer of around 10^8–10^9 plaque-forming units (PFU)/mL as the virus stock suspension.

Experimental System

A microwave oven (Panasonic, NN-T945SF, 2.45 GHz, continuous irradiation) with two one-inch holes in the backside was used in this study. Because common filter holders could not survive in the microwave, a custom-made quartz filter holder was placed inside the microwave.

[**] Polyacrylonitrile (PAN) and cross-linked PAN nanofiber filter were tested and the results are displayed in Appendix B.

To support the filter material and to enhance heat transfer, a SiC disk was employed inside the quartz reactor.

The experimental set-up for testing the inactivation of the virus is shown in Figure 5-1. Six Lpm of dry air was passed through a six-jet Collison nebulizer (Model CN25, BGI Inc., MA) to aerosolize the viruses. A second air stream passed through the humidifier and then rejoined the flow. After the combined flow passed through the mixing chamber, it was split three equal ways, and each stream proceeded toward the filtration unit at 4 Lpm, corresponding to a face velocity of 5.3 cm/s, which is a standard face velocity for ventilation system testing (U.S. Army, 1998). Of the three flows, two were directed to filter holders outside the microwave, one with and one without an HVAC filter, as controls. The third was equipped with an HVAC filter 47 mm in diameter (effective diameter 40 mm for the quartz reactor used) inside the microwave oven. The filters inside and outside the microwave oven were labeled A and B, respectively. The BioSamplers downstream of the microwave/filtration system and non-irradiated filter were labeled C and D, respectively. The BioSampler downstream of the empty filter holder (control) was labeled E.

For in-flight microwave decontamination, microwave irradiation was applied for three 10-min cycles that included selected periods of irradiation—1, 2.5, 5 and 10 min/10 min—at three different microwave power levels, 125, 250 and 375 W. To select the microwave application conditions, the thermal stability of three test filters was analyzed with TGA/SDTA (851E, Mettler–Toledo Inc., OH), and the temperature of filters on the SiC disk under different applied conditions was measured with an IR pyrometer (OS533E, Omega Engineering Inc., CT). After irradiation, the test filter was taken off the filter holder in the experimental system and subjected to wrist-action shaking (Model 75, Burrell Scientific, PA) with a shaking angle of 20° for 15 min

to extract the viruses (Woo et al., 2010). The extracted MS2 was assayed with *E. coli* as a host by the single-layer method (EPA, 1984). For enumeration of MS2 viruses within an adequate count range of 30-300 PFU/mL, 1 mL of diluted MS2 was mixed with 9 mL of #271 agar and 1 mL of #271 medium with log phage *E. coli* and poured into the Petri dish. The mixture was solidified and then the plate was stored in the incubator at 37 ^{o}C for one night before counting.

The effectiveness of this process was evaluated by using two parameters: survival fraction (SF) and IE. The SF under microwave irradiation was calculated by comparing the viable MS2 in the two filters:

$$\mathrm{SF} = \frac{C_{\mathrm{A}}}{C_{\mathrm{B}}} \tag{5-1}$$

where C_A and C_B are the viral concentrations collected by filters A and B, respectively.

Viral aerosols penetrating the test filters under microwave irradiation were collected in BioSamplers containing 15 mL of DI water. The IE through the microwave/filtration system was obtained by comparing the viable MS2 concentration in the two BioSamplers:

$$\mathrm{IE} = \frac{C_{\mathrm{E}}}{C_{\mathrm{C}}} \tag{5-2}$$

where C_C and C_E are the concentrations of viruses collected in the BioSamplers C and E, respectively.

The filtration efficiency of the filter itself ($1\text{-}C_D/C_E$) was used to confirm the stability of this system after each test. The pressure drop of the filter was measured by a Magnehelic gauge to evaluate the degradation or change of filters after decontamination test. Triplicate experiments and duplicate assays were carried out, and 1-way ANOVA was used for statistical analysis after confirming over 90% of normality (Design-Expert® 8.0).

The scanning electron microscopy (SEM, JEOL JSM-6330F, JEOL Inc., MA) images of virus-contaminated filters were taken after conventional oven heating and after microwave irradiation heating to investigate non-thermal effects of microwave irradiation. A conventional oven (ISOTEMP® oven 230G, Fisher Scientific, PA) was used to provide purely thermal effects. Filters contaminated with a virus suspension of 10^{10} PFU/mL of DI water were either microwaved or inserted into a conventional oven for 30 mins.

Results and Discussion

Temperature Measurement of Test Filters

TGA was used to determine the appropriate temperature range for microwave assisted HVAC filtration because of the concern that the polymer fiber of the filter might experience melting or other mutations during the thermal process. For filters A and B, two endothermic events were observed at 125-130 ^{o}C and ~170 ^{o}C while for filter C no endothermic or exothermic event was observed over the 25~300 ^{o}C range (results not shown). Therefore, the temperature of 125 ^{o}C was selected as the maximum temperature for microwave irradiation to avoid filter

TGA/DTA was used to determine the appropriate temperature range for microwave-assisted HVAC filtration because of the concern that the polymer fiber of the filter might experience melting or other mutations during the thermal process. As displayed in Figure 5-2A, no residual moisture loss around 100 ^{o}C was observed in all three filters, confirming the hydrophobicity of filter material. For filters 1 and 2, two endothermic events were observed at 125–130 ℃ and at ~170 ℃; for filter 3 no endothermic or exothermic event was observed over the 25~300 ℃ range, as shown in Figure 5-2B. Therefore, 125 ℃ was selected as the maximum temperature for microwave irradiation to avoid filter damage. The temperature profiles of the filters supported on a SiC disk running with a flow rate of 4 Lpm at different microwave power levels and application times are displayed in Figure 5-3 A linear increase in temperature as

application time increased was expected. However, the results showed a different trend. At 250 W, the temperature did not increase much after 2.5 min, likely due to the balance between heating by microwave irradiation and cooling by the air stream. At 375 W for 10 min/cycle, the max temperature was around 120 ℃, whereas it reached 165 ℃ without airflow, illustrating the cooling effect by the air stream. Based on the temperature measurement, a maximum power level of 375 W was selected to investigate the IE and SF in this study. For further investigations, higher power levels of 500 W and 750 W were selected for filter 3 because of its high thermal stability as mentioned previously.

Inactivation Efficiency and Survival Fraction

For filter 1, the IE of the microwave irradiation assisted filtration system and the SF on the filter surface as a function of microwave power at four different microwave application times are displayed in Figures 5-4A and 5-4B, respectively. As shown, IE increased and SF decreased as microwave power was increased and as the application time was extended. For the IE, changes to both microwave power level ($p<0.01$) and application times ($p<0.01$) were significant. The IE is attributed to two factors: 1) physical capture by the filtration mechanism and 2) inactivation of viruses during flight. At the lowest setting—125 W for 1 min/cycle—no additional disinfection was observed beyond the inherent log removal efficiency of 0.53 (i.e., 71%) coming from the physical filtration efficiency ($1-C_D/C_E$) of filter 1 (~73%). At a power level of 375 W, 3.0 and 3.5 logs of the viable MS2 were disinfected when microwave irradiation was applied for 5 and 10 min/cycle, respectively. This suggests that an application time of 5 min/cycle is sufficient to disinfect MS2. Significant influences of both microwave irradiation time ($p = 0.02$) and power level ($p = 0.03$) upon SF were seen. The trends of SF were similar to those of IE, although a much lower SF was expected at higher microwave power levels because of the longer exposure time of 30 mins for the SF as compared to the shorter flight time of less than 5 s for the IE.

However, at 375 W applied for 5 and 10 mins/cycle, a higher value of log IE was observed than the absolute value of log SF.

Physical capture is one possible reason for the higher log IE. However, the log IEs after deducting the inherent removal efficiency were still higher than the absolute values of the log SF (2.5 and 2.9 vs. 1.8 and 2.5). This may be explained by the high temperature of the SiC disk. Damit et al. (2010) reported that the exposure of MS2 to the high temperature of 250 ℃ for 1 s resulted in 4-log SF. The temperatures of the SiC disk at 375 W immediately after irradiation at 5 and 10 min/cycle were 172 ℃ and 203 ℃, respectively, whereas the temperatures of the filters on the SiC disk were 107 ℃ and 117 ℃. Thickness of the SiC disk was 2.54 cm, and viruses flying through the disk were exposed to these high temperatures for 0.5 s. This exposure during flight could attribute to the higher IE. For filter 2, similar results were seen, as shown in Figures 5-4C and 5-4D, although the inherent filtration efficiency was slightly higher than that of filter 1. For filter 3, IE and SF at 375 W, 500 W, and 750 W are displayed in Figures 5-4E and 5-4F. As shown, the IE and SF at 375 W are similar to those for filters 1 and 2, although the higher inherent filtration efficiency was around 95%. At 500 W and 750 W, log SFs of -3.47 and -4.23 were seen, respectively. The temperatures of filter 3 on the SiC disk at 500 W and 750 W for 10 min/ cycle were 143 ℃ and 171 ℃, respectively. This result suggests that the thermal stability of filter material is an important factor for microwave disinfection applications.

Effective Temperature

Comparing the microwave irradiation power level and application time data revealed that filter disinfection can be characterized by a threshold temperature, i.e., the temperature at which inactivation starts to increase sharply. Similarly an effective temperature, defined as the minimum temperature that must be reached for effective disinfection (2-log or greater), can also be identified. The threshold and effective temperatures can be estimated in Figure 5-5, which

displays log IE and log SF as a function of the temperature reached after microwave irradiation application. The data pattern greatly resembles a two-stage process—an initial accumulation of energy, and then a catastrophic release, simply indicating a threshold temperature has been reached. The IE remains unsatisfactory until the threshold temperature of around 90 ℃, and it reaches 2 logs at 109 ℃. The SF also starts to rise around 90 ℃ and reaches 2 logs at 116 ℃. Once the filter reaches this temperature, effective disinfection of the virus can be assumed. IE and SF of each filter against MS2 can also be expressed as a function of temperature (T) via a log-linear relationship above the threshold temperature, as displayed in Table 5-1. Although different intercepts and slopes were expected because of different inherent physical removal efficiency and thermal properties of filter, the difference was not significant ($p<0.05$). Furthermore, when the intercepts of log IE were corrected by deducting the inherent filtration efficiency, the results showed no difference among all three filters ($p = 0.02$). Therefore, in and near the temperature region studied, the IE and SF of MS2 for a microwave-irradiation-assisted filtration system can generally be expressed as:

$$\log (IE) - \log (IE)_{\text{inherent filtration}} = \log (IE)_{\text{microwave}} = -7.57 + 0.08\,T \quad (5\text{-}3)$$

$$\log (SF) = 5.01 - 0.06\,T \quad (5\text{-}4)$$

Thus, for an HVAC filter having 99.9% filtration efficiency to reach 6-log IE for MS2, the necessary temperature is ~132 ℃.

Although thermal effect was a major factor for microwave inactivation, Khalil and Villota (1989) compared the distortion of RNA subunits in *Staphylococcus aureus* after microwave and conventional heat treatments, and found destruction of the 23S RNA by only microwave treatment, indicating the possibility of non-thermal effect. In addition, Betti (2004) reported a non-thermal effect of microwaves against plants and viruses at a sublethal temperature, and Wu

and Yao (2010) confirmed visible changes of bacteria and fungi after microwave heat treatment by ESEM. Hence, in this study non-thermal effects were investigated by studying the morphological changes and SFs with and without microwaves at the same temperature. Figure 5-6 displays the temperature profiles of the conventional and microwave ovens. Temperatures of the conventional oven were selected based on the temperature profiles of the microwave oven at 250 W and 375 W. The conventional oven's temperature was stable for 30 min of test time. For the microwave oven operated at 250 W, a steady-state temperature profile was observed after 10 min. However, temperatures around 90 ℃ at 250 W might be insufficient to inactivate MS2. Therefore, 375 W was selected for observations of morphological changes through SEM.

Figure 5-7 displays SEM images of untreated, conventional-oven-treated, and microwave-treated virus-contaminated filters. As shown in Figures 5-7B and 5-7C, the heat of both the conventional oven and the microwave oven made the water evaporate (or removed it in some other way), and then aggregation was observed. However, no significant difference in morphology was seen, even though the concentration of microwave-treated viruses was lower than that of conventional-oven-treated viruses. SFs of viruses on the substrates after heat treatment by microwave oven and conventional oven were also compared but no significant difference was shown, indicating that no non-thermal effect of microwaves can be elucidated in this study.

Effect of Relative Humidities on Inactivation Performance

Relative humidity is another key parameter for the inactivation of viruses. However, when a SiC disk is used, it is difficult to determine the effect of relative humidity because of the overwhelming thermal effect of the SiC disk as compared to relative humidity. Relative humidity is another key parameter affecting the inactivation of viruses. However, when a SiC disk is used, it is difficult to determine the effect of relative humidity because of the overwhelming thermal

effect of the SiC disk as compared to relative humidity. Therefore, to investigate the effects of relative humidity, a quartz frit was used as a support instead of a SiC disk. IE through the system and SF on the filter surface as a function of microwave power level applied to filter 1 for 5 min/cycle under three relative humidities are displayed in Figures 5-8A and 5-8B, respectively. IE (p = 0.01) significantly increased and SF ($p<0.01$) significantly decreased as the application time increased. By design the quartz frit could not absorb microwave irradiation, which resulted in a lower filter temperature and less pronounced viral inactivation capacity compared to those with the SiC disk. Log IEs of 0.8, 0.9, and 1.3 were obtained at relative humidities of 30%, 60%, and 90%, respectively, at 500 W (p <0.01). Unlike the results with a SiC disk, log IE corrected for filtration efficiency of the filter itself was lower than the absolute value of log SF, indicating that the lower temperature of the support is insufficient to inactivate MS2. At the higher power level, a high IE and lower SF were seen under high relative humidity, which may be explained by the mechanism of microwave irradiation. The higher water content can contribute to more efficient heating induced by water's molecular vibrations (Fisher et al., 2011). However, the relative humidity effect was not observed at 500 W for 10 min/cycle in Figures 5-8C and 5-8D. The different phenomenon can be explained by the increased concentration of water vapor at higher temperature and the higher temperature itself. At high relative humidity, final temperatures were 27 ℃, 43 ℃, 66 ℃, and 81 ℃ after 5 min/cycle, and 49 ℃, 62 ℃, 78 ℃, and 89 ℃ after 10 min/cycle at 125, 250, 375, and 500 W, respectively. The results suggest that relative humidity is a significant parameter from 50~80 ℃ and that it ceases to be significant above 90 ℃.

Degradation of Filters after Microwave Irradiation

Table 5-2 shows that pressure drops of the test filters after microwave treatment were measured to inspect for degradation of the filter. Under the operating condition, the initial

pressure drops (at 5.3 cm/s) of 0.45, 0.62, and 1.20 inches H_2O for filters 1, 2 and 3, respectively, were maintained throughout several microwave irradiation tests at 375 W for 10 min/cycle. There was no significant difference in pressure drop between control and treated filters, indicating no melting or degradation. SEM images also showed no visible morphological changes.

Comparison to Other Disinfection Technologies

Numerous disinfection technologies, including energetic techniques and chemical treatments, with or without filtration systems have been studied. A study investigating bleach disinfection with 0.1% sodium hypochlorite aerosol and UV germicidal irradiation (UVGI) with a wavelength of 254 nm achieved 2-log SF of MS2; however, bleach and UVGI have limitations of chemical release and low penetration, respectively (Vo et al., 2009). Rengasamy et al. (2010) and Woo et al. (2011) confirmed the inactivation effect of biocidal filters incorporated antimicrobial agents, e.g., silver copper, oxygen species, titanium oxide and dialdehyde, but these filters could not reached 2-log SF for 30 mins. Compared to other filter disinfection technologies, the microwave-assisted filtration system was effective without any filter damage and chemical formation.

As direct disinfection technologies without filter, Kettleson et al. (2009) reported electrostatic precipitator (ESP) at $\pm$6 kV showed 2-log IE of MS2 and that at -10 kV could reach above 6-log IE. To compare these results with the present study is difficult because of different inactivation mechanisms (thermal effect vs. radical reaction). However, ESP disinfection should be cautioned about the formation of ozone. Grinshpun et al. (2010) demonstrated dry heat treatments of MS2 at 125 ℃ for 0.24 s resulted in 2-log IE. This value is similar to that corrected by deducting the inherent filtration efficiency was considered, confirming thermal effect of microwave.

Summary

This study demonstrates that microwave assisted filtration is an efficient approach for inactivating viral aerosols. Microwave power and application time are key operating parameters for controlling the disinfection effectiveness of viral agents. Both factors combine to yield a threshold temperature of around 90 ^{o}C. Relative humidity is another pivotal parameter for viability of viruses at medium temperature, but it becomes insignificant at high temperatures above 90 ^{o}C. If thermally stable filter material is applied, a high inactivation efficiency of around 5-log through the system can be reached at lower temperatures compared to other dry heat treatments.

Table 5-1. Linear relationship of the IE and SF of MS2 with temperature (T)

Filter 1	Log IE = -7.14 (-7.65)[a] + 0.087T (p=0.04)	Log SF = 4.67 - 0.057T (p<0.01)
Filter 2	Log IE = -6.69 (-7.46) + 0.077T (p=0.02)	Log SF = 4.81 - 0.060T (p<0.01)
Filter 3	Log IE = -6.57 (-7.60) + 0.078T (p<0.01)	Log SF = 5.05 - 0.061T (p<0.01)
All filters[b]	Log IE = -6.83 (-7.57) + 0.080T (p=0.02)	Log SF = 5.01 - 0.060T (p<0.01)

[a]The values in parentheses in log IEs are the intercepts calculated with inherent filtration efficiency deducted.
[b]The relationships were obtained from all IEs and SFs above threshold temperature of three filters.

Table 5-2. Pressure drop (face velocity of 5.3 cm/s) of three filters after microwave treatment at 375 W for 10 mins/cycle

	Pressure drop (inH_2O)		
No. treatment	Filter 1	Filter 2	Filter 3
0 (Control)	0.45	0.62	1.2
1	0.45	0.62	1.2
2	0.45	0.60	1.2
5	0.46	0.60	1.2

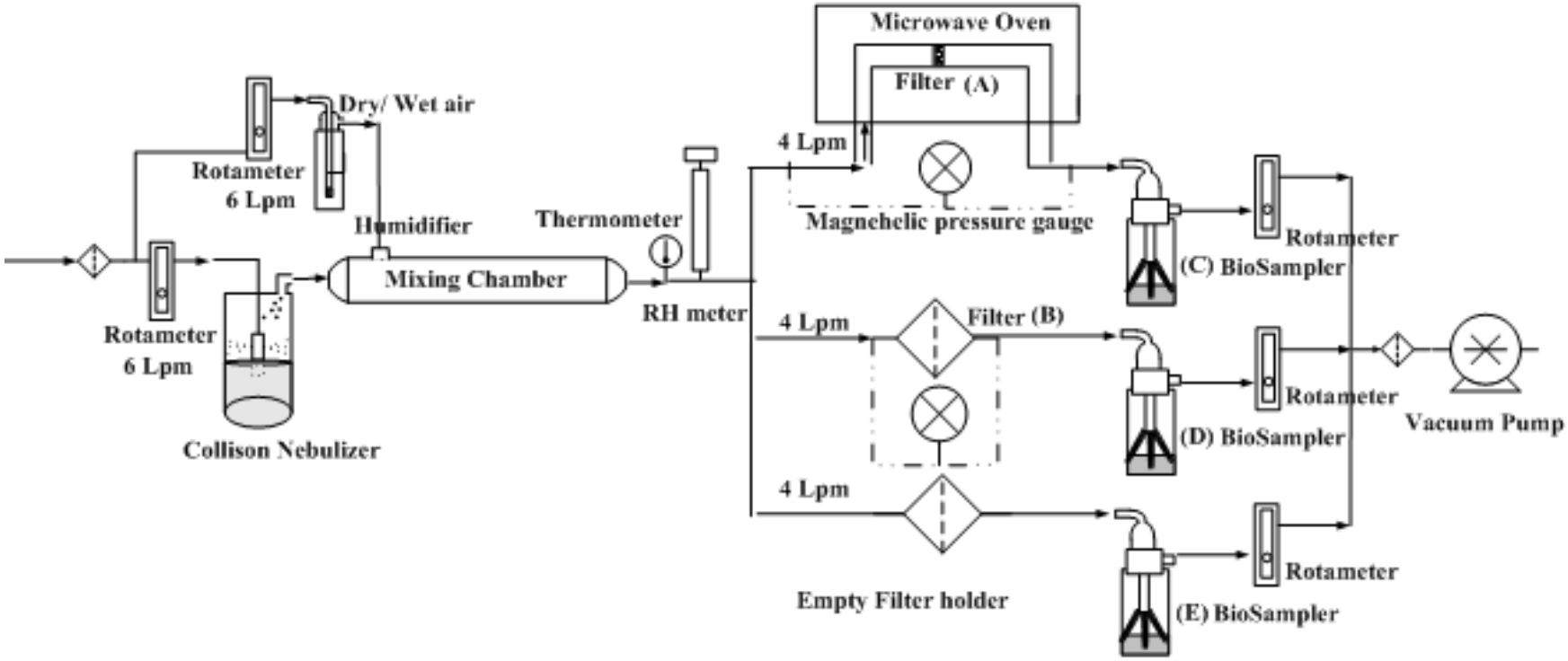

Figure 5-1. The experimental set up for microwave irradiation assisted filtration.

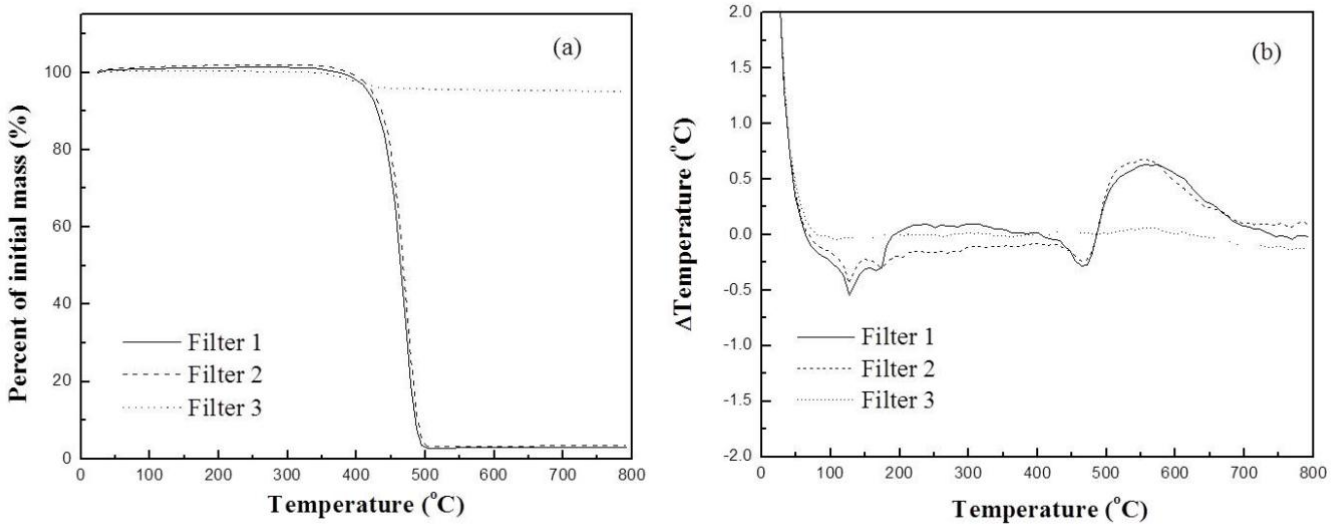

Figure 5-2. Thermal stability for three filters of A) Thermogravimetric analysis (TGA) and B) differential thermal analysis (DTA) curves for three filters.

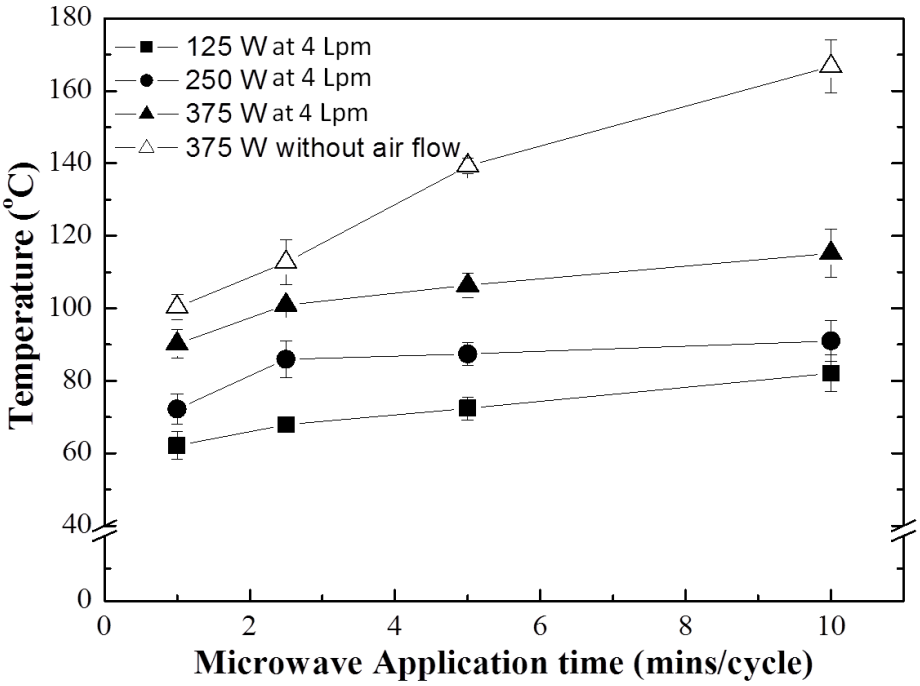

Figure 5-3. Temperature of the filters as a function of microwave application time at three different microwave power levels

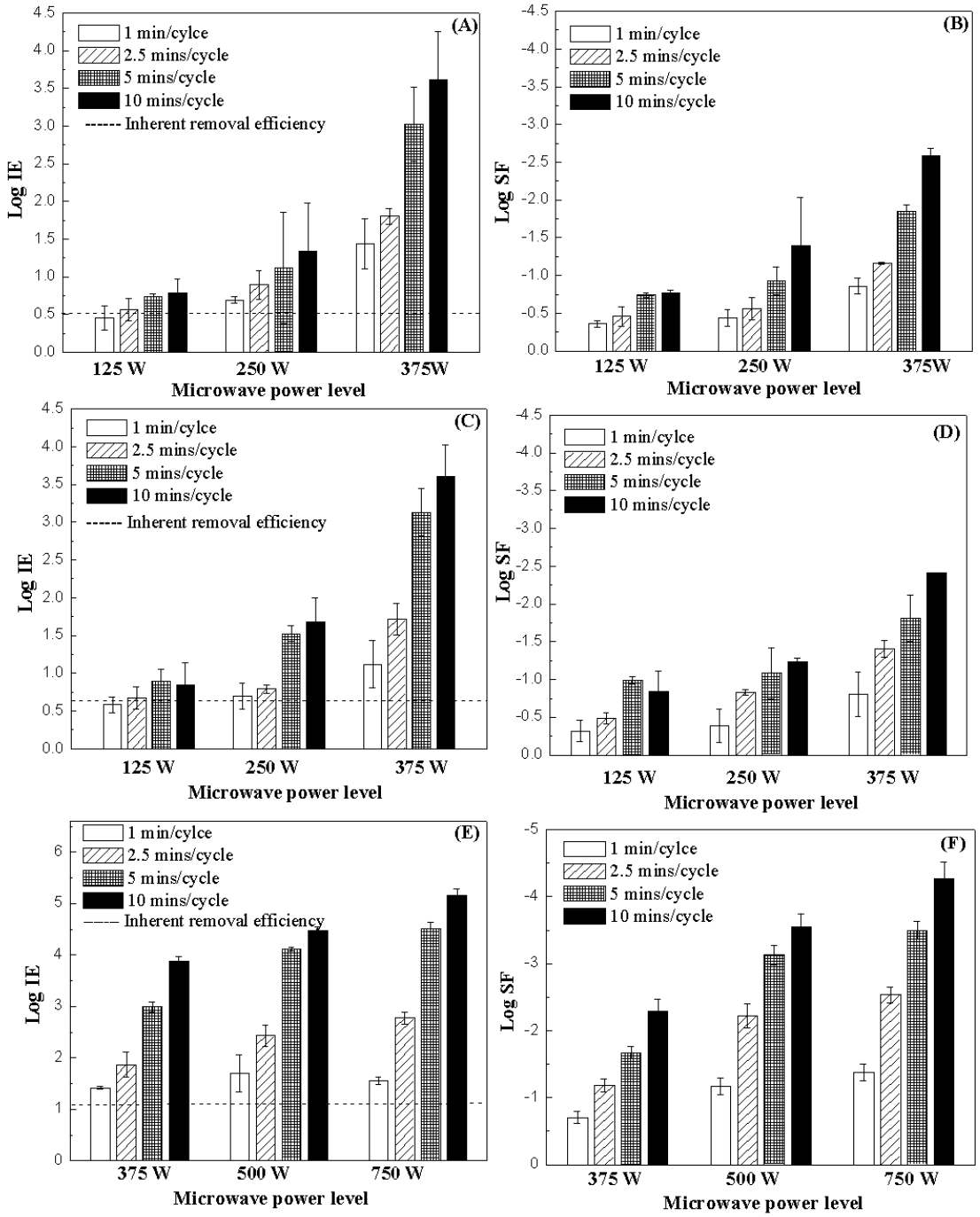

Figure 5-4. Log inactivation efficiency and log survival fraction: A) and B) filter A, C) and D) filter B, and E) and F) filter C

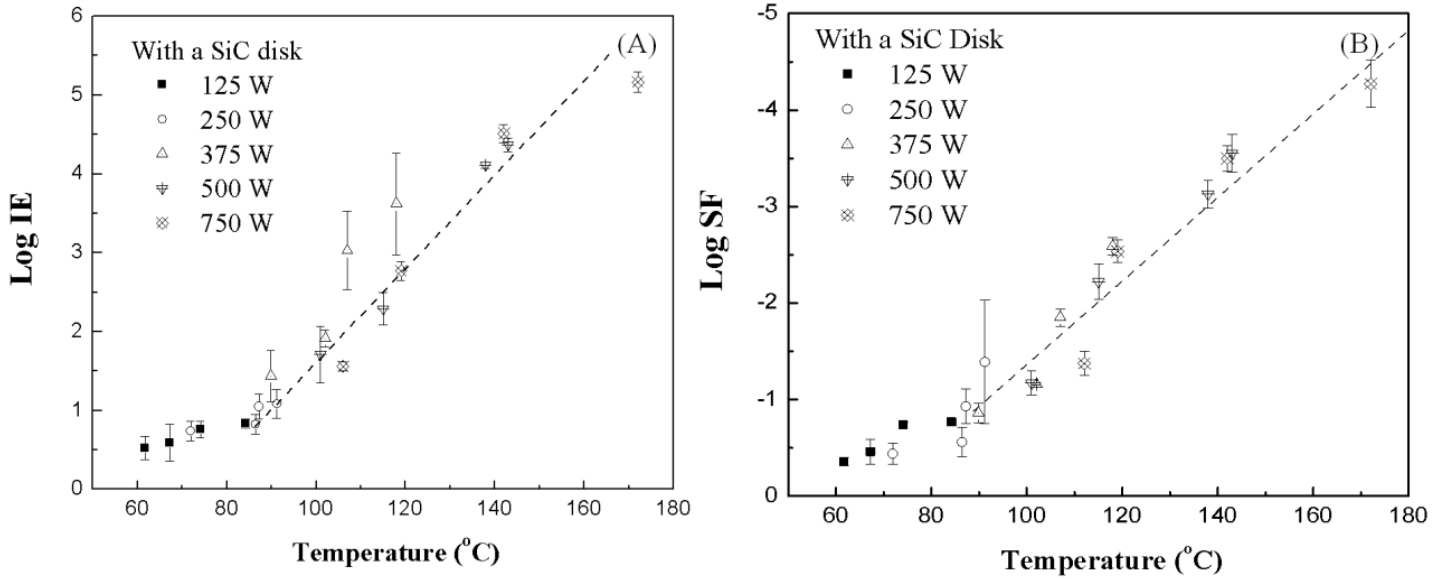

Figure 5-5. Microwave inactivation performance: A) Log inactivation efficiency and B) log survival fraction as a function of the temperature reached during microwave irradiation. Filter 1 for 125, 250 and 375 W and Filter 3 for 500 and 750 W

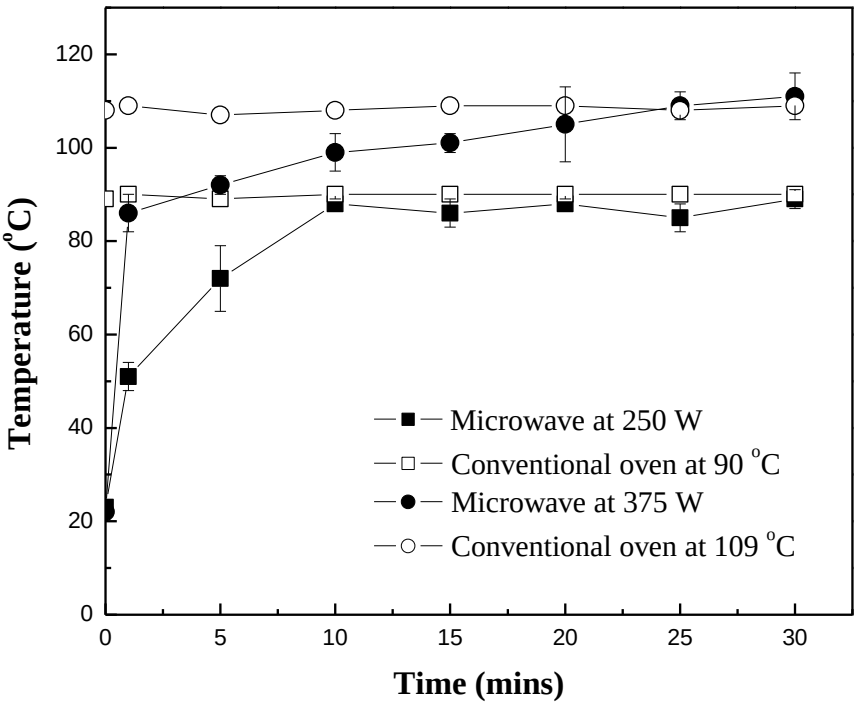

Figure 5-6. Temperature of microwave and conventional ovens as a function of application time

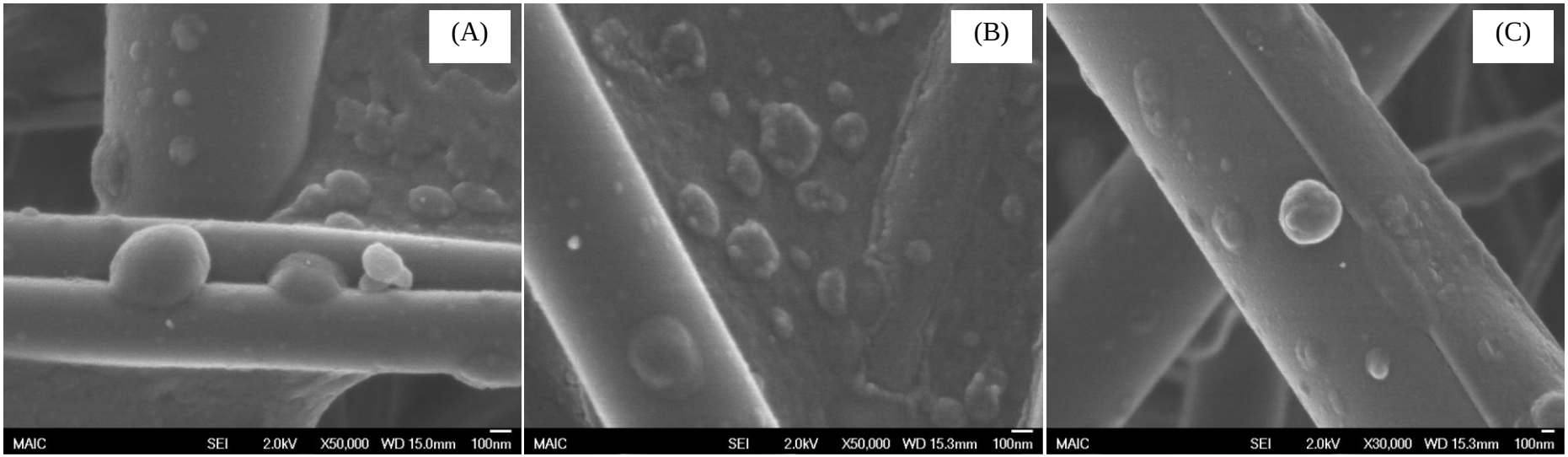

Figure 5-7. SEM images: A) untreated- virus contaminated filter, B) conventional heat treated- virus contaminated filter, and C) microwave treated-virus contaminated filter. Magnifications of A)-C) 50,000×

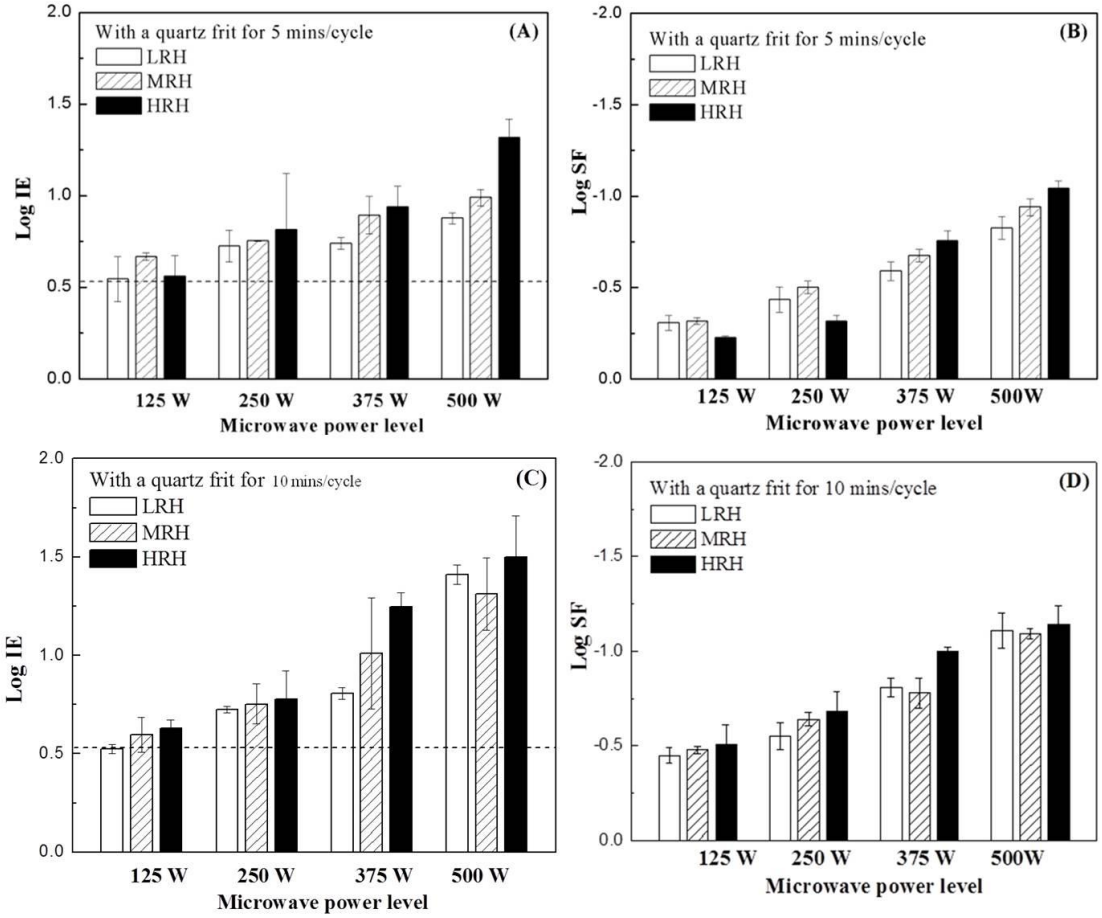

Figure 5-8. Log inactivation efficiency by microwave irradiation assisted filtration system and and Log survival fraction on filter surface as a function of microwave power level: A) and B) for 5 min/cycle and C) and D) for 10 min/cycle

CHAPTER 6
EFFECTS OF RELATIVE HUMIDITIES AND AEROSOLIZED MEDIA ON UV DECONTAMINATION OF VIRAL AEROSOLS LOADED FILTER[††]

Background

The increasing threat of bioterrorist attacks (e.g., ebola virus) and recent outbreaks of airborne pathogenic infections (e.g., SARS, H1N1, Avian Flu) have raised the level of public interest in biological aerosols and protection methods that prevent their spread (Drazen, 2002; Prescott et al., 2006; CDC, 2009). Filtering facepiece respirators (FFRs) certified by the National Institute for Occupational Safety and Health (NIOSH) are mandated by 40 CFR 84 to be worn by healthcare personnel and are recommended as a protective device for the general public during a pandemic event. Several factors influence the effectiveness of the intended protection offered by the FFRs, including the bioaerosol transmission mode and environmental conditions.

Because aerosol size is a pivotal parameter for filtration efficiency understanding the transmission mode of viral aerosols is critical to protection of the public against major airborne pathogen pandemics. Three critical transmission modes are recognized for the spread of infectious viruses (CDRF, 2006): (1) Droplet transmission, which results from infected individuals generating droplets containing microorganisms by coughing, sneezing, singing and talking. Droplets of various sizes produced by an infected person are propelled short distances through the air to a susceptible host, and the infection occurs through contact with a mucous membrane. (2) Aerosol transmission, which includes the dispersion of droplet nuclei that remain airborne in air after evaporation of droplets and dust particles carrying the microorganism. Owing to the small size of the inhalable droplet nuclei and dust particles, disease can be widely spread by this mode. (3) Fomite transmission, which includes both

[††] Reprinted with permission from Woo, M.- H., Anwar, D., Smith, T., Grippin, A., Wu, C.- Y., & Wander, J. Investigating the effects of relative humidities and nebulized media on UV inactivation of viral aerosols loaded filter. Submitted to *Applied &Environmental Engineering.*

direct body-to-body contact and indirect contact through a contaminated object (e.g., towel or mask). Controlling this mode is a chronic problem in healthcare facilities. One infected patient serving as a source can easily infect other—especially immunocompromised—patients through activity in the facility.

As implied above, the FFR is a device that efficiently captures viruses transmitted by droplet and aerosol modes. However, infectivity of the captured viruses persists, which makes the contaminated FFR a fomite. In addition, reaerosolization of viruses captured on the FFR is a possibility; transient, high rates of air flow (e.g., coughing and sneezing) aggravate the probability of reaerosolization (Rengasamy et al., 2010). NIOSH projected that during a 42-day influenza pandemic the healthcare sector alone would require over 90 million masks, a demand that could create a supply shortage that would leave millions in unnecessary danger of infection (CDRF, 2006). One possible buffer against this threat, recovering and reusing FFRs after inactivating the viruses that they capture and thus allowing them to be reused several times, has been shown to be technically feasible (Heimbuch et al., 2011) and appears consistent with 29 CFR 1910.134(h)(1) (OSHA, 2012). However, imprecision in the definition of the term "single-use" as applied to disposable N95 FFRs—the Centers for Disease Control and Prevention (CDC) recommends continuous or intermittent wearing for no more than 8 hours and only until the mask becomes wet, dirty or contaminated, ceases to seal to the wearer's face or develops elevated flow resistance (CDC, 2011)—and the specification in 29 CFR 1910.134(d)(1)(ii) that respirators must be NIOSH-certified (OSHA, 2012), a certification that applies only to new disposable respirators, poses a procedural obstacle to implementation of this concept, even in a declared emergency (FDA, 2007), that remains to be resolved.

Decontamination of used FFRs plays an important part in preventing both reaerosolization of viral particles collected on a filter surface and fomite transmission, and

can extend filter life. Several inactivation methods, including microwave irradiation, UV irradiation and biocidal surfaces (Vo et al., 2009; Fisher et al., 2009; Lee et al., 2009; Zhang et al., 2010) have been shown to decontaminate viral aerosols collected on filters. Antimicrobial agents such as phenols, alcohols, heavy metals, and quaternary ammonium compounds can be incorporated into air filters; however, the biocidal filters that have been tested release small quantities of toxic chemicals (Lee et al., 2009; Woo et al., 2011; Rengasamy et al., 2010), as can chloramines (Gowda et al., 1981) . The use of direct microwave irradiation to kill microorganisms through thermal and non-thermal effects has also been demonstrated in various studies in solid media, but this method requires a microwave absorber (typically water, activated carbon or silicon carbide) and may damage the material (Fisher et al., 2009; Heimbuch et al., 2011; Zhang et al., 2010; Rengasamy et al., 2010).

UV irradiation delivers sufficient energy to be a practical antimicrobial method. UV-C irradiation is a recognized method for inactivating a wide variety of biological agents and in particular airborne microorganisms (Prescott et al., 2006). At a wavelength of 254 nm, a UV-C photon striking a biological cell is selectively absorbed by one of adjacent pairs of thymine or uracil nucleotide bases in deoxyribonucleic acid (DNA) or ribonucleic acid (RNA), causing them to form covalent bonds with each other and interrupting hydrogen bonds with adenine bases in the complementary DNA/RNA strain. Pyrimidine dimers of thymine/uracil bases distort the shape of DNA/RNA, altering the double-helical structure and preventing the cell's accurately transcribing or replicating its genetic material, which ultimately leads to the death of the cell (Perier et al., 1992; Kowalski, 2009; Prescott et al., 2006). Many studies (Farhad, 2004; Memarzadeh et al., 2010; Ryan et al., 2010; Chuaybamroong et al., 2011) have reported that UV intensity, exposure time, lamp placement and air movement patterns influence its inactivation efficiency (IE) against microbes.

A study by Viscusi et al. (2009) investigating the effect of UV light on the performance of FFRs found no net change in the functionality of the masks after UV radiolysis. Most studies have focused on the relationship between decontamination efficacy and two parameters, UV intensity and exposure time (Viscusi et al., 2009). None has considered other important parameters (e.g., relative humidity (RH), nebulized medium, and transmission mode) that influence susceptibility of viral agents collected on fibrous filters.

The objective of this study was to investigate the IE of UV irradiation against viruses collected through different transmission modes under various environmental conditions. For this, the filters were contaminated by two pathways (droplet and aerosol) using three spraying media (i.e., deionized (DI) water, beef extract (BE) in filtered, sterile DI water, and an artificial saliva (AS)) at three RH conditions (i.e., low (LRH, 30±5%), medium (MRH, 60±5%), and high relative humidity (HRH, 90±5%)). UV irradiation was applied at a constant intensity of 1.0 mW/cm^2 for different time intervals.

Materials and Methods

MS2 Preparation

MS2 bacteriophage (MS2; ATCC, 15597-B1) was used as the test agent. MS2 (Φ= 27.5 nm) has a non-enveloped, icosahedral capsid (Prescott, Harley, & Klein, 2006; Brion & Silverstein, 1999) and is commonly used as a nonpathogenic surrogate for human pathogenic viruses (e.g., rotavirus, influenza, poliovirus, and rhinovirus) for the following reasons: physical characteristics similar to those of human pathogenic viruses, need of only BSL-1 containment, and ease of preparation and assay (Brion & Silberstein, 1999). A freeze-dried MS2 culture was suspended in DI water at a titer of approximately 10^{11}–10^{12} plaque-forming unit (PFU)/mL and this stock was stored at 4 ℃. The virus stock was successively diluted to 10^8–10^9 PFU/mL with 1X phosphate buffered saline (PBS) and used for the experiment.

A single-layer bioassay with a host of *Escherichia coli* (ATCC, 15597) was used to enumerate the infectious viruses (EPA, 1984). Tryptone–yeast extract–glucose broth (TSB 271) and culture medium 271 were prepared following the American Type Culture Collection (ATCC) procedure for MS2 assay. Freeze-dried *E. coli* were suspended in 1X PBS, inoculated into a solidified agar plate (1.5% agar) with a sterilized loop, and incubated at 37 ℃ overnight. The single colony from the plate was transferred into TSB 271 and set to grow at 37 ℃ overnight. Culture medium 271 (100 mL) was inoculated with 0.3 mL of the *E. coli* culture from TSB 271 and incubated at 37 ℃ for 3 hrs. A 1-mL aliquot of inoculated *E. coli* culture was added to a sterile conical tube containing 9 mL of soft agar (0.5% agar) in a water bath between 40 ℃ and 50 ℃. One millimeter of MS2 was added to the tube containing *E. coli* and agar, the mixture was shaken thoroughly, and then it was poured into a petri dish. To attain the countable range of 30–300 PFU/mL, serially diluted MS2 samples were used. After the agar hardened, the plate was inverted and placed in an incubator at 37 ℃ overnight. Plaques on each plate were enumerated and the titer of the sample was determined by multiplying the dilution factor times the plaque count.

Spraying Medium

Three types of spraying media were tested, DI water, BE and AS. DI water was included to explore properties of the naked virus. BE (0.3 vol %) was used to provide nutrients, which can also contribute encasement. Beef extract is a mixture of peptides, amino acids, nucleotide fractions, organic acids, minerals and some vitamins, derived from infusion of beef (Cote, 1999). AS (0.6 vol %), 0.3% mucin from porcine stomach (Sigma–Aldrich, M1778) plus salts in DI water as a mucus simulant was used to mimic human respiratory fluid. Mucin—viscous glycoproteins comprising approximately 75% carbohydrate and 25% amino acids linked via glycosidic bonds between *N*-acetylgalactosamine and serine or

threonine resides—readily forms a gel in water (Bansil et al., 1995). The details of AS composition were reported in Woo et al. (2010).

Droplet and Aerosol Loading System

The experimental set-up for loading droplets and aerosols containing viruses onto the substrate is displayed in Figures 6-1A and 6-1B, respectively. A 2.4-MHz ultrasonic nebulizer (241T, Sonear, Farmingdale, NY, USA) was used to generate droplets containing viruses with a flow rate of 2 Lpm. The MS2 suspension in the reservoir was prepared by dispersing 1 mL of stock solution in 25 mL of spraying medium (i.e., DI water, BE or AS). Circular coupons (Φ= 2.54 cm) were cut from a 3M 1870 (NIOSH-certified N95) FFR. The droplets produced entered the chamber and loaded onto the surface of FFR coupons for 5 min. Each filter was then cut into four equal quadrants for UV exposure. Droplet size is affected by environmental conditions such as RH and temperature. Loading of droplets onto filter coupons was conducted at room temperature (20 ± 3 ℃) and HRH.

A Collison nebulizer (CN25, BGI Inc., Waltham, MA, USA) was used to generate the aerosol containing viruses, with a flow rate of 6 Lpm. The MS2 suspension in the nebulizer was prepared by dispersing 2 mL of viral stock solution in 50 mL of nebulizer medium. The aerosol from the nebulizer entered the mixing chamber and was mixed with dry or wet air as appropriate to adjust RH. Loadings were applied at each of the three RHs (LRH, MRH, and HRH). The flow was split into three streams toward the filters (Φ= 47 cm, 3M 1870) to deliver 4 Lpm, corresponding to a face velocity of 5.3 cm/s, a standard face velocity for air filter system testing (U.S. Army, 1998). After loading with aerosol for 30 min at the selected RH, the filter was removed and cut into equal quadrants to prepare for UV exposure.

UV Exposure

During UV exposure, the UV-C (254 nm) lamp (UVG-11, Ultraviolet Products, Cambridge, UK) was adjusted to a height of 10 cm. UV intensity of 1.0 mW/cm^2 was

measured using a radiometer (PS-300, Apogee, Logan, UT, USA). The quadrants were placed on a petri dish in a chamber and exposed to UV for different exposure times (0–2 h) at the selected RH. One quadrant used as a control was not exposed to UV; the other three were exposed to UV for different times. All were evaluated after the maximum exposure time for a fair comparison.

Dry/wet air was fed into the chamber to adjust the relative humidity in the system. After the maximum exposure time, each quadrant was placed in a 50-mL conical tube containing sterilized DI water and agitated with a wrist action shaker (Model 75, Burrell Scientific, PA) inclined 20^{o} for 15 min to extract MS2. The MS2 extracted was assayed with the single-layer method. IE was determined by comparing the count from the irradiated coupon with that from the paired control:

$$\mathrm{IE} = \frac{PFU_{\mathrm{ctl}}}{PFU_{\mathrm{exp}}} \tag{6-1}$$

Triplicate tests for each condition and duplicate assay were conducted. Two-way analysis of variance (ANOVA) and three-factor ANOVA were used for statistical analysis (Design-Expert® 8.0). The coefficient of variation of amounts loaded on the quadrants was less than 20%. Scanning electron microscopic (SEM, JEOL JSM-6330F, JEOL Inc.) images of filters contaminated with viruses generated in different media were taken and compared to investigate the protective effect of solid components.

Results and Discussion

Effect of Transmission Mode with Different Media

Log IE is plotted in Figure 6-2 as a function of UV irradiation time for both droplet and aerosol modes with three different nebulizer media. HRH was applied for both loading and UV irradiation. For droplet transmission mode, the log IEs were 4.32, 2.32, and 1.98 after 60-min irradiation in DI water, AS and BE, respectively, whereas for aerosol transmission mode,

the log IEs were 5.01, 2.68 and 2.32 in DI water, AS and BE, respectively. The IEs in this figure depend on three parameters:

1) UV irradiation time: Extending the irradiation time increased the IE because the UV dose increased. When the application time was changed from 30 to 60 min, the dose of UV irradiation doubled from 1.8 J/cm^2 to 3.6 J/cm^2, increasing the amount of damage to nucleic acids.

2) Transmission mode: IE for aerosols was higher than for droplets. Water in the droplets absorbs UV (Prescott et al., 2006; Kowalski, 2009), and shielding of viruses near the center of the aggregate likely also contributes to this trend. The size of droplets generated from the ultrasonic nebulizer was around 9–10 μm (Woo et al., 2010) whereas aerosols from the Collison nebulizer measured 1–2 μm (May, 1973). The evaporation time for a 1-μm droplet at HRH is 0.0077 s at 20 ℃. As the residence time of aerosol in the mixing chamber was 0.21 s, these particles reached equilibrium during transit. However, the evaporation time of 9–10 μm droplets at HRH and 20 ℃, 0.63–0.7 s, is much longer than the residence time. So the larger droplets retain much of their water at contact.

The equations used are as follows (Hinds, 1999):

$$t_{\text{evaporation time}} = \frac{R\rho_{\text{p}} d_{\text{d}}^2}{8D_{\text{v}}M\left(\frac{p_{\text{d}}}{T_{\text{d}}} - \frac{p_{\infty}}{T_{\infty}}\right)} \tag{6-2}$$

where R is the ideal gas law constant, ρ_{p} is the density of particle, d_{d} is the droplet size, D_{v} is the diffusion coefficient of water vapor molecule, M is the molecular weight of water, T_{∞} and p_{∞} are the temperature and pressure away from the droplet surface, i.e., the environmental conditions, and T_{d} and p_{d} are the same conditions at the droplet surface. Room temperature (20 ℃) was applied for T_{∞} and the equation below was used to determine T_{d}.

$$T_{\text{d}} = T_{\infty} + \frac{(6.65 + 0.345T_{\infty} + 0.0031T_{\infty}^{\ 2})(S_R - 1)}{1 + (0.082 + 0.00782T_{\infty})S_R} \tag{6-3}$$

where S_R is the saturation ratio. The partial pressure in kPa at a given temperature in K is calculated according to

$$p_{\mathrm{d}} = \exp(16.7 - \frac{4060}{T_{\mathrm{d}} - 37}) \tag{6-4}$$

3) Spraying medium: IEs in AS and in BE were much lower than in DI water for both aerosol and droplet transmission. The likely reason for this difference is a protective effect caused by solids in both AS and BE. Based on the composition of the media, the volume fractions of solids in DI water, BE and AS were 1×10^{-4}, 3.1×10^{-3} and 6.0×10^{-3}, respectively, after complete evaporation—DI water has a much lower solid content. This mode of protection is supported by SEM images, shown in Figure 6-3, of filters contaminated with MS2 viruses aerosolized in different media. Images of MS2 generated in DI water and loaded on the filter (Figure 6-3B) show aggregates in the range 100 nm–1 μm on the substrate. Riemenschneider et al. (2010) and Jung et al. (2009) reported MS2 aggregates of around 200 nm for the MS2 suspension and 30–200 nm for captured aerosol particles.

MS2 aerosolized in BE instead of DI water was captured as oval-to-spherical features as shown in Figure 6-3C. As displayed in Figure 6-3D, precipitated BE solids formed a thick shell encapsulating the MS2 virions and/or aggregates. The solids in AS are water-insoluble mucin and various water-soluble salts. To test the hypothesis that the salts and mucin act separately to afford protection (Lee et al., 2011), MS2 was aerosolized from AS media prepared both with and without mucin. As aerosolized virions and aggregates load onto the filter, it is possible for them to form a wide size range of superaggregates. Figure 6-3H shows that grape-shaped superaggregates were observed in the absence of mucin. Multivalent cations of the soluble salts (Mg^{2+} and Ca^{2+}) can interact with negatively charged features on the surface of MS2 to promote a high degree of virus aggregation (Sjogren and Sierka, 1994). Encasement by a thin layer through the crosslinking network (Figure 6-3F) appears to result

from gel formation caused by the presence of mucin. The similarity of the underlying structures in Figures 6-3F and 6-3H suggests that mucin contributes little or nothing to the aggregation process and simply covers the final configuration.

To isolate the UV protection effect of water-insoluble mucin in AS, the IEs of MS2 nebulized in mucin-free AS medium and mucin medium were investigated. For fair comparison, 0.3% and 0.6% of volume fractions were considered. As shown in Figure 6-4, for volume fraction of 0.3%, the log IEs in 0.3% mucin-free AS were 3.66, 4.33 and 4.94 after 30-, 60-, and 120-min irradiation, respectively, whereas the log IEs in 0.3% mucin medium were 3.12, 3.94, and 4.37 after 30-, 60-, and 120-min irradiation, respectively. The lower log IEs in mucin-free AS compared to those in DI water suggest a protective effect of water-soluble salts. The higher IE in 0.6% mucin-free AS compared to 0.3% mucin-free AS was expected because salts increase hydration and then more water can shield viruses. Contrary to that expectation, the difference between 0.3% and 0.6% mucin-free AS was not significant. The log IEs in 0.3% mucin-free AS were higher than those in 0.3% mucin medium (salt-free AS), indicating better protection by water-insoluble mucin than by various water-soluble salts. Relatively higher IEs in both mucin-free AS and salt-free AS than those in AS suggest that both encasement by water-insoluble mucin and aggregation by water-soluble salts contribute protection.

In addition, that the encasement in BE provided better protection than in AS—even through the volume fraction of solid in BE is only half of that in AS—appears to indicate that the organic solids in BE are stronger absorbers at 254 nm and thus provide more-effective protection from UV radiation.

Effect of RH during Both Loading and Inctivation

Log IEs measured after aerosol loading for 30 min followed by UV exposure for 60 min at different RHs are displayed in Figure 6-5; the corresponding general factor ANOVA

results appear in Table 6-1. Because the strong effect of the spray medium (> 80% contribution, not shown) made it difficult to distinguish the RH effect, two-way ANOVA was also conducted for each spray medium. Referring to Figure 6-5, upon completion of the experiment, the highest inactivation efficiency, around log 5.8, was seen in filters subjected to UV after applying the MS2 in DI water at LRH. However, it should be noted that the actual IE at this condition might be somewhat higher because values measured under LRH during UV inactivation after aerosol loading in both LRH and MRH conditions were at the detection limit of our experimental system.

For MS2 delivered in DI water, both RH during UV inactivation ($p < 0.0001$) and RH during aerosol loading ($p < 0.0001$) are significant, as is the interaction for both RHs ($p = 0.0118$). This may be attributed to a combination of intrinsic susceptibility of MS2 and UV exposure susceptibility of MS2, augmented by stress imposed on MS2 by aerosolization under different loading RHs. The second susceptibility was the more important parameter because the contribution of RH during inactivation (75%, not shown) was five times that of RH during aerosol loading (15%, not shown). In general, IEs at LRH were higher than those at both MRH and HRH, suggesting a protective contribution by a water layer. This is broadly consistent with a report that inactivation efficiency of UV against microbes dramatically dropped off above 70% RH (Burgener, 2006).

Unlike in DI water, IEs in BE were not significantly influenced by RH during virus loading, during UV irradiation for 60 min, or by their interaction—IE was in the range of 2.4–2.8 logs under all nine sets of RH conditions. The contributions of both RH regimes are less than 6%, although the contribution of RH during inactivation is 1.9 times that of RH during virus loading, suggesting some effect of water on protection by the solid content. To investigate the protective effect of solid contents in BE directly, intensities of a 1.0-mW/cm^2 UV beam after penetrating BE solutions of different concentrations were compared. Values

of 0.97, 0.78, 0.62 and 0.41 mW/cm^2 were found after penetration of solutions containing 0%, 0.1%, 0.3%, and 0.5% BE, respectively, verifying the conclusion above that UV absorbers in BE contribute significantly to its observed protective effect.

In AS, IEs fell in the range 2.7–3.2 logs under all conditions, showing that dissolved solids in these experiments eliminated sensitivity of the MS2 particles to RH during loading. However, RH during inactivation was a statistically significant factor (p = 0.0204). To distinguish the significance of the RH levels, a Tukey comparison was conducted and a difference was identified at HRH. Compared to BE, AS was less protective—even though the solid fraction of AS is larger—and the contribution of RH at both stages was larger (38%, not shown) in AS than in BE (6%, not shown). These are consistent with conclusions above from SEM images and UV absorption results that the two solid media act by different routes: solids in BE appear to encase the virions in a shell that provides environmental protection and some UV screening. In contrast multivalent cations in AS appear to gather virions and promote formation of superclusters that are coated with a layer of mucin as a gel, which affords less protectivity and is more sensitive to water than the BE shell

Virus Susceptibility

When microbes are exposed to a biocidal factor, first-order decay of viability is commonly observed (Brickner et al., 2003), and the IE of UV irradiation as a function of time can be defined as:

$$IE = \frac{N_o}{N_s} = (A \times e^{-KCt})^{-1} \tag{6-5}$$

where A is the fraction of the total initial population subject to fast decay, N_s is the concentration of airborne virus surviving after UV exposure, N_o is the concentration of airborne virus before UV exposures, C is the UV intensity factor (W/m^2), t is time (s), and K is the virus susceptibility factor (m^2/J).

Although this equation gives a straight line in a semi-logarithmic representation, two characteristics at the beginning and end (e.g., shoulder (IE < 90%) and tailing) were not incorporated (Kowalski and Bahnfleth, 2000; Brickner et al., 2003). The shoulder represents the threshold dose; if the dose is insufficient, the virus shows negligible response or even recovers from the damage. Meanwhile, the slow decay curve at tailing might be from a resistant minority of viruses and/or reaching the detection limit (Kowalski & Bahnfleth, 2000).

Table 6-2 lists first-order decay *K*s derived from the experimental results. A higher *K* was observed for both loading and exposure in LRH. In addition, and as expected, *K* at LRH in DI water was higher (by more than 10 x) than in AS or BE. Reported UV susceptibilities of some other viruses are listed in Table 6-3. *K* for viruses is in the range 0.01 – 10. The value of MS2 in DI water is similar to that of corona virus, which is of the same genomic type. Low *K* values for double-stranded and DNA-type viruses were expected both because their undamaged strands are able to repair UV-damaged segments and because RNA is a stronger UV absorber than DNA (Kowalski, 2009). However, for dsDNA type, values of *K* were found to vary widely, depending on the individual characteristics of viruses, rather than following a simple classification by genome type.

Summary

This study examined the effect of transmission mode and environmental conditions on sensitivity of MS2 coli phage to UV disinfection. IE was lower following droplet transmission than aerosol transmission, largely owing to the higher water content of the larger droplets, which shields viruses from UV exposure. Lower *K*s were observed for viruses in BE and AS than in DI water, which is attributed to protective effects exerted by solids present in the respective media. In these experiments BE was slightly more protective than AS and acted by some different mechanisms. The protective effect of solids followed the order water-

insoluble solid (beef extract powder) > water-insoluble viscous solid (mucin) > water-soluble solid (salts). When these solids were present, RH was not a significant parameter in decontamination by UV exposure. If the susceptibility factor is obtained for the target microbial species, the appropriate UV dose for surface decontamination can be determined.

Table 6-1. Statistics in general factor Analysis of Variances

	p value
Three-factor ANOVA for three media	
spray medium	< 0.0001*
RH during UV inactivation	0.0197*
RH during aerosol loading	< 0.0001*
Spray×RH during aerosol loading	< 0.0001*
Two-way ANOVA for DI water	
RH during aerosol loading	< 0.0001*
RH during UV inactiation	< 0.0001*
RH during UV inactivation × RH during aerosol loading	0.0118*
Two-way ANOVA for beef extract	
RH during aerosol loading	0.2202
RH during UV inactivation	0.4188
RH during UV inactivation × RH during aerosol loading	0.6278
Two-way ANOVA for artificial saliva	
RH during aerosol loading	0.4569
RH during UV inactivation	0.0204*
RH during UV inactivation × RH during aerosol loading	0.9983

SS: sum of squares DF: degree of freedom MS: mean square *Significant parameter

Table 6-2. Virus susceptibility factor *K* (m^2/J) for aerosol transmission under different conditions

RH condition		*K* in		
Loading	UV exposure	DI water	AS	BE
LRH	LRH	0.764	0.056	0.046
	MRH	0.267	0.043	0.040
	HRH	0.273	0.045	0.039
MRH	LRH	0.222	0.061	0.051
	MRH	0.189	0.058	0.044
	HRH	0.209	0.051	0.041
HRH	LRH	0.231	0.055	0.042
	MRH	0.222	0.056	0.044
	HRH	0.207	0.044	0.038

Table 6-3. Virus susceptibility factors (m^2/J) from other studies

Test microbe	Type	< 68%RH	>75% RH	Reference
Adenovirus	dsDNA	0.039	0.068	Walker & Ko (2007)
Vaccinia	dsDNA	6.01	1.42	McDevitt et al (2007)
Phage T7	dsDNA	0.33	0.22	Tseng & Li (2005)
Phage Phi 6	dsRNA	0.43	0.31	Tseng & Li (2005)
Phage phi X174	ssDNA	0.71	0.53	Tseng & Li (2005)
Corona virus	ssRNA	0.38	-	Walker & Ko (2007)

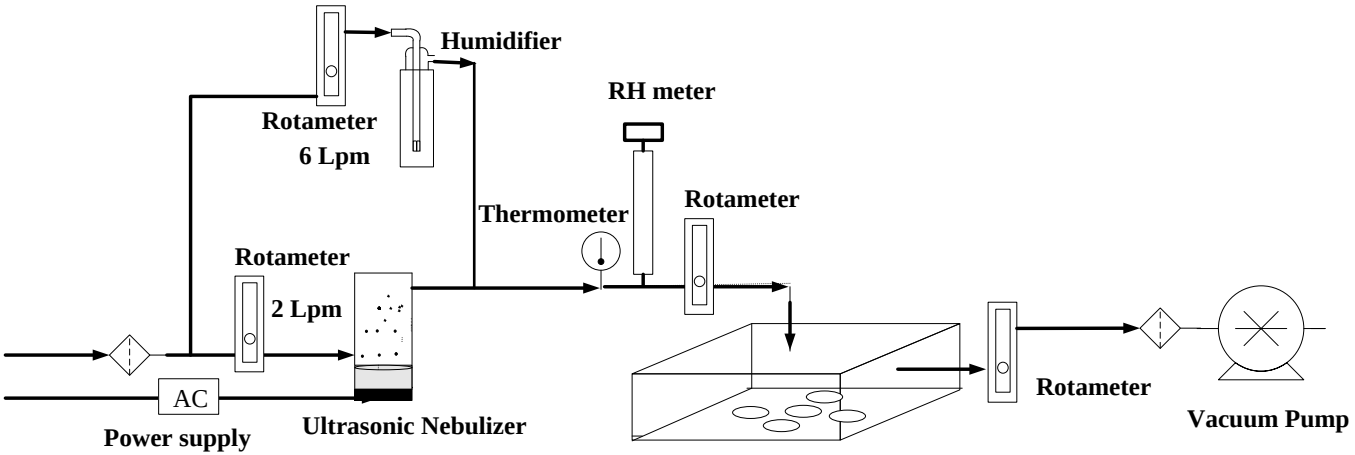

(A)

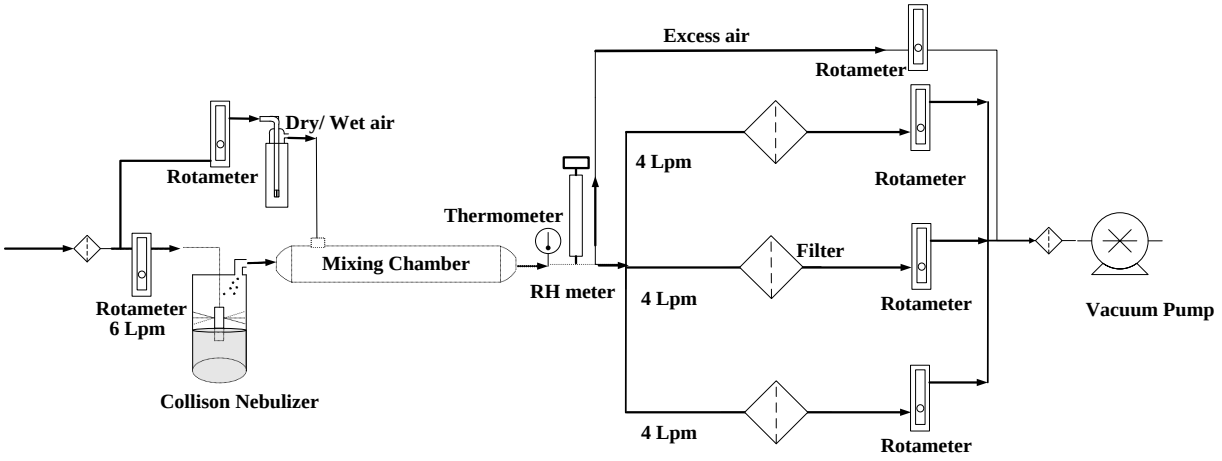

(B)

Figure 6-1. Schematic diagrams: A) droplet loading system and B) aerosol loading system

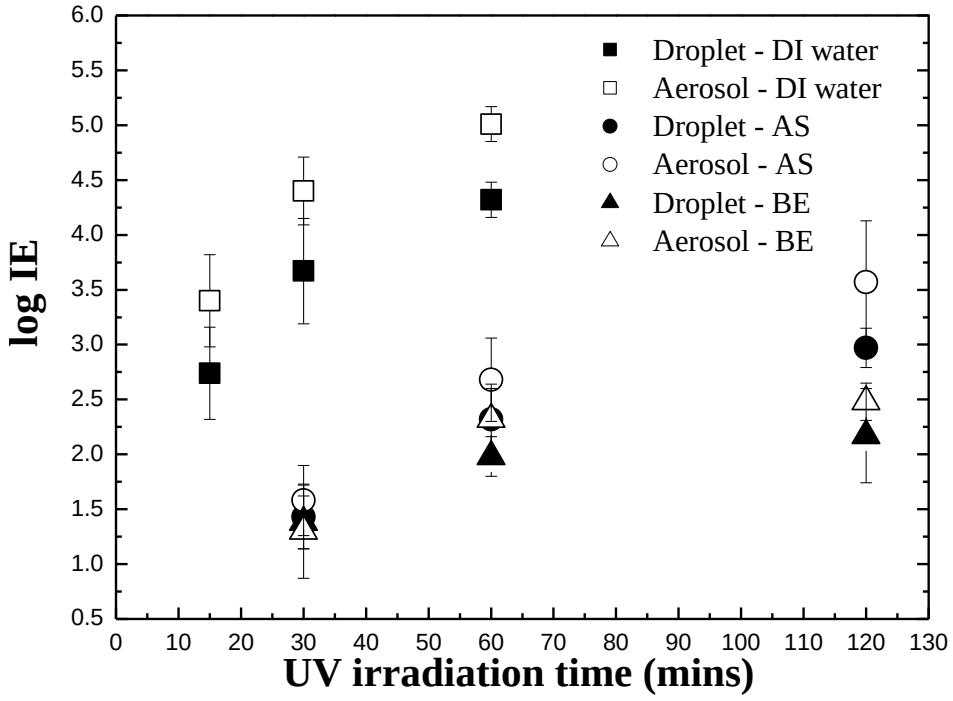

Figure 6-2. Log inactivation efficiency by UV exposure at HRH for droplet and aerosol transmission mode as a function of UV irradiation time in different nebulizer media at HRH during virus loading

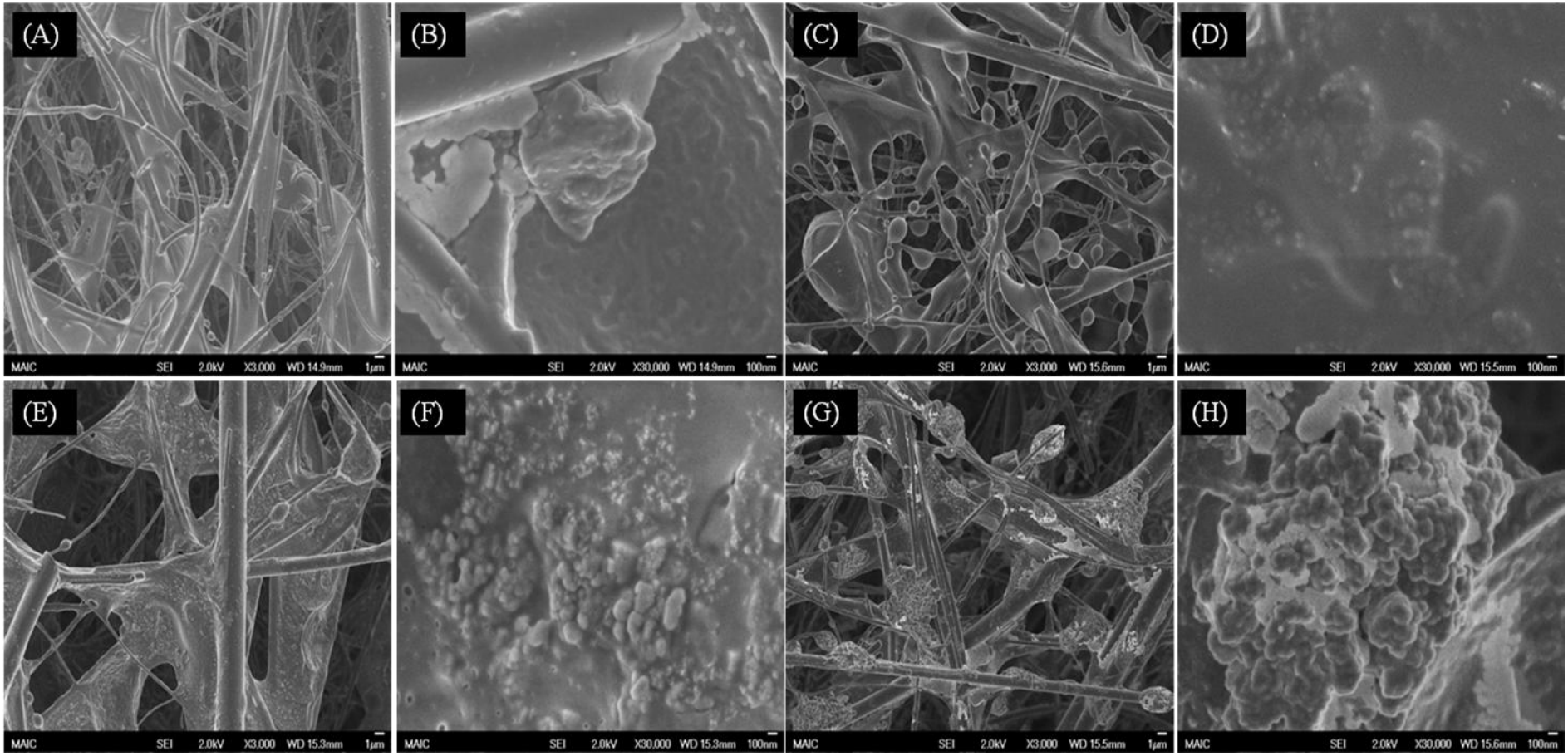

Figure 6-3. The SEM images of the filter contaminated with viruses aerosolized: A) and B) DI water, C) and D) 0.3% beef extract, E) and F) artificial saliva, and G) and H) artificial saliva without mucus under HRH. Magnification of A), C), E), and G) 3,000× and B), D), (F), and H) 30, 000×.

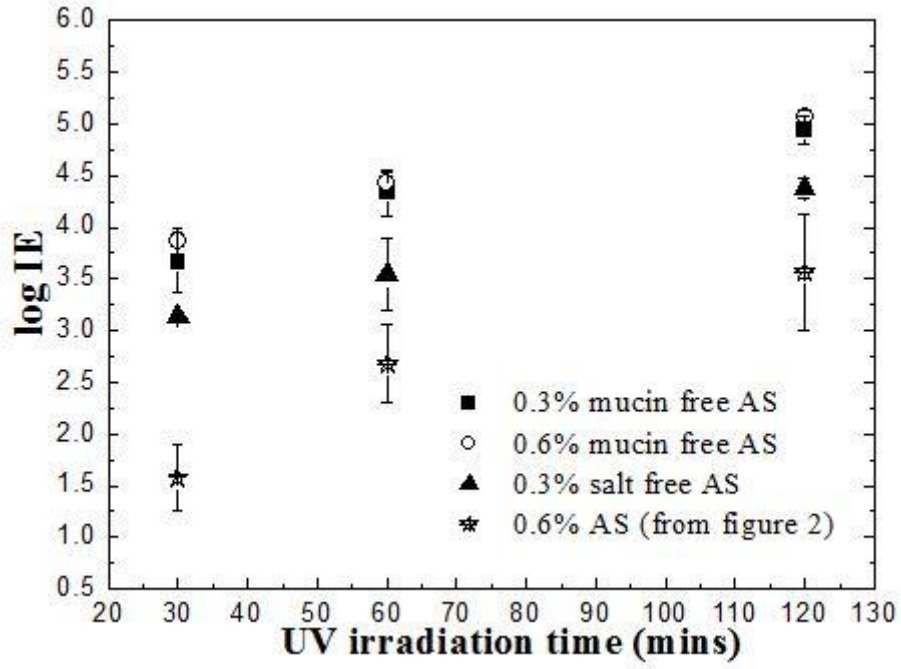

Figure 6-4. Log IE after virus loading and UV exposure at HRH for aerosol transmission mode as a function of UV irradiation time in 0.3% and 0.6% mucin-free artificial saliva and 0.3% salt-free artificial saliva

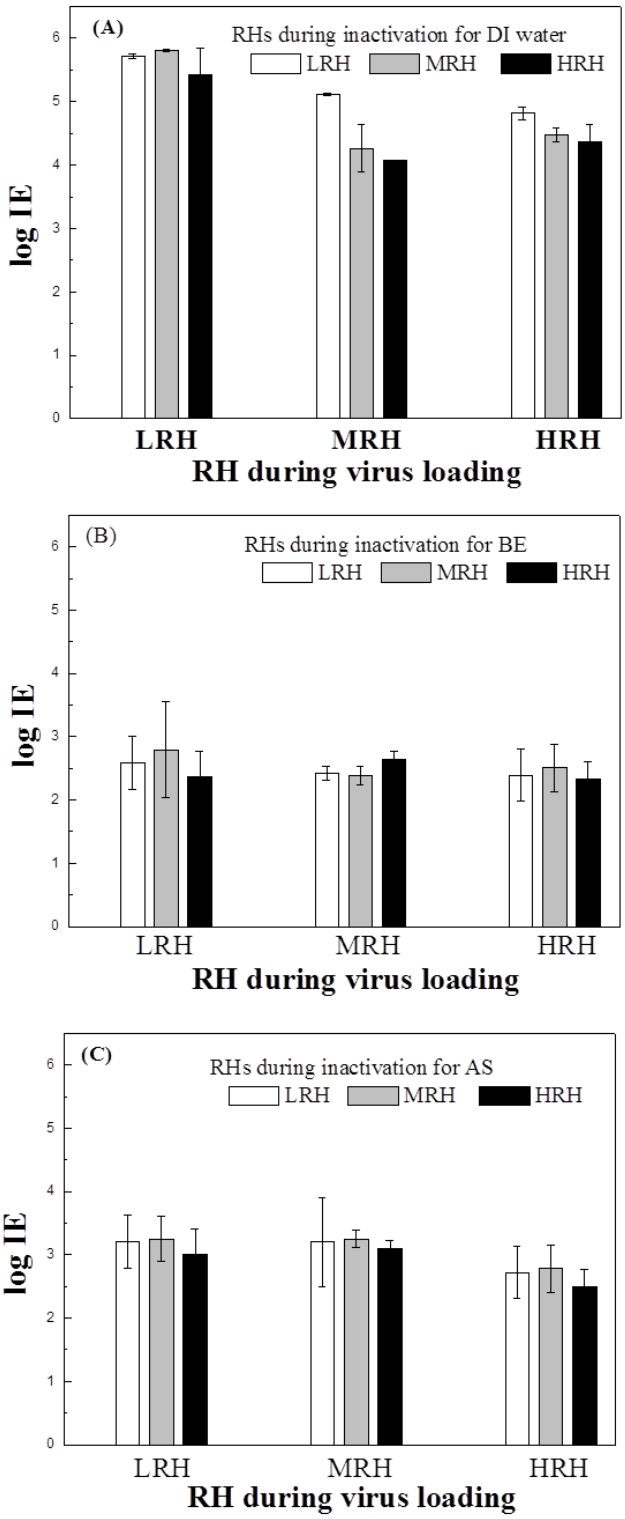

Figure 6-5. Log natural decay and inactivation efficiency as a function of relative humidity during both loading and UV inactivation: A) DI water, B) 0.3% beef extract, and C) artificial saliva.

CHAPTER 7
EFFECTS OF RELATIVE HUMIDITIES AND SPRAY MEDIA ON SURVIABILITY OF VIRAL AEROSOLS

Background

Viral aerosols, such as smallpox virus, SARS virus, and influenza virus, have been identified as the most common cause of respiratory infectious diseases acquired from recent outbreaks (CDRF, 2006; CDC, 2009). Because they are related to the severe pandemic events causing death (CDC, 2009), the public's concern about the viral aerosol hazard has been spurred, and their interest in the protection device such as a respirator and inactivation technology like ultraviolet germicidal irradiation (UVGI) to prevent their spread has increased. The performance of the protection and decontamination is determined by several factors related to the characteristics of viruses. For example, filtration efficiency is dependent on the size distribution of aerosols containing viruses (Hinds, 1999), and inactivation efficiency of UVGI is determined by relative humidity (RH) and media related to susceptibility of viral aerosol as well as intensity and exposure time of UV (Woo et al., Submitted).

To improve the efficacy of filtration and inactivation technology, understanding the characteristics of viral aerosol is of seminal importance. The naked virion ranges from 20 nm to 300 nm in diameter but viruses in natural system exist in various size ranges from ultrafine (< 0.1 μm), submicron (< 1 μm), to supermicron (> 1 μm) because of aggregation of several viruses, attachment of viruses onto other airborne particles, or encasement of viruses by droplets of respiratory secretions. Inhaled particles can deposit in various respiratory regions. After they are deposited, the aggregates may disperse into numerous individual virions. More than 400 different viruses with different lethal doses (LDs) result in human diseases such as rubella, influenza, measles, mumps, smallpox, and pneumonia, which involve the respiratory system either directly or indirectly (Prescott et al., 2003). Some viruses cause diseases with

only few lethal doses. For instance, ebola virus (Φ= 30 nm), with a lethal dose of 10-100, results in ebola hemorrhagic fever with fatality in humans ranging from 50-89% (Biosafety level 4) (Brion and Silverstein, 1999). If one aggregate of ebola viruses is released from a filter surface and inhaled into the respiratory system as a 300 nm particle, the viruses may disperse in the pulmonary fluid and the final dose of 1000 can exceed well over the lethal level.

The aggregation, attachment, and encasement of viruses also facilitate resistance to environmental stresses, because of shielding effect (Kowalski & Bahnfleth, 2007) and different stability at each condition. Lipid viruses are stable at lower RH, whereas non-lipid viruses are stable at higher RH (Benbough, 1971). In addition, viruses lose their viabilities in the presence of a NaCl- or peptone containing medium, whereas phenylanine protects a virus from inactivation at various RH levels (Dubovi & Akers, 1970; Trouwborst & de Jong, 1973). Tseng and Li (2005) demonstrated that both the morphology of the virus particles and the presence or absence of a lipid envelope significantly affected the collection efficiency of four bioaerosol samplers and the viability of collected virus sample.

The purpose of this study was to investigate the environmental condition like spray medium and RH on the stability for virus. By comparing the infectious viruses obtained by plaque assay with total viruses obtained from polymerase chain reaction (PCR), the stability factor was determined for different environmental conditions. Such information can provide a very useful tool in designing an effective strategy to improve filtration and inactivation efficiency and for assessing the risk imposed by respiratory deposition of viral aerosol.

Materials and Methods

Test Virus and Spraying Medium

As a viral simulant, MS2 bacteriophage (MS2) was selected after considering several factors including ease, economics, biosafety level, size, shape, host, and available molecular

techniques. MS2 (Φ = 27 nm) is an icosahedral, non-enveloped, linear ssRNA genome virus which only infects *Escherichia coli* (*E. coli*) strain C3000. In addition, it contains four important proteins (i.e., capsid coat protein, RNA replicase β chain protein, lysis protein, assembly protein), and can be easily analyzed by PCR and enzyme-linked immunosorbent assay (ELISA). It is commonly used as a non-pathogenic surrogate to human pathogenic viruses (e.g., rotavirus, influenza, poliovirus, and rhinovirus) (Brion & Silverstiein, 1999).

The MS2 virus stock was prepared by suspending freeze-dried MS2 (ATCC® 15597-B1™), which contain a small amount of milk proteins and organic molecules for virus preservation, in filtered deionized (DI) water to a titer of 10^{11}–10^{12} plaque-forming units (PFU)/mL and stored at 4 °C. A single layer bioassay was used to enumerate the infectious viruses with *E. coli* (ATCC® , 15597) as the host. The details of the assay are described in Woo et al. (2011).

Three types of spraying media (i.e., DI water, 0.3 vol% beef extract (BE) and artificial saliva (AS)) were selected. DI water was included to explore properties of the naked virus whereas BE was used to provide a source of protein, which can also contribute encasement, and AS was used to mimic human respiratory fluid. The details of AS composition were reported in Woo et al. (2010). For fair comparison of protein effect between BE and AS, 0.3 vol% was selected because the concentration of the protein component (mucin) in AS was 0.3 vol%.

Experimental Design and Tasks

The schematic of the experimental set-up is shown in Figure 7-1. Four tasks of experiments (i.e., collection efficiency of BioSampler (Task 1), the particle size distribution (Task 2), plaque assay (Task 3), and PCR analysis (Task 4)) were performed in this study. For Task 1, PSL particles (Duke Scientific) with different sizes from 30 nm to 300 nm were used to determine the collection efficiency of BioSampler at the specific size and flow rate.

As displayed in Figure 7-1A, a six-jet Collison nebulizer (BGI Inc., CN25) was used to generate aerosols containing viruses with a flow rate of 6 Lpm. The second dry air was added to the mixing chamber to achieve LRH in the system and then rejoined the aerosol flow. After penetrating the mixing chamber, the aerosols in the combined flow were collected in the BioSampler (SKC Inc., Eighty Four, PA, USA) containing 15 mL of DI water at different flow rates. The collection efficiency of the BioSampler is defined as:

$$E_{dp}(\%) = (1 - \frac{N_{dp,down}}{N_{dp,up}}) \times 100 \quad (7\text{-}1)$$

where $N_{dp,\,down}$ and $N_{dp,\,up}$ are the number concentrations of particles collected by condensation particle counter (CPC) at specific particles size (d_p) downstream and upstream of the BioSampler, respectively.

For Tasks 2-4, the MS2 in three different spraying media (i.e., DI water, 0.3 % BE, and AS) was used instead of PSL particles in DI water. To elucidate RH effect on the stability of viruses, three RHs ((i.e., low RH (LRH, 30±5%), medium RH (MRH, 60±5%), and high RH (HRH, 90±5%)) were applied. Task 2 experiments were performed to measure the number, surface, and mass-based particle size distributions of viral aerosol by using scanning mobility particle sizer (SMPS) whereas Task 3 experiments were to obtain size distribution of the infectious viruses at specific sizes by using plaque assay. The experimental set-ups for Tasks 2-4 is illustrated in Figure 7-1B. For Task 3, by adjusting the applied voltage on the DMA, only particles of the corresponding size can penetrate the electrostatic classifier. Seven specific sizes from 30 nm, which is related to the MS2 virion, to 230 nm, which is close to the upper limited particle size measured by the SMPS at a flow rate of 1.5 Lpm and 5 more sizes (i.e., 60, 90, 120, 150, and 180 nm) between them were studied. The size-classified particles were collected by the BioSampler. To minimize any loss in collected viruses over long sampling time and reaerosolization, a flow rate of 4.5 Lpm and sampling time of 5 mins

were applied (Riemenschneider et al., 2010). The number of viable viruses collected in BioSamplers was enumerated by using the single layer bioassay. The size distribution function of infectious viruses based on the results of the plaque assay was calculated following Equation 7-2.

$$PFU/cm^3 = \frac{C_{PFU} \times V}{C_{Eff} \times Q_{inlet} \times \Delta \log d_p \times t} \quad (7\text{-}2)$$

where C_{PFU} is the virus concentration in the collection medium of the BioSampler, V is the volume of the collection medium of the BioSampler, C_{Eff} is the correction factor for the collection efficiency of the BioSampler for specific particle size from Task 1, Q_{inlet} is the inlet flow rate of DMA, t is the collection time of the BioSampler, and $\Delta\log d_p$ is logarithm of the bin size of the DMA.

The number of MS2 PFU per particle ($N_{PFU)}$ was determined by dividing the C_{PFU} by the total aerosol particles and the theoretical N_{PFU} was calculated with the volume fraction of MS2 in the solid content in the spray medium for the given particle size, according to Equation 7-3.

$$N_{Theo\ PFU} = \frac{V_{dp} \times F_{MS2}}{\left(\frac{\pi}{6} d_{MS2}{}^3\right)} \quad (7\text{-}3)$$

where V_{dp} is the volume of the droplet nulei, F_{MS2} is the volume fraction of infectious viruses obtained from the plaque assay for MS2 stock suspension, and d_{MS2} is the size of MS2 virion (27 nm). Based on the composition of the media, the volume fractions of solids in DI water, BE and AS were 1×10^{-4}, 3.1×10^{-3} and 6.0×10^{-3}, respectively. The corresponding particle size of MS2 aerosols generated were 0.046 d_d, 0.145 d_d, and 0.179 d_d, respectively, when d_d is the diameter of the droplet.

The liquid sample assayed in Task 3 was also used for PCR to determine the concentration of total viruses including infectious and non-infectious viruses with an assumption of no RNA distortion during the test (Task 4).

Before proceeding to the PCR, nucleic acid extraction was conducted with 4-mL samples from the BioSampler. Because the concentration was insufficient to compare, this sample was concentrated to 280 µL by using an Amicon ultra-centrifugal device (UFC 810096, Millipore, Bedford, MA, USA). The concentrated sample was processed using RNA extraction with a QIAamp Viral RNA mini kit (QIAGEN Inc., Valencia, CA, USA) and then the aliquots were stored at -80 °C.

Real-time PCR assays were designed in O'connell et al. (2006), and the sequence data for MS2 were obtained as a target of RNA replicase β from National Center for Biotechnology Information (NCBI) with accession number of NC_001417. The target sequences were as follow:

MS2-F and MS2-R: Forward and reverse primers binding to target sequences on the internal MS2 bacteriphage control, 80 pmol/ µL each.

MS2-F: 5'-TGG CAC TAG CCC CTC TCC GTA TTC ACG-3'

MS2-R: 5'-GTA CGG GCG ACC CCA CGA TGAC-3'

MS2 ROX/Probe: Taqman probe that hybridizes to a target sequence on the MS2 internal control 80 pmol/ µL.

5' ROX-CAC ATC GAT AGA TCA AGG TGC CTA CAA GC-BHQ2-3'

In this study, primers and probe used were obtained from Applied Biosystem (ABI). Enzyme and buffers used were from the Invitrogen Superscript™ Platimium kit.

One step Quantitative PCR (qPCR) was carried out on ABI 7500 under the following condition: incubation at 50 ^{o}C for 15 mins followed by further incubation at 95 ^{o}C for 2 mins and then 40 cycles of amplification with denaturation at 95 ^{o}C for 15 s and annealing and

extension at 60 ^{o}C for 30 s, acquiring on the ROX channel and FAM channel. MS2 RNA (165948, Roche Diagnostics, Indianapolis, IN, USA) with 5 serial dilutions and DNase–RNase-free water sterilized were substituted for MS2 RNA sample as the positive and negative controls.

By comparing the threshold cycle (C_T) for positive control to that for RNA samples, the total number of viruses (both infectious and non-infectious viruses) was calculated. The number of MS2 RNA per particle (N_{RNA}) was then determined by dividing it by the total aerosol particles measured by the CPC following Equation 7-4, and then the stability factor of virus can be obtained by comparing the N_{RNA}/N_{PFU}.

$$N_{RNA} = \frac{RNA(ng)\,in\ the\ Sample \times (10^{-9}\ g/ng)}{\left(\frac{1.0\times10^{6}\ g}{1mol}\right)\times\left(\frac{1mol}{6.02\times10^{23}\ molecules}\right)} \Big/ N_{aerosol\ particles} \times C_{eff} \qquad (7\text{-}4)$$

Results and discussion

Collection Efficiency of BioSamplers

Figure 7-2 shows the collection efficiency of the BioSampler as a function of particle size. At a flow rate of 12.5 Lpm, the collection efficiency increased as particle size increased except ultrafine size (~30 nm), which is explained by the major collection mechanisms of impaction and centrifugation for large particles and diffusion for small particles (Hinds, 1999). At 4.5 Lpm, the collection efficiency for all particle size tested was below 15%, which is presumably expressed by the reduced collection by inertia impaction and centrifugation because of low flow rate. Lin et al. (2000) investigated the effect of flow rate on collection efficiency of BioSampler and observed increases in collection efficiency as a function of flow rate. They used three flow rates of 8.5, 10.5, and 12.5 Lpm and large particles (0.8 and 1.0 μm), supporting higher collection efficiency at 12.5 Lpm for large particles. Hogan et al. (2005) also noted that low collection efficiency of below 20% at the flow rate of 3.5-12.5

Lpm for 25 nm particle. In addition, because liquid behavior in BioSampler was turbulent beyond 8.7 Lpm, the collection efficiency of 300 nm dramatically increased after 8.7 Lpm. The data reported by Hogan et al. (2005) agree well for smaller (30 nm) and larger particles (300 nm) tested. Because a flow rate of 4.5 Lpm was employed for further test to avoid reaerosolization (Riemenschneider et al., 2010), the collection efficiency of 12%, 8%, 6%, 4%, 4%, 6%, and 7% for 30, 60, 90, 120, 150, 180, and 230 nm, respectively, were applied as a correction factor for other tasks.

Size Distribution of MS2 in Different Environmental Conditions

Figure 7-3 displays the number-based particle size distribution for aerosols generated from MS2 suspension in DI water, BE, and AS under three RHs. As shown, the particle size distribution MS2 aerosols had a mode at approximately 27 nm, corresponding to the size of MS2 virion, at LRH/RT. The number-based particle size distributions for aerosols generated from MS2 suspension in DI water slightly increased as RH increased, as well as geometric standard deviation (GSD). This is explained by incomplete evaporation of water at higher RH condition although theoretically there was sufficient residence time for complete evaporation for three RHs.

The particle size distribution of MS2 aerosol generated in BE and AS was shifted to the larger particle size compared to that in DI water. The modes of MS2 aerosol generated in DI, BE, and AS were 28 nm, 68 nm, and 151 nm, respectively, at LRH. The mode shifted to the larger size according to the increased volume fraction of spray medium, as explained in Hinds (1999) and Hogan et al. (2005). These values for BE and AS shifted to the smaller and larger size, respectively, compared to the expectation of 84 nm and 106 nm. The larger size of AS is presumably because of the intrinsic property of mucin component in AS. Mucin is a viscous glycoprotein, which is 75% carbohydrate and 25% amino acids linked via glycosidic bonds between *N*-acetylgalactosamine and serine or threonine resides (Bansil et al., 1995).

Hence, gel formation of mucin can readily retain the water contents and retard the evaporation of water at even LRH condition.

Size Distribution of infectious MS2

The particle size distribution of infectious MS2 in DI water is displayed in Figure 7-4. To investigate the dimension of the particle size distribution of MS2, it was compared to number- and mass-based particle size distributions. The results showed that it followed the volumetric distribution. To verify this trend, the infectious PFU/particle was calculated and then regression analysis was conducted. The results are shown in Figure 7-5. When the same process was carried out for MRH and HRH, similarly, the slope of least square regression obtained for three RHs of around 3 was observed, as seen in Table 7-1. However, at MRH, the number of infectious virus was smaller compared to LRH although total particle concentration was higher. This can be explained by the different stability on RH (Prescott et al., 2006). Different from the other two RHs, the number of infectious MS2 at 30 nm was much lower than expected, indicating lower stability of virion at MRH condition. The slopes of N_{PFU} for BE and AS for three RHs were also obtained and listed in Table 7-1. The values are lower than that of DI water. They were were between 2 and 3 in BE whereas around 2 in AS.

Figure 7-6 shows the RNA of MS2 generated in DI water as a function of particle diameter at three RHs as well as the theoretical value ($N_{theo\ RNA}$) with an assumption of negligible impurity. Similar to N_{PFU}, the regression analysis of N_{RNA} for DI water was conducted as well as BE and AS, and the results are listed in Table 7-2. The slopes of N_{RNA} values in BE and AS were significantly lower than that of DI water. It can be explained by the higher volume fraction resulting from the presence of solid contents. BE consists of insoluble solids with hydrophobicity, causing the hydrophobic interaction with MS2 that attach MS2 to the surface of insoluble salts. The slope of N_{RNA} in AS was less compared to

the BE. This might be explained by the higher volume fraction and the surfactant property of mucin. Mucin tends to adsorb to hydrophobic surfaces via protein-surface interactions while holds water molecules via their hydrophilic oligosaccharide clusters. When MS2 was captured by mucin through hydrophobic interaction with MS2 protein, the hydrophilic part enabled viruses not to stick (Shi et al., 2000). Mantle and Husar (2003) reported that preincubation of plasmid-bearing *Yersinia enterocolitica* with intestinal mucin significantly reduced subsequent binding of the organism to polystyrene, suggesting that mucin may mask hydrophobic adhesions on the bacterial surface and make the microorganism more hydrophilic.

The stability of MS2 at specific sizes at different RHs was compared using the stability factor (N_{PFU} / N_{RNA}), as displayed in Figure 7-7. The stability of MS2 generated in DI water followed the order LRH > HRH > MRH ($p< 0.001$, Turkey's comparison < 0.05 for all), supporting Floyd et al. (1977). The stability factor of MS2 generally increased as a function of particle size, indicating the shielding effect of bigger particles. Indeed, the stability factor of MS2 at MRH was very small at smaller size; however, the value dramatically increased at larger size. For BE, it should be noted that the stability factors were higher compared to these value for DI water, indicating protection effect of beef extract. Schaffer et al. (1976) and Benbough (1971) reported low protein content in the medium led to a sharp decrease in viability and Schaffer et al. (1976) showed that the minimum concentration of protein for virus stability was 0.1%. The slightly lower stability of MS2 in BE at LRH might be explained by stress of MS2 by crystallization of solute (Trouwborst & de Jong, 1973; Hinds, 1999). With the same context, protective effect of AS was confirmed with the higher stability value compared to that for solute-free medium although lower stability factor was expected because of adverse effect of saliva component (Barlow & Donaldson, 1973). Woo et al. (2012, submitted) reported the SEM image of super-aggregates when AS was applied to

generate viruses, supporting the cross-linking effect of mucin. The viability of MS2 captured inside mucin linkage might be higher than naked MS2. The effect of RH on stability factor was negligible. It might be explained by the holding of water molecules via their hydrophilic oligosaccharide clusters (Shi et al., 2000). There is less MS2 in a particle, resulting in lower shielding effect. Although higher volume fraction in AS was shown compared to BE, the lower survival fractions in AS were generally observed. Because the volume contents of insoluble salts (0.3%) are the same, the possible reason might be soluble salt in AS, supported by Benbough (1971) that the soluble salt content of the suspending medium was the main reason of the low viability at MRH. This result suggested that AS showed both protective effect by insoluble mucin components and adverse effect by soluble salt components.

Summary

Both particle size distributions of infectious and total viruses in pure media without solute follow volumetric size distribution, whereas those in spray medium with solute follow lower dimension size like surface or number. Aggregation by MS2 itself and encasement by inert salts afford higher stability factor because of shielding effect and reduction of the air/water interface. In addition, for MS2 aerosols generated in gel-formation media like artificial saliva, the protection effect was observed but the effect of relative humidity could not be distinguished.

Table 7-1. Slope of least squares regression for N_{PFU} as a function of particle size for different spray medium at three relative humidities.

Spray medium	Slope of N_{PFU} (R^2)		
	LRH	MRH	HRH
DI water	2.98 (0.98)	3.22 (0.95)	2.83 (0.99)
Beef extract	2.43 (0.98)	2.38 (0.98)	2.37 (0.98)
Artificial Saliva	2.11 (0.98)	1.98 (0.91)	2.01 (0.92)

Table 7-2. Slope of least squares regression for N_{RNA} as a function of particle size for different spray medium at three relative humidities

Spray medium	Slope of N_{RNA} (R^2)		
	LRH	MRH	HRH
DI water	3.41 (0.99)	3.45 (0.99)	3.35 (0.99)
Beef extract	2.37 (0.99)	2.15 (0.98)	2.03 (0.99)
Artificial Saliva	1.82 (0.96)	1.83 (0.99)	1.83 (0.98)

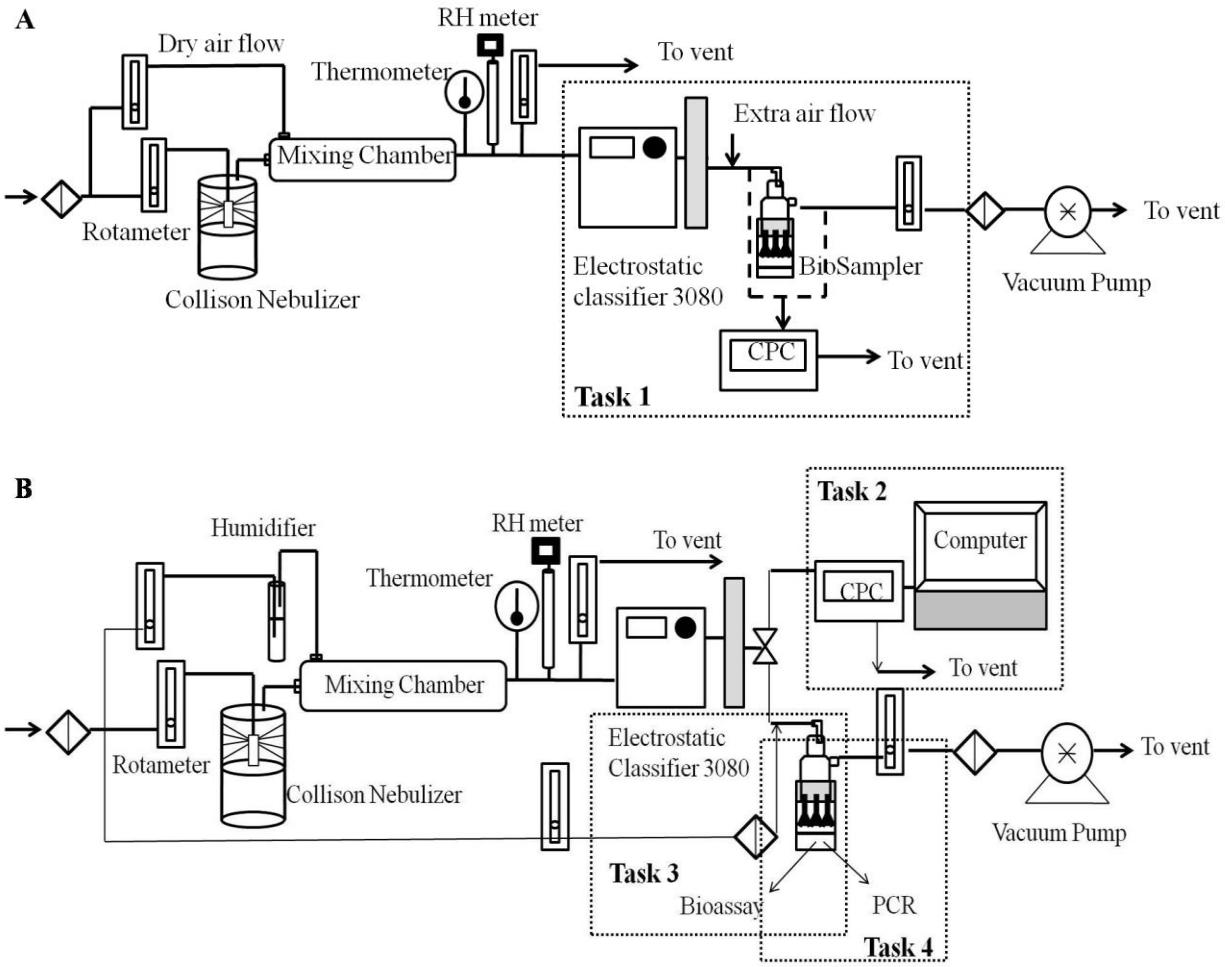

Figure 7-1. Schematic diagram of the experimental set-up: A) the system used to determine t he collection efficiencies of BioSampler as a function of particle sizes (Task 1) and B) the system used to measure particle size distribution (Task 2) and to evaluate viable (Task 3) and total (Task 4) viruses.

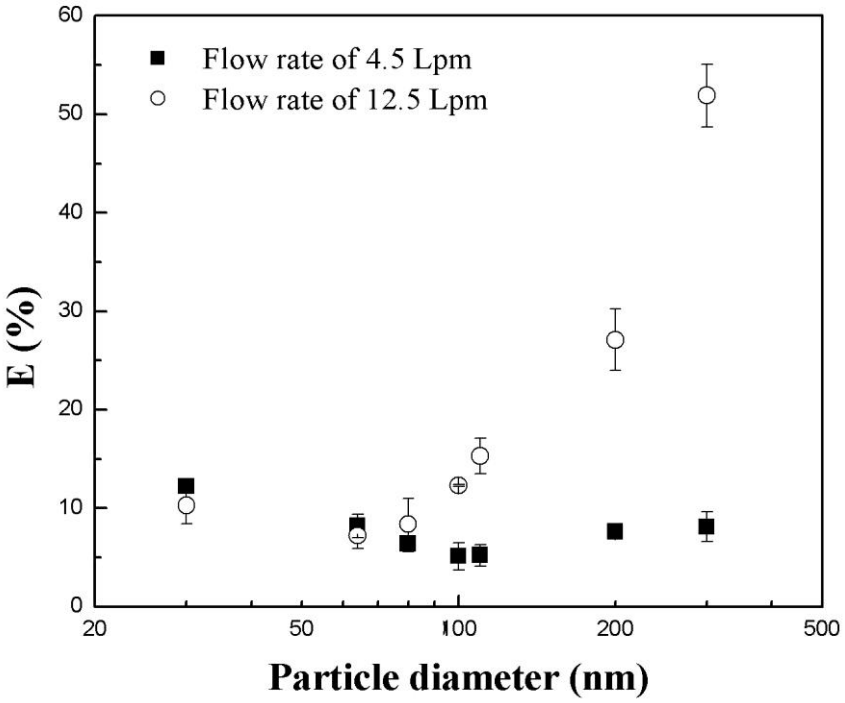

Figure 7-2. Collection efficiency of BioSampler as a function of particle diameter with a sampling flow rates of 4.5 and 12.5 Lpm.

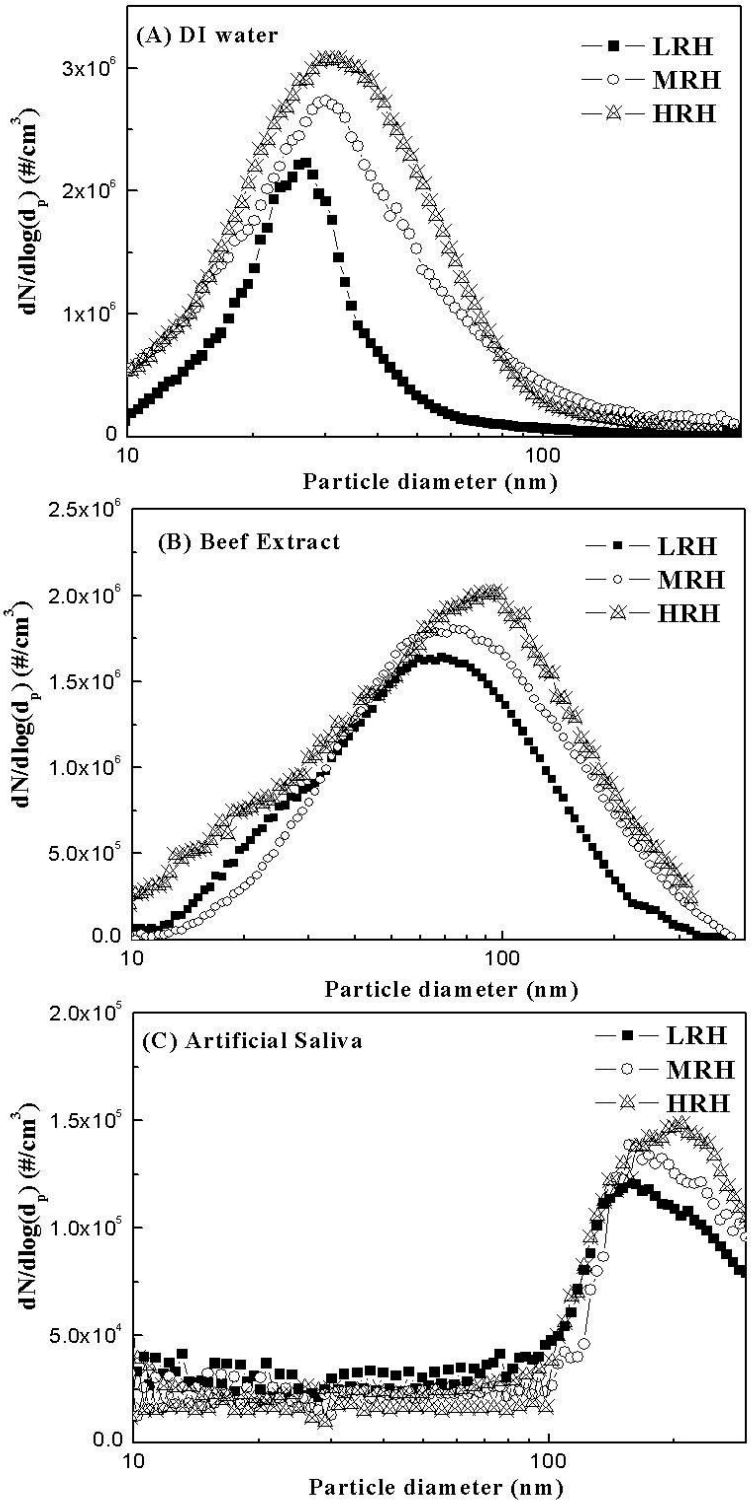

Figure 7-3. Particle size distribution of MS2 aerosols generated with DI water, beef extract, and artificial saliva at three relative humidities

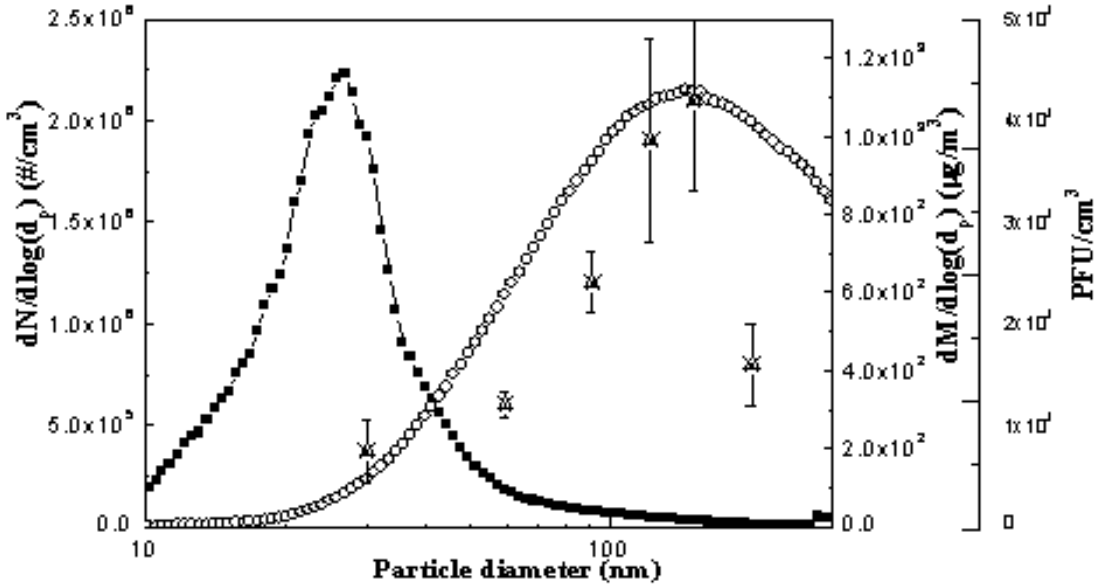

Figure 7-4. Particle size distribution of number- (solid) and mass- (empty) based MS2 aerosols obtained from monitoring the SMPS and infectious viruses (cross) through plaque assay. Error bar indicates the standard deviation of triplicate test.

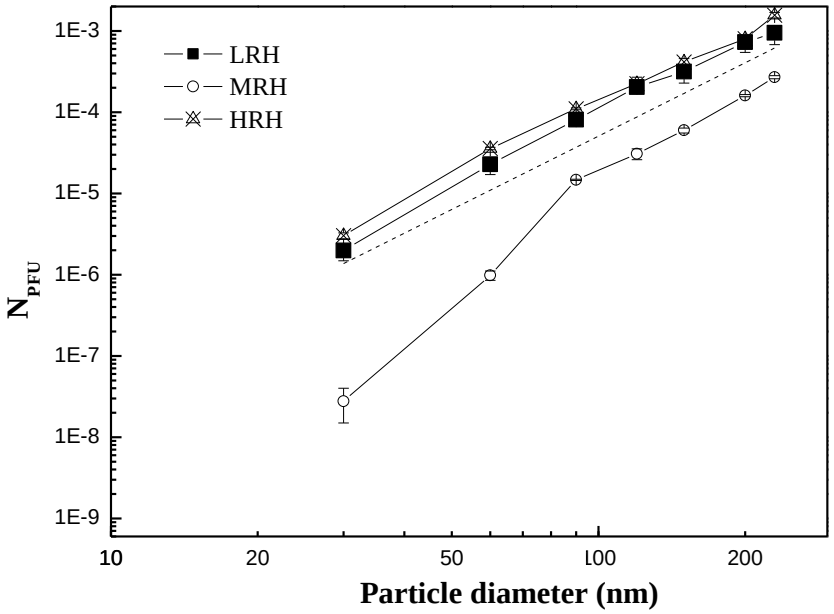

Figure 7- 5. The infectious MS2 per particle generated in DI water as a function of particle size at three relative humidities. Dash line represents the theoretical PFU per particle. Error bar indicates the standard deviation of triplicate test.

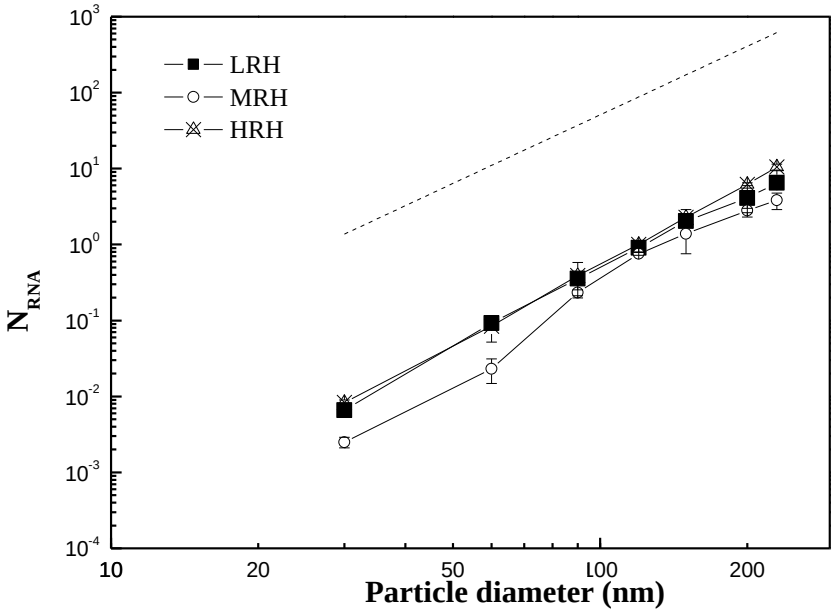

Figure 7-6. The MS2 RNA per particle generated in DI water as a function of particle size at three relative humidities. Dash line represents the theoretical PFU per particle. Error bar indicates the standard deviation of triplicate test.

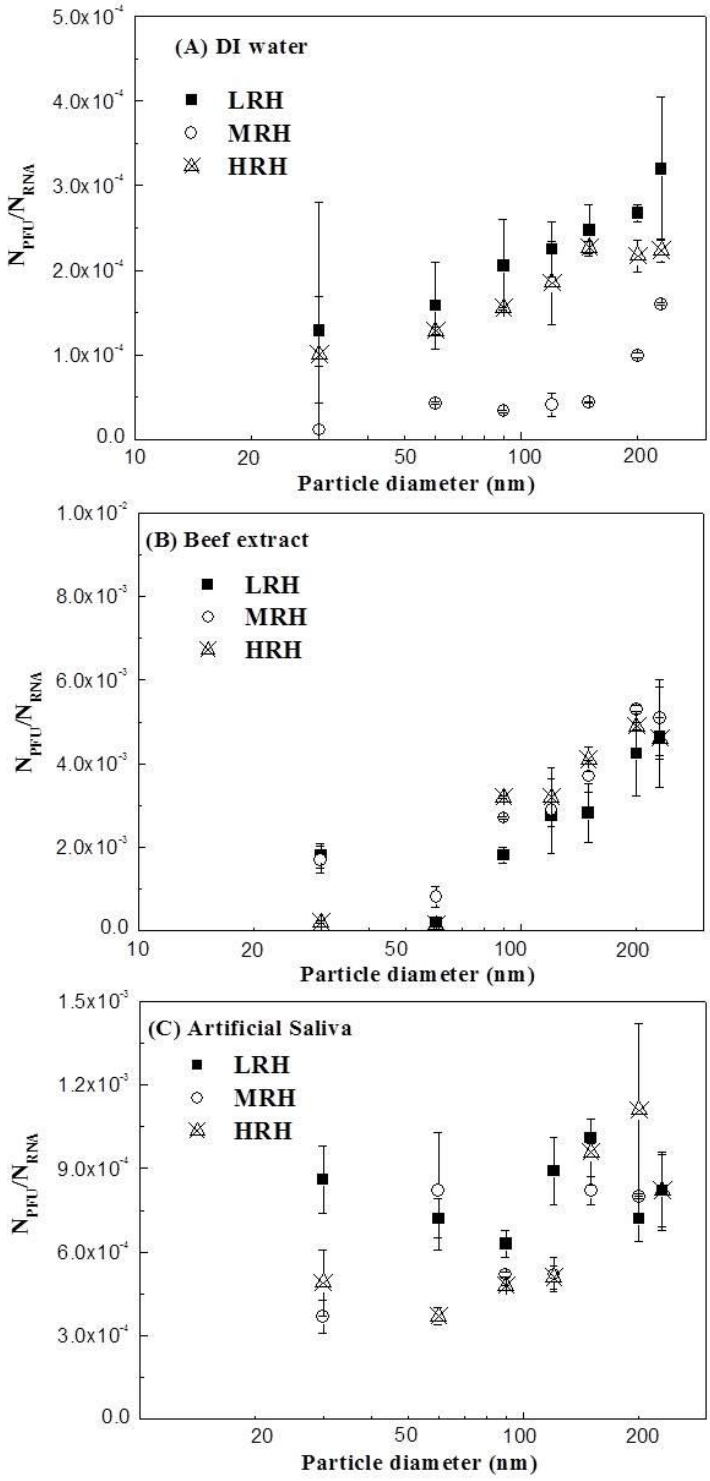

Figure 7-7. Stability factors of MS2 as a function of diameter at three relative humidities: A) DI water, B) beef extract, and C) artificial saliva

CHAPTER 8
CONCLUSIONS AND RECOMMENDATIONS

This doctoral research has focused on inactivation of viral aerosol using various novel decontamination methods. Firstly, to properly evaluate the decontamination/inactivation technologies, a droplet/aerosol loading system, which can produce the representative human respiratory secretions and can be applied for consistent and controlled delivery of aerosolized droplets containing viral agents, was developed in order to properly evaluate and compare techniques for decontamination. Because this system can be applied for inactivation of air/objects contaminated by all transmission modes, i.e., aerosol, droplet, and contact transmissions, it can be used to determine the protocol for decontamination test.

The DAC/DAS filter was prepared by periodate oxidation of a cellulose filter or incorporated starch. The treated filter presented a slightly higher viable removal efficiency and a significantly lower relative survival fraction as treatment time increased. Increasing the residence time by lowering the filtration velocity resulted in a higher viable removal efficiency and lower survival fraction. The removal efficiency and relative survival fraction of the treated filter increased and decreased, respectively, with increasing relative humidity. The pressure drop of the treated filter was significantly lower than that of the untreated filter, which resulted in a higher filter quality. The DAC filter with sufficient moisture content had a higher removal efficiency, lower pressure drop, and better disinfection capability, which are all important attributes for practical biocidal applications. All biocidal filters (DAS/DAC) showed a significantly lower relative survivability than untreated filters, and the relative survivability decreased as the concentration of DAS or treatment time for DAC increased.

For inactivation through microwave-irradiation assisted HVAC filtration system, the distortion by thermal effect was identified to be the major mechanism. Both survival fraction and inactivation efficiency measures changed sharply above a threshold temperature of around 90 ℃ and reached 2 log at 109 and 116 ^{o}C, respectively. Relative humidity is a

significant parameter from 50~80 ℃ and but it ceases to be significant above 90 ℃. Therefore, relative humidity is not a pivotal parameter for inactivation of viral aerosols. The heating by microwave irradiation was a key factor for inactivation performance, the temperature can be selected if the target IE and SF were suggested with simply two equations below;

$$\log (IE) - \log (IE)_{\text{inherent filtration}} = \log (IE)_{\text{microwave}} = -7.57 + 0.08\ T \quad (8\text{-}1)$$

$$\log (SF) = 5.01 - 0.06\ T \quad (8\text{-}2)$$

Unlike microwave results, relative humidity is an important parameter for UV disinfection of filters as well as the solid component in spraying medium. High water content that absorbs UV and shielding of viruses near the center of the aggregate might be responsible for lower inactivation. When protective medium is present, RH is not a significant parameter. These environmental conditions are not only important for disinfection technology but also for susceptibility of virus itself.

Both particle size distributions of infectious and total viruses in pure media without solute follow volumetric size distribution, whereas those in spray medium with solute follow a lower dimension size. Aggregation by MS2 itself and encasement by inert salts contribute to a higher stability factor because of shielding effect and reduction of the air/water interface. In addition, for MS2 aerosols generated in gel-formation media like artificial saliva, the protective effect was observed but less than inert salts.

Based on the knowledge learned and experiences gained in this research, recommendations are made to help further advance the application of novel decontamination method against viral aerosols: 1) Development of an analytical model for disposition of viruses in aerosol in different spray media is recommended. The model can be a very useful tool in designing an effective strategy to improve filtration and inactivation efficiency and for assessing the risk by respiratory deposition of viral aerosol. 2) Characterization of virus

between 20-230 nm size range was not enough to complete the model. To further expand the applicability of the model, the stability factor of a wider size range should be included. 3) Further studies to elucidate the aggregation and encasement by TEM will be helpful. TEM can be taken after staining the lipid with selective concentration of dye (uranyl acetate). Although higher dye concentration allows easy observation of the morphology of MS2, it can also alter isoelectric point, resulting in different aggregation modes. Hence, after determining the optimal dye concentration for MS2, the morphology by TEM should be observed. 4) Microwave-incorporated HVAC ventilation system for real application should be tested because the energy/cost is another impotent factor with performance. For real application, the consumption of cost/energy should be considered. 5) Because the relative humidity in duct is between 65-85% and the condition is sufficient for mold and fungi to grow, dialdehyde starch/cellulose is possible to be applied. Aldehyde has a biocidal effect against mold and some fungi. It will be helpful to use these filters against duct-type microbes.

APPENDIX A
PRELIMINARY TEST FOR DROPLET LOADING CHAMBER

Methods

Before building the droplet loading chamber, an experiment was conducted to verify the uniform deposition of aerosols using a small chamber, as shown in Figure A-1. 600 mg/L of fluorescein was applied for evaluating the distribution of the deposition. The fluorescein aerosols were generated by an ultrasonic nebulizer with a flowrate of 0.5 Lpm for 5 minutes. Four Lydall square filters with 1 inch length, placed in the small chamber as shown in Figure A-2, were used as the collection media. After the loading, the fluorescein was extracted by 50 mL solution of 0.1 N NH_4OH for 30 mins using a wrist action shaker. The fluorescein concentration was then analyzed by a fluorometer (Turner Fluorometer, Model 112).

Determination of Operating Conditions

Before and after experiments, the chamber was decontaminated by isopropyl alcohol for 30 mins. Six samples were placed onto the support on the turntable using sterile forceps. Theoretically, a titer of around 10^7 PFU/mL in the ultrasonic nebulizer with 5 min loading time should provide sufficient loading density (>10^3 PFU/cm^2). The titer was prepared by adding 0.3 mL virus stock suspension into 30 mL artificial saliva. The droplets from the ultrasonic nebulizer after passing the distributer entered the chamber through 6 inlets. The size of generated and loaded droplets can be affected by the frequency of the ultrasonic generator and environmental conditions such as RH and temperature. For this study, the frequency of the generator was 2.4 MHz and the environmental conditions were 20±2 ℃ and 35±5%. Low RH was chosen because the survivability of MS2 is high under this condition. After loading, the residual droplets were allowed to clear for 5 mins, and the FFR samples were taken out for extraction and assay.

The optimal conditions to extract the virus from the FFRs were investigated by comparing virus counts under different agitation methods, extraction media, and extraction

times. The experimental procedures were as follows: (1) a glass fiber filter (GelmanScience, No. 61630) of 25 mm diameter was loaded with a known virus titer, and (2) applied filter was agitated to extract the viruses for a select period of time by a select agitation method after waiting for 10 mins, as listed in Table A-1.

To evaluate if the viability of virus is influenced by the ultrasonic process, bioaerosols produced at different times were collected by a Biosampler and their viabilities were compared. The MS2 survival efficiency might be affected by the nebulization fluid, the storage time, and the extraction time. To examine the MS2 survivability in the spray medium, deionized (DI) water and artificial saliva (AS) were tested. The ultrasonic nebulizer was run with a flow rate of 1 Lpm and a loading time of 5 min. After the loading, 0.25 M glycine solution was applied to extract the MS2 on the filter by the wrist action shaker to analyze the virus concentration. The sample extraction times were 1, 2, and 5 mins. The sample was then kept in the refrigerator for 2 days for the second analysis. Survival fraction was defined as the ratio of virus concentrations after two days to the virus concentration in the extraction solution at the initial time.

Results

Fluorescein Test

The calibration results of the fluorometer under 4 modes, shown in Figure A-3, indicate this fluorometer has a good performance for the concentration range of interest to this study. The results of deposition experiment are shown in Table A-2, which displays the reading from the fluorometer under a certain mode and then converted according to the calibration curve to acquire the concentration. The final concentration was averaged from the 3 modes (i.e. 1×, 3×, and 10×). The corresponding CV was 4.69%, which satisfies the criterion of 20% and demonstrates the uniformity of this method.

Determination of Extraction Conditions

In terms of the agitation method, as displayed in Figure A-4, the shaking method by the wrist action shaker (Model 75, Burrell Scientific, Pittsburgh, PA) had 1.25, 1.54, and 1.89 times higher extraction efficiency than vortexing, rotating, and sonication, respectively. This is different from previous research on best extraction method. Edward et al (2004) showed a similar efficiency in extracting MS2 from FFR coupons between vortexing and shaking. Kim et al (2008) showed that shaking had twice higher efficiency than vortexing. However, ATCC medium (organic matter) was used instead of 0.25M glycine and BG spores was applied in lieu of MS2 bacteriophage, respectively. In other words, the efficiency may be species and medium dependent.

With regard to the extraction medium, as shown in Figure A-5, glycine had the higher extraction efficiency. Hence, in this study, 0.25 M glycine was selected as the extraction buffer instead of DI water or 1X PBS. There are two possible reasons for its higher extraction efficiency. First, glycine is a zwitterion which can combine with both cations and anions and provide more reaction sites. Second, glycine has a high ionic strength which can reduce the double layer strength on particle surface (Roger et al. 1993). Regarding the extraction time, the effect is shown in Figure A-6. Fifteen mins of extraction shows the best extraction efficiency. Less than 10 mins may not be sufficient to extract the virus efficiently while greater than 15 mins may cause damages to virus due to mechanical stress and long air contact time. From these results, the best condition to extract the sample is to use 25 mL of 0.25 M glycine solution in a wrist action shaker with a 10^{o} angle for 15 mins.

Viability during Ultrasonic Nebulization

The impact of ultrasonic nebulization on virus viability in the nebulizer reservoir was investigated by measuring the viable counts over time. The results show no significant difference in virus viability between 0 and 30 mins (p=0.10). Apparently, the heat shock from

ultrasonic vibration did not cause damage to the MS2 in the reservoir during droplet generation. To determine the ultrasonic effect on virus aerosol during droplet generation the viability of the viruses collected in the BioSampler after 5 and 10 mins of generation was examined. The theoretical concentration in BioSampler after 5 mins of nebulization is 3×10^5 PFU/mL when the virus titer in the reservoir is 1.0×10^7 PFU/mL. The 5 mins time-weighted (0-5 and 5-10 mins) average concentration of collected viruses in the BioSampler was around 3.2×10^5 PFU/mL, which is similar to the theoretical value. As demonstrated, the ultrasonic generator can be used to produce droplets containing viruses without adverse effects on their viability.

Effect of Saliva on Viability

As shown in Table A-3, the extraction time does not affect the survival fraction significantly. However, the survival fractions were higher when applying AS than DI water. The around 1 survival fractions from AS also imply that MS2 concentration can still be accurately analyzed after 2 days if AS is used as the medium and the sample is kept in the refrigerator.

Table A-1. Several agitation methods to extract the MS2 bacteriophage onto filter

Agitation Method	Applied time (mins)	Final time*	Specific conditions
Shaking	1, 2, 5, 10,15, 30,45 and 60	15 mins	10^{o} angle
Vortexing	1, 2, 5, 10, 30, and 60	1 min	3200 rpm
Rotating	1, 3, 5, 10, 30, and 60	10 mins	8 rpm
Sonication	1, 5, 10, and 15	10 mins	40 KHz

Final time *: Used for comparison as shown in Figure A-4

Table A-2. Fluoroscein concentrations of 4 filters under 3 reading modes

No.	1X		3X		10X		
	Reading	Con. (µg/L)	Reading	Con. (µg/L)	Reading	Con. (µg/L)	Avg. Con. (µg/L)
1	8.09	585.50	23.70	589.97	51.96	586.02	587.16
2	7.23	522.73	21.25	527.63	46.43	524.58	524.98
3	7.82	565.80	22.98	571.65	49.90	563.13	566.86
4	7.84	567.26	23.00	572.16	50.40	568.69	569.37

Table A-3. The survival fraction for two media after 48 hour of storage time (in duplicate)

Time	DI water			Artificial saliva		
	Concentration (PFU/mL)		Survival fraction	Concentration (PFU/mL)		Survival fraction
(mins)	0 days	2 days		0 days	2 days	
1	284	223.5	0.78	260	240.5	0.93
2	283	275	0.97	290	306	1.06
5	257	225.5	0.88	295	301	1.02

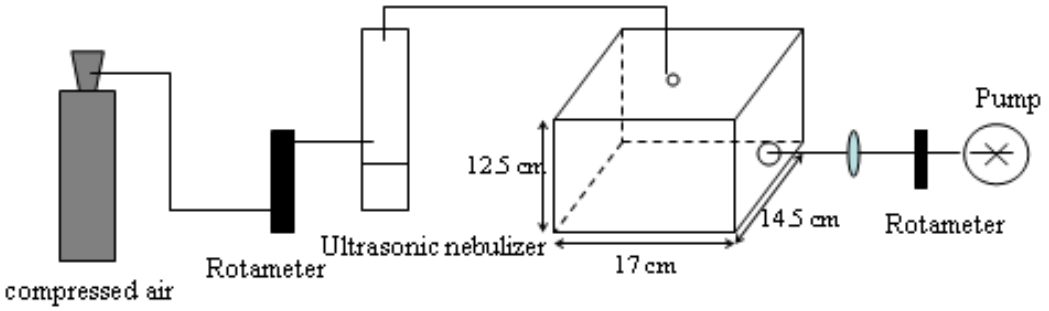

Figure A-1. Experimental set-up for aerosol loading experiment by using a small chamber

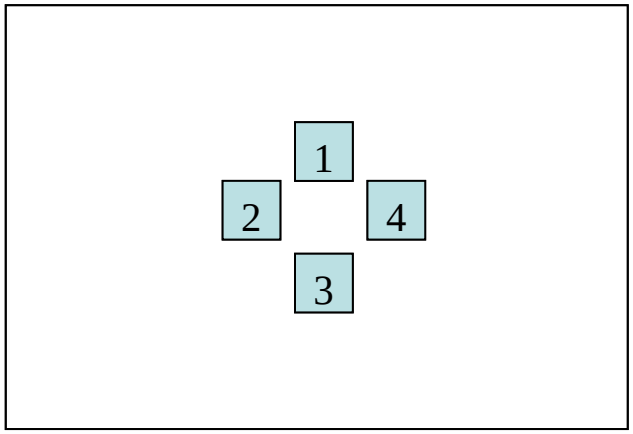

Figure A-2. Filter location in the small chamber for uniform distribution experiment

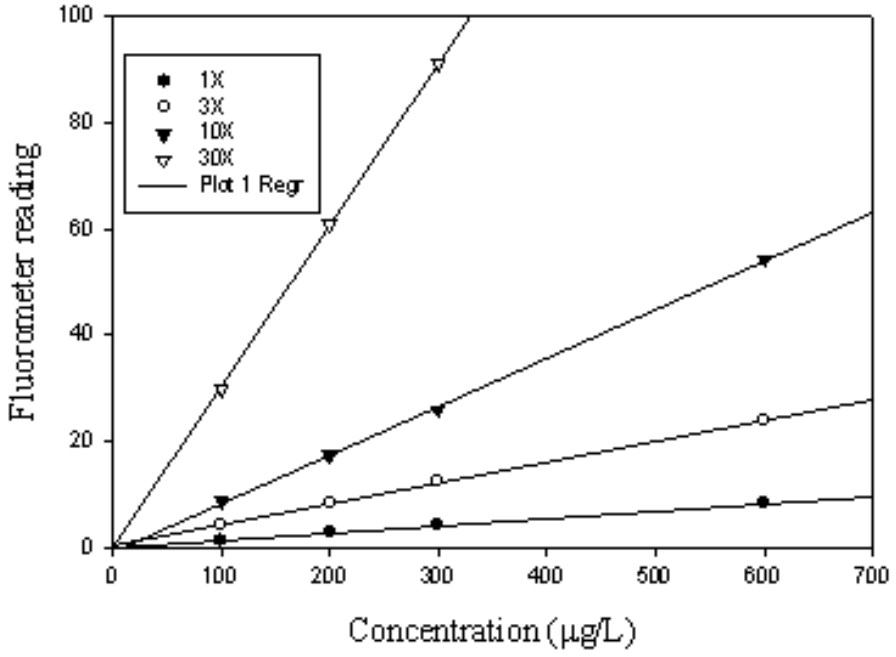

Figure A-3. Calibration curves of the fluorometer under 4 modes

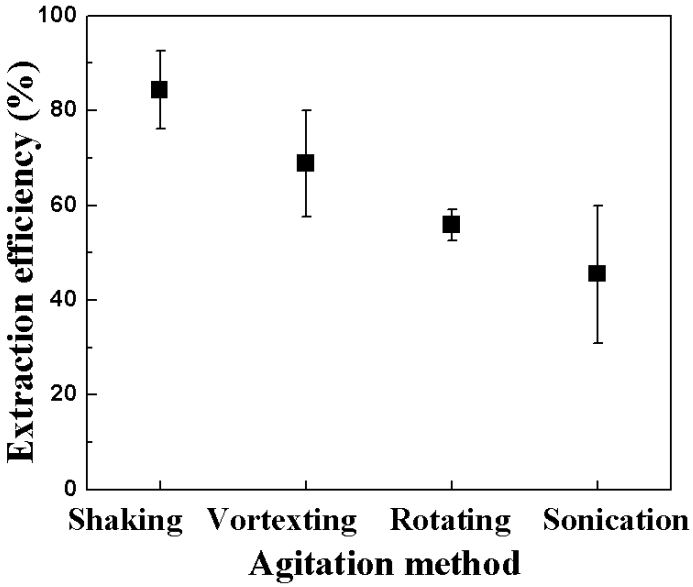

Figure A-4. MS2 extraction efficiency based on agitation method. The error bar represents one standard deviation

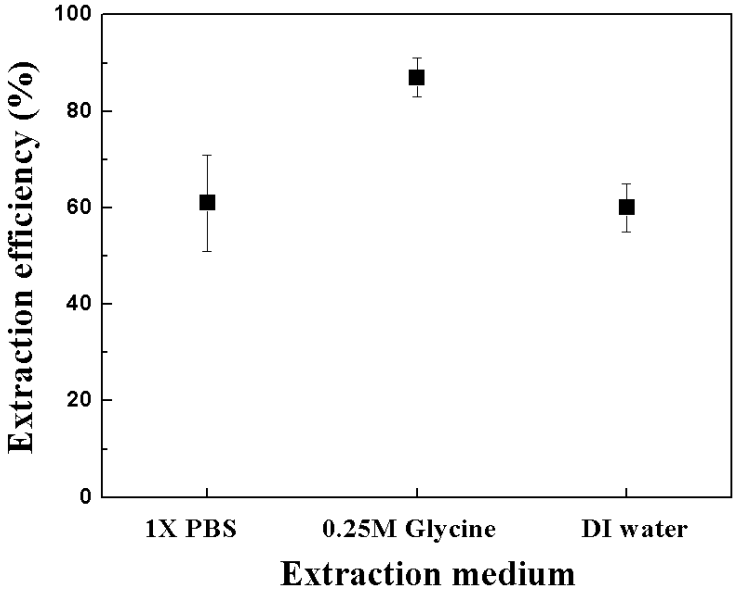

Figure A-5. MS2 extraction efficiency based on extraction medium. The error bar represents one standard deviation

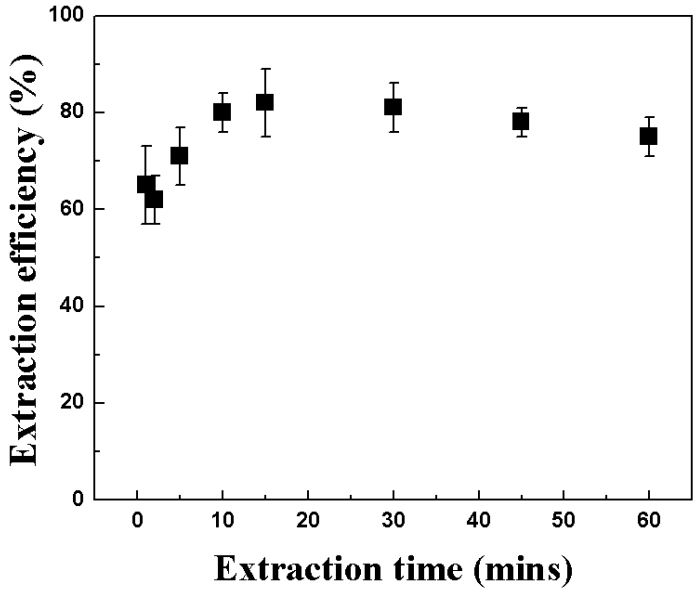

Figure A-6. MS2 extraction efficiency based on extraction time. The error bar represents one standard deviation

APPENDIX B
MICROWAVE-ASSISTED PAN-NANOFIBER FITRATION SYSTEM FOR VIRAL AEROSOL

The static on-filter MS2 inactivation tests were carried out under 500 W microwave power. As shown in Table B-1, in less than 90 seconds the survival dropped below 2 log inactivation. These results suggest that the microwave irradiation can effectively decontaminate the filters with loaded MS2.

To evaluate the inactivation performance of microwave-irradiation assisted nanofiber filtration system during in-flight filtration against MS2, the experimental system as displayed in Figure 5-1 was used. The similar operating conditions were applied. Duplicate experiments were carried out for MS2 with PAN nanofiber filter. The inactivation efficiency (C_E/C_E) for MS2 under different microwave powers and time intervals when PAN was employed are shown in Figure B-1. As shown, the inactivation effect of microwaves against MS2 is dependent on both microwave power and time. 2.4-log IE was shown with continuous microwave treatment at maximum power (500 W). However, the mechanical property of PAN filter was altered after continuous test because of high temperature, which makes partially crosslinked (x-linked) filter. To avoid this phenomenon, x-linked PAN having high thermal stability was employed instead of PAN filter. Without filter damage, the similar inactivation result was shown (Figure B-2). This inactivation effect for virus is less than that of *E. coli* shown in *Zhang et al*. (2010). This may be explained as MS2 having higher heat resistance compared to *E. coli.*

Table B-1. Survival fraction of microorganisms under microwave irradiation – Static on-filter inactivation at 500 W

		Microwave irradiation time			
		30 s	45 s	60 s	90 s
MS2	Mean	33.25%	–	4.14%	0.81%
	SD	6.34%	–	0.81%	0.34%

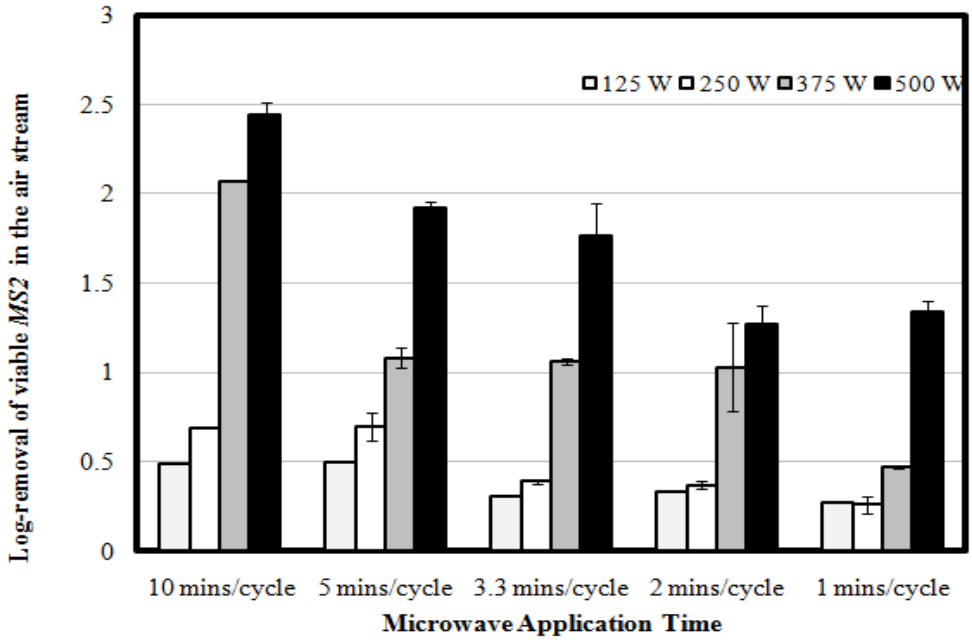

Figure B-1. Log Inactivation efficiency by microwave irradiation assisted filtration system for PAN nanofiber filter as a function of microwave application time

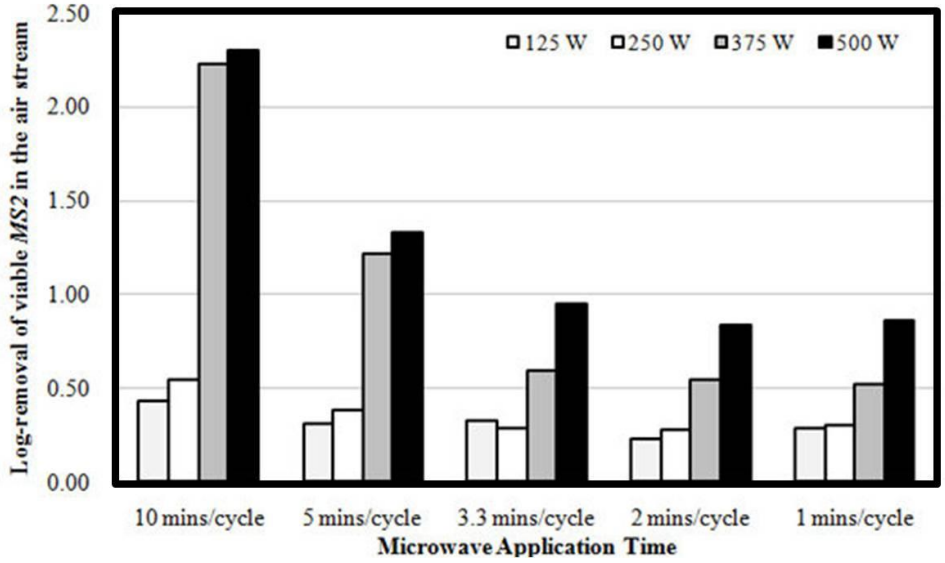

Figure B-2. Log Inactivation efficiency by microwave irradiation assisted filtration system for x-PAN nanofiber filter as a function of microwave application time

LIST OF REFERENCES

Aps, J. K.M., & Martens, L.C. (2005). Review: The physiology of saliva and transfer of drugs into saliva. *Forensic Science* 150, 119–131.

Aranha-Creado, H., & Brandwein, H. (1999). Application of bacteriophages as surrogates for mammalian viruses: A case for use in filter validation based on precedents and current practices in medical and environmental virology. *Journal of Pharmacy Science & Technology* 53, 75–82.

Baron, P., Estill, C., Deye, G., Hein, M., Beard, J., Larsen, L., & Dahlstrom, G. (2008). Development of an aerosol system for uniformly depositing *Bacillus anthracis* spore particles on surfaces. *Aerosol Science & Technolgy* 42, 159–172.

BeMiller, N., & Whistler, R. (2009). *Starch: Chemistry and Technology*. New York: Elsevier's Science and Technology.

Benbough, J. E. (1971). Some factors affecting the survival of airborne viruses. *Journal of Genetics Virology* 10, 209–220.

Betti, L., Trebbi, G., Lazzarato, L., Brizzi, M., Calzoni, G.L., & Marinelli, F., et al. (2004). Nonthermal microwave radiations affect the hypersensitive response of tobacco to tobacco mosaic virus. *The Journal of Alternative and Complementary Medicine* 10, 947-957.

Brion, G. M. and Silverstein, J. (1999). Iodine disinfection of a model bacteriophage, MS2, demonstrating apparent rebound. *Water Resource.* 33, 169–179.

Brickner, P., Vincent, R., First, M., Nardell, E., Murry, M., & Kaufman, W. (2003). The application of ultraviolet germicidal irradiation to control transmission of airborne disease: bioterrorism countermeasure. *Public Health Reports*, 118, 99–118.

Bruck, C.W. (1991). *Sterilization of medical products*; Polyscience Publications: Morin Heights.

Campanha, N.H., Pavarina, A.C., Brunetti, I.L., Vergani, C.E., Machado, A.L., Spolidorio, D.M.P. (2007). Candida albicans inactivation and cell membrane integrity damage by microwave irradiation. *Mycoses* 50, 140–147.

CDC (2009). Fact sheet: novel H1N1 flu situation update. Available at <http://www.cdc.gov/h1n1flu.update.htm>, September 15, 2009.

CDC (2011). Ancillary Respirator Information. Available at <http://www.cdc.gov/niosh/npptl/topics/respirators/disp_part/RespSource3.html>, March 22, 2011.

CDRF (2006). Reusability of facemasks during an influenza pandemic: facing the flu, *National Academies Press*, Washington D.C.

Celandroni, F., Longo, I., Tosoratti, N., Giannessi, F., Ghelardi, E., & Salvetti, S., et al. (2004). Effect of microwave radiation on Bacillus subtilis spores. *Journal of Applied Microbiology* 97, 1220–1227.

Chuaybamroon, P., Thunyasirinon, C., Supothina, S., Sribenjalux, P., & Wu, C. Y. (2011). Performance of photocatalytic lams on reduction of culturable airborne microorganism concentration. *Chemosphere*, 83, 730–735.

Cote, R. J. (1999). Media composition, microbial, laboratory scale. In: Flickinger and Drew (Eds.), *Encyclopedia of bioprocess technology: fermentation, biocatalysis, and bioseparation*. John Wiley & Sons, Inc.: New York, pp 104–122.

Damit, B., Lee, C. N, & Wu, C. Y. (2011). Flash infrared radiation disinfection of fibrous filters contaminated with bioaerosols. *Journal of Applied Microbiology* 110, 1074–1084.

Diaz–Arnold, A. M., & Marek, C. A. (2002). The impact of saliva on patient care: A literature review. *Journal of Prosthetic Dentistry* 88, 337–343.

Dodds, M. W. J., Johnson, D.A., & Yeh, C. K. (2005). Health benefit of saliva: a review *Journal of Dentistry* 33, 223–233.

Doguid, J. P. (1946). The size and the duration of air-carriage of respiratory droplets and droplet nuclei. *Journal of Hygiene* 44, 471–479.

Dubovi, E. J. (1971) Biological activity of the nucleic acids extracted from two aerosolized bacterial viruses. *Applied Microbiology* 21, 761–762.

Dubovi, E. J. and Akers, T. G. (1970) Airborne stability of tailless bacterial viruses S-13 and MS-2. *Applied Microbiology* 19, 624–628.

Drazen, J. M. (2002). Smallpox and bioterrorism. *The New England Journal of Medicine*, 346, 1262–1263.

Dreyfuss, M.S. & Chipley, J.R. (1980). Comparison of effects of sublethal microwave radiation and conventional heating on the metabolic activity of Staphylococcus aureus. *Applied &Environmental Microbiology* 39, 13–16.

ECDC (2009). daily update—Pandemic (H1N1) 2009.Available at <http://ecdc.europa.eu/en/healthtopics/Documents/091020_Influenza_AH1N1_Situation_Report_0900hrs.pdf>, September 18, 2009

Edward, D., Man, J., Brand, P., Kaststra, J., Sommerer., K., & Stone, H. et al. (2004). Inhaling to mitigate exhaled bioaerosols. *PNAS.* 101, 17383–17388.

EPA (1984). USEPA manual methods for virology. *US Environmental Protection Agency, Research and Development*, 600/4-84-013, Cincinnati, OH.

Favero, M.S. & Bond, W.W. (1991). *Disinfection, sterilization, and preservation*; Lea & Febiger: Philadelphia

FDA (2007) *Emergency Use Authorization of Medical Products*. U.S. Department of Health and Human Services, Food and Drug Administration, July 2007. Available at <http://www.fda.gov/RegulatoryInformation/Guidances/ucm125127.html>, May 3, 2008

.Feather, G. & Chen, B. (2003). Design and use of a settling chamber for sampler evaluation under calm-air conditions. *Aerosol Science & Technology* 37, 261–270.

Fiegel, J., Clarke, R., & Edwards, D. A. (2006). Airborne infectious disease and the suppression of pulmonary bioaerosols. *Drug Discovery Today* 11, 51–57.

Fisher, E., Rengasamy, S., Viscusi, D., Vo, E. & Shaffer, R. (2009). Development of a test system to apply virus containing particles to filtering facepiece respirators for the evaluation of decontamination procedure. *Applied & Environmental Microbiology* 75, 1500–1507.

Fisher, E.M., Williams, J.L., & Shaffer, R.E. (2011). Evaluation of Microwave Steam Bags for the Decontamination of Filtering Facepiece Respirators. *PLoS ONE* 110: e18585.

Floyd, R., & Sharp, D. G. (1977). Aggregation of poliovirus and reovirus by dilution in water. *Applied & Environmental Microbiology* 33, 159–166.

Gabbay, J., Borkow, G., Mishal, J., Magen, E., Zatcoff, R., & Shemer-Avni, Y. (2006). Copper oxide impregnated textiles with potent biocidal activities. *Journal of Industrial Textile*. 35, 323–335.

Goldblith, S.A. & Wang, D.I.C. (1967). Effect of microwaves on Escherichia coli and Bacillus subtilis. *Applied Microbiology* 15, 1371–1375.

Gowda, N, Trieff, N., & Stanton, J. (1981). Inactivation of Poliovirus by Chloramine-T. *Applied & Environmental Microbiology* 42, 469–476.

Grinshpun, S.A., Adhikari, A.A, Li, C., Yermakov, M., Reponen, L, Johansson, E.J., & Trunov, M. (2010). Inactivation of aerosolized viruses in continuous air flow with axial heating. *Aerosol Science & Technology* 22,1042–1048.

Hou, Q.X., Liu, W., Liu, Z.H., Duan, B., & Bai, L.L. (2008). Characteristics of antimicrobial fibers prepared with wood periodate oxycellulose. *Carbohydrogen Polymer*. 74, 235–240.

Hamid, M., Thomas, T., El-Saba, A., Stapleton, W., Sakla, A. Rahman, A. (2001). The effects of microwaves on airborne microorganisms. *Journal of Microwave Power and Electromangetic Energy* 36, 37–45.

Heimbuch, B., Wallace, W., Kinney, K., Lumley, A., Wu, C.-Y., & Woo, M.-H. et al., (2010). A Pandemic Influenza Preparedness Study: Use of energetic methods to decontaminate Filtering Facepiece Respirators Contaminated with H1N1 Aerosols and Droplets. *American Journal of Infection Control* 39, 1–9.

Herrera, P., Burghardt, R., Huebner, H.J., & Phillips, T.D. (2004). The efficacy of sand-immobilized organoclays as filtration bed materials for bacteria. *Food Microbiology*. 21, 1–9.

Hinds, W. C. (1999). *Aerosol Technology*. New York: John Wiley and Sons, Inc.

Humphrey, S. P., & Williamson, R. T. (2001). A review of saliva: Normal composition, flow and function. *Journal of Prosthetic Dentistry* 85, 162–169.

Jung, J., Lee, J., & Kim, S. (2009). Generation of nonagglomerated airborne bacteriophage particles using an electrospray technique. *Analytical Chemistry* 81, 2985–2990.

Kettleson, E.M., Ramaswami, B., Hogan, C.J., Lee, M.H., Statyukha, G., & Biswas, P. et al. (2009). Airborne Virus Capture and Inactivation by an Electrostatic Particle Collector. *Environmental Science & Technology* 43, 5940–5946.

Khalil, H. & Villota, R. (1989). The effect of microwave sublethal heating on the ribonucleic acids of *Staphylococcus aureus*. *Journal of Food Protection* 52, 544–548.

Kim, U.J. & Kuga, S. (2004). Reactive interaction of aromatic amines with dialdehyde cellulose gel. *Cellulose.* 4, 287–293.

Kowalski, W. & Bahnfleth, W. (2007). UVGI design basics for air and surface disinfection. *HVAC engineering* 100–111.

Kowalski, W. (2009). *Ultraviolet Germicidal Irradiation Handbook*. Springer.: New York

Kujunzic, E., Matalkah, F., Howard, C., Hernandez, M., & Miller, S. (2006). UV air cleaners and upper-roon air ultraviolet germicidal irradiation for controlling airborne bacterial and fungal spores. *Journal of Occupational Environmental Hygiene* 3, 536.

Lang, R. (1962). Ultrasonic atomization of liquid. *Journal of Acoustical Society America.* 34, 6–8.

Lee, I.S., Kim, H.J., Lee, D.H., Hwang, G.B. Jung, J.H., & Lee, M., et al. (2011). Aerosol particle size distribution and genetic characteristic of aerosolized influenza A H1N1 virus vaccine particles. *Aerosol and Air Quality Research* 11, 230–237.

Lee, J.H., Wu, C.Y., Lee, C.N., Anwar, D., Wysocki, K.M., & Lundgren, D.A. et al. (2009). Assessment of iodine-treated filter media for removal and inactivation of MS2 bacteriophage aerosols. *Journal of Applied Microbiology* 107, 1912–1923.

Li, C.S., Hao, M.H., Lin, W.H., Chang, C.W., & Wang, C. S. (1999). Evaluation of microvial samplers for bacterial microorganisms. *Aerosol Science & Technology* 30, 100–108.

Lin, C.Y. & Li, C.S. (2003). Inactivation of microorganisms on the photocatalytic surfaces in air. *Aerosol Science & Technology* 37, 939–944.

Lin, X., Reponen, T., Willeke, K., Wang, Z., Grinshpun, S.A., & Trunov, M. (2000). Survival of airborne microorganisms during swirling aerosol collection. *Aerosol Science & Technology* 32, 184–196.

Mantle, M., & Husar, S.D. (1993). Adhesion of *Yersinia enterocolitica* to Purified Rabbit and Human Intestinal Mucin. *Infection and Immunity* 61, 2340–2346.

Marple, V., & Rubow, K. (1983). An aerosol chamber for instrument evaluation and calibration. *American Industry Hygiene Association Journal* 44, 361–367.

May, K. R. (1973). The collision nebulizer: Description, performance and application. *Journal of Aerosol Science* 4, 235–238.

McCrumb, F. (1961). Aerosol infection of man with Pasteurella tularensis *Bacteriology Review* 25, 1912–1923.

McDevitt, J.J., Lai, K.M., Rudnick, S.N., Houseman, E.A., First, M.W., & Milton, D.K. (2007). Characterization of UVC light sensitivity of vaccinia virus. *Applied & Environmental Microbiology* 73, 5760–5766.

Mcdonnell, G. & Russell, A.D. (1999). Antiseptics and disinfectants: activity, action, and resistance. *Clinical Microbiology Reviews.* 12, 147–179.

Metcalf, E. & Eddy, F. (2004) *Wastewater Engineering: Treatment and reuse*; McGraw-Hill, Inc: New York.

Miller M.B. (2009). Removal of waterborne pathogens using an antimicrobial filter media, *Proceeding of the 2009 Georgia Water Resources Conference.*

Morawska, L., Johnson, G., Ristovski, Z., Hargreaves, M., Mengersen, K., Corbett, S., et al., (2009). Size distribution and sites of origin of droplets expelled from the human respiratory tract during expiratory activities. *Journal of Aerosol Science* 49, 256–269.

Munro, L. (2007) *Basics for microbiology laboratory*. North Carolina: Contemporary publishing compamy of raleigh, Inc.

NIOSH (2005). Determination of particulate filter penetration to test against liquid articulates for negative pressure, air-purifying respirators standard testing procedure (STP). Pittsburgh, PA.

O'Connell, K. P., Bucher, J. R., Anderson, P. E., Cao, C. J., Khan, A. S., Gostomski, M. V. & Valdes, J. J. (2006) Real-time fluorogenic reverse transcription-PCR assays for detection of bacteriophage MS2. *Applied & Environmental Microbiology* 72, 478–483.

OSHA (2012). Available at <http://www.osha.gov/pls/oshaweb >, January 15, 2012.

Para, A., Karolczyk-Kostuch, S., & Fiedorowicz, M. (2004). Dihydrazone of dialdehyde starch and its metal complexes. *Carbohydrogen Polymer* 56, 187–193.

Park, D.-K., Bitton, G., & Melker, R. (2006). Microbial inactivation by microwave radiation in the home environment. *Journal of Environmental Health* 69, 17–24.

Park, J., Yoon, K., Kim, Y., Byein, J., & Hwang, J. (2009). Removal of submicron aerosol particles and bioaerosols using carbon fiber ionizer assisted fibrous medium filter media. *Journal of Mechanical Science & Tech*nology 23, 1846–1851.

Pellerin, C. (1994). Alternatives to incineration: there's more than one way to remediate. *Environmental Health Perspectives* 102, 840–845.

Perier, C., Bové, J., & Vila, M. (2011). Mitochondria and Programmed Cell Death in Parkinson's Disease: Apoptosis and Beyond. *Antioxidant Redox Signal* July 18. [Epub ahead of print]

Phelan, A.M., Neubauer, C.F., Timm, R., Neirenberg, J., & Lange, D.G. (1994). Athermal alterations in the structure of the canalicular membrane and ATPase activity induced by thermal levels of microwave radiation. *Radiation Research* 137, 52–58.

Power, E.G.M. & Russell, A.D. (1990). Sporicidal action of alkaline glutaraldehyde: factors influencing activity and a comparison with other aldehydes. *Journal of Applied Bacteriology* 69, 261–268.

Prescott, L. M., Harley, J. P., & Klein, D. A. (2006) Microbiology, New York, NY: McGraw Hill Companies, Inc. pp. 142–146.

Radley, J. A. (1976). *Starch Production Technology*. London: Applied Science Publisher, Inc.

Ratnesar-Shumate, S., Wu, C.Y., Wander, J., Lundgren, D., Farrah, S., Lee, J.H., et al. (2008) Evaluation of physical capture efficiency and disinfection capability of an iodinated biocidal filter medium. *Aerosol Air Quality Research* 8, 1–18.

Rengasamy, S., Fisher, E., & Shaffer, R. (2010) Evaluation of the survivability of MS2 viral aerosols deposited on filtering face piece respirator samples incorporating antimicrobial technologies. *American Journal of Infection Control* 38, 9–17.

Riemenschneider, L., Woo, M.- H., Wu, C.Y., Lundgren, D. A., Wander, J., & Lee, J.H. et al. (2010). Characterization of reaerosolization from impingers in an effort to improve airborne virus sampling. *Journal of Applied Microbiology* 108, 315–324.

Ryan, K., McCabe, K., Clements, N., Hernandez, M., & Miller, S. (2010). Inactivation of airborne microorganisms using novel ultraviolet radiation sources in reflective flow-through control devices. *Aerosol Science & Technology* 44, 541–550.

Salgado, C. D., Farr. B. M., Hall, K. K., & Hayden, F. G. (2002). Influenza in the acute hospital setting. *The Lancet Infectious Diseases* 2, 145–155.

Shi, L., Ardehali, R., Caldwell, K.D., & Valint, P. (2000). Mucin coating on polymeric material surface to suppress bacterial adhesion. *Colloids and Surfaces B: Biointerfaces* 17, 229–239.

Silver, S., Phung, L., & Silver, G. (2006). Silver as biocidaes in burn and wound dressings and bacterial resistance to silver compounds. *Journal of Industrial Microbiology Biotechnology* 33, 627–634.

Sjogren, J.& Sierka, R. (1994). Inactivation of phage MS2 by iron-aided titanium dioxide photocatalysis. *Applied and Environmental Microbiology* 60, 344–347.

Song, L. (2008). Antibacterial and antiviral study of dialdehyde polysaccharides. *Dissertation in University of Florida*.

Song, L., Cruz, C., Farrah, S. R., & Baney, R. H. (2009). Novel antiviral activity of dialdehyde starch. *Electronic Journal of Biotechnology* 12, 1–5.

Tabak, L. A. (1995). In defense of the oral cavity: structure, biosynthesis, and function of salivary mucin. *Annual Review of Physiology* 7, 547–564.

Tellier, R. (2006). Review of aerosol transmission of influenza. *Emergenvy Infection. Disease* 12, 1657–1661.

Tseng, C. & Li, C. S. (2005). Inactivation of virus containing aerosols by ultraviolet germinidal irradiation. *Aerosol Science & Technology* 39, 361–366.

U.S. Army (1998) Filter medium, fire-resistant, high efficiency, military Specification MIL-F-51079D, Aberdeen Proving Ground, MD: U.S. Army Armaments Munitions and Chemical Commands.

Valegard, K., Lijas, L., Fridborg, K., & Unge, T. (1990). The three-dimensional structure of the bacterial virus MS2. *Nature* 345, 36–41.

Varavinit, S., Chaokasem, N., & Shobsngob, S. (2001). Covalent immobilization of a glucoamylase to bagasse dialdehyde cellulose. *World Journal of Microbiology & Biotechnology* 17, 721–725.

Veelaert, S., Devit, D., Gotlieb, K. F., & Verhe, R. (1997). The gelation of dialdehyde starch. *Carbohydrate Polymer* 32, 131–139.

Veerman, E. C. I., van den Keybus, P. A. M., Vissink, A., & Nieuw Amerongen, A. V. (1996). Human glandular salivas: their separate collection and analysis. *European Journal of Oral Science* 104, 346–352.

Verdenelli, M.C., Cecchini, C., Orpianesi, C., & Dadea, G.M. (2003). A. Efficacy of antimicrobial filter treatments on microbial colonization of air panel filters. *Journal of Applied Microbiology* 94, 9-17.

Vingerhoeds, M. H., Blijdenstein ,T. B. J., Zoet F. D., & Aken, G. A. V. (2005). Emulsion flocculation induced by saliva and mucin. *Food Hydrocolloids* 19, 915–922.

Viscusi, D. F., Bergman, M. S., Eimer, B. C., & Shaffer, R. E. (2009) Evaluation of five decontamination methods for filtering facepiece respirators. *Annual Occupational Hygiene* 53, 815–817.

Vo, E., Rengasamy, S., & Shaffer, R. E. (2009). Development of a test system to evaluate procedures for decontamination of respirators containing viral droplets. *Applied & Environmental Microbiology* 75, 7303–7309.

Walker, C. M., & Ko, G. (2007). Effect of ultraviolet germicidal irradiation on viral aerosol. *Environmental Science & Technology* 41, 5460–5465.

Watanabe, K., Kakita, Y., Kashige, N., Miake, F., & Tsukiji, T. (2000). Effect of ionic strength on the inactivation of micro-organisms by microwave irradiation. *Letters in Applied Microbiology* 31, 52–56.

Williamson, K., Wommack, K., & Radosevich, M. (2003). Sampling natural viral communities from soil for culture-independent analyses. *Applied & Environmental Microbiology* 69, 6628–6633.

Willeke, K., Lin, X., &Grinshpun, A. S. (1998) Improved aerosol collection by combined impaction and centrifugal motion. *Aerosol Science & Technology 28*, 439–456.

Wong, L., & Sissions, C. H. (2001). A comparison of human dental plaque microcosm biofilms grown in an undefined medium and a chemically defined artificial saliva. *Oral Biology* 46, 477–486.

Woo, I.-S., Rhee, I.-K., & Park, H.-D. (2000). Differential damage in bacterial cells by microwave radiation on the basis of cell wall structure. *Applied & Environmental Microbiology* 66, 2243–2247.

Woo, M. H., Hsu, Y. M., Wu, C. Y., Heimbuch, B., & Wander, J. (2010). Method for contamination of filtering facepiece respirators by deposition of MS2 viral aerosol. *Journal of Aerosol Science* 41, 944–952.

Woo, M. H., Lee, J. H., Rho, S. G., Ulmer, K., Welch, J., & Wu, C. Y. (2011). Evaluation of the performance of dialdehyde cellulose filters against airborne and waterborne bacteria and viruses. *Industrial & Engineering Chemistry Research* 50, 11636–11643.

Woo, M.- H., Anwar, D., Smith, T., Grippin, A., Wu, C.- Y., & Wander, J. (2012).Investigating the effects of relative humidities and nebulized media on UV inactivation of viral aerosols loaded filter. Submitted to *Applied &Environmental Engineering.*

Wu, Y. & Yao, M. (2010a). Inactivation of bacteria and fungus aerosols using microwave irradiation. *Journal of Aerosol Science* 41, 682–693.

Wu, Y. & Yao, M. (2010b). Effects of microwave irradiation on concentration, diversity and gene mutation of culturable airborne microorganisms of inhalable sizes in different environments. *Journal of Aerosol Science* 42, 800–810.

Yang, S. H., Lee, G. W. M., Chen, C. M., Wu, C. C., & Yu, K. P. (2007). The size and concentration of droplets generated by coughing in human subjects. *Journal of Aerosol Medicine* 20, 484–494.

Yu, J., Chang, P., & Ma, X. (2010). THe preparation and properties of dialdehyde starch and thermoplastic dialdehyde starch. *Carbohydrate Polymer* 79, 296–300

Zhang, Q., Damit, B., Wlech, J., Park, H., Wu, C. Y., & Sigmund, W. (2010). Microwave assisted nanofibriuos air filtration for disinfection of bioaerosols. *Journal of Aerosol Science* 41, 880–888.

BIOGRAPHICAL SKETCH

Myung-Heui Woo was born in Mokpo, South Korea, in 1980, and was raised through her high school years there. She attended the Department of Chemistry in Korea University and received *Summa cum laude* for her Bachelor of Science in 2004. In 2006, she received her master's degree in physical chemistry from Korea University. She served as a graduate research assistant and teaching assistant, involved in projects titled "Zirconium Phosphate sulfonated poly (Fluorinated arylene ether)s composite membranes for PEMFCs at 100-140 ^{o}C"

In 2007, Myung-Heui Woo enrolled at University of Florida to pursue a Ph.D. in Environmental Engineering Sciences and served as a research and teaching assistant.